Weyl Semimetals and Holography

with a hint of Massive Spinors

Master Thesis by:
Z.W. Sybesma

Under the Supervision of:
Prof. Dr. Ir. H.T.C. Stoof
& V.P.J. Jacobs, MSc.

Institute for Theoretical Physics,
Utrecht University

December 26, 2012

Contents

Chapter 1

Introduction

The AdS/CFT correspondence relates a weakly interacting gravity theory in a $D+1$-dimensional anti-de Sitter (AdS) bulk spacetime to a strongly interacting conformal field theory (CFT) on the D-dimensional boundary of the AdS bulk [1]. Via the weakly interacting gravity bulk the AdS/CFT correspondence potentially enables us to perform computations on strongly interacting field theories where regular perturbation theory breaks down [2, 3, 4].

A quantum critical point (QCP) governs quantum phase transitions. See Figure 1.1 for an illustration. A condensed matter system exactly at a QCP has a divergent correlation length. This renders

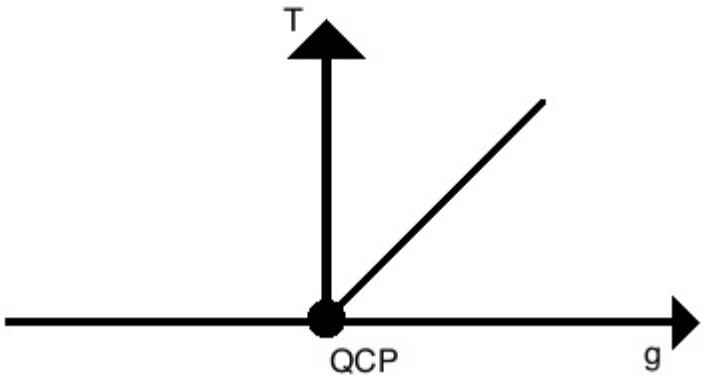

Figure 1.1: This graph illustrates a phase diagram. By T we denote temperature and g is some coupling constant of the theory. The diagonal line denotes a phase transition line governed by the quantum critical point (QCP) at the origin.

the system to be scale invariant and hence a relativistic condensed matter system exactly at a QCP is governed by a CFT. Perturbations around the QCP can be realized [5]. For instance by putting a black brane in the gravitational bulk. A black brane is a black hole with a planar rather than a spherical topology. In this thesis we will require a brane since we want to have a theory with planar topology on the boundary. The Hawking temperature associated with this black brane breaks the conformal symmetry on the boundary. The boundary theory now possesses a temperature scale. This setup is sketched in Figure 1.2. Moreover we can add electric charge to the black brane to acquire a scale of chemical potential on the boundary. In addition we can break the relativistic scaling between space and time on the boundary by generalizing the AdS background to the Lifshitz background [6, 7]. The Lifshitz background admits anisotropic scaling.

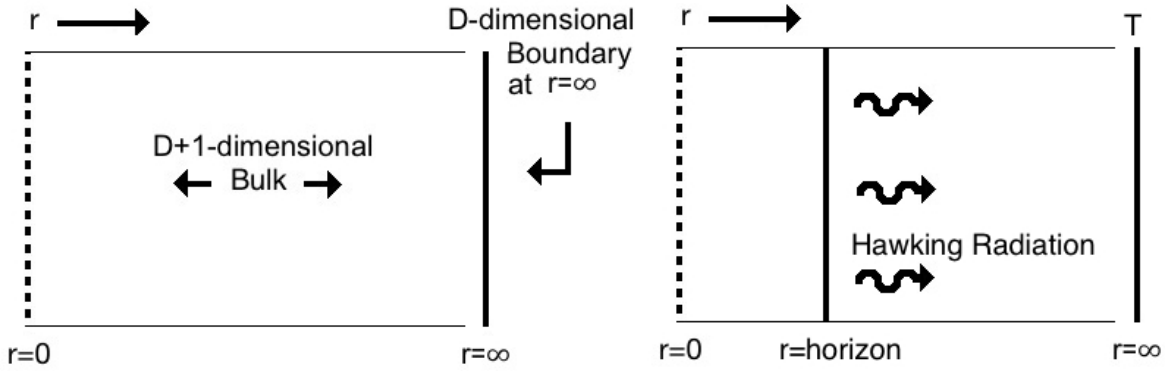

Figure 1.2: This picture illustrates the setup. The coordinate r is called the holographic coordinate and is the coordinate associated to the extra dimension of the bulk with respect to the boundary. The boundary sits at $r = \infty$. The first picture describes an AdS space with a CFT on the boundary. The second picture indicates that there is a black brane in the interior of the bulk spacetime.

An important point is that it is not clear until now what the nature of the QCP described by AdS/CFT is. We do not know what kind of phase transition it governs. Therefore we do not only hope that we can acquire more insights in strongly interacting condensed matter systems by studying this correspondence, but in addition the condensed matter systems may help us to learn more about the AdS/CFT correspondence itself.

In this thesis we are interested in two $D = 3 + 1$-dimensional fermionic systems. We apply the holographic description proposed by [8, 9] to compute retarded single-particle propagators of those systems. Single-particle propagators are crucial in condensed matter physics because of experimental access. This description ensures that the obtained propagators obey the sum rule,

$$\frac{1}{\pi}\int d\omega \mathrm{Im}\left[G_{R,\alpha\alpha'}(\mathbf{k},\omega)\right] = \delta_{\alpha\alpha'}, \tag{1.1}$$

which is a direct consequence of the elementary anti-commutation relations for fermionic single-particle operators. The resulting propagator is strongly interacting via AdS/CFT and can be decomposed in a non-interacting propagator on the boundary and a self-energy term which follows from interactions with a bulk fermion.

The first system we study is a massive Dirac spinor in presence of a strong interaction via AdS/CFT. We compute the retarded single-particle Green's functions of this system at finite temperature and finite chemical potential. Moreover, the result of breaking relativistic scaling is considered. This system might be the basis for a model of for instance atoms at unitarity which commonly have non-relativistic dispersion relations [7, 5]. We study the spectral functions which are directly obtained from the Green's functions. The spectral function gives the density of states and dispersion relations of the system.

The second system we consider is when we break a particular symmetry in a massless Dirac spinor theory. Recall that a Dirac spinor is composed of two chiral spinors. Breaking a particular symmetry changes the dispersion relation described by one Dirac cone into the dispersion relation described by two chiral cones with some separation in between. This is illustrated in Figure 1.3. The chiral cones describe a Weyl semimetal[1] [9, 10] in a low-energy range.

[1] A semimetal is a gapless semiconductor. In addition, a Weyl semimetal is a semimetal with touching valence and

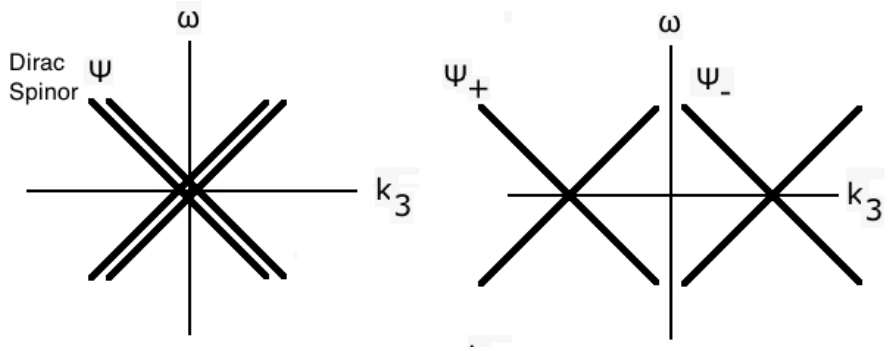

Figure 1.3: The first graph denotes the dispersion relations of a Dirac spinor. On the horizontal axis we find momentum and on the vertical axes we have energy. In $D = 3 + 1$ dimensions a Dirac spinor is composed of two chiral spinors Ψ_+ and Ψ_- the following way: $\Psi = (\Psi_+, \Psi_-)$ [11]. By breaking a specific symmetry in the Dirac spinor theory we obtain a momentum-space separation between the chiral spinors, which otherwise would be degenerate in momentum space.

The separation between the chiral cones induces a fictitious magnetic field in momentum-space generated by monopoles at the points the origin of each chiral cone [12, 13]. The effect is topological since the number of monopoles is quantized. See Figure 1.4 for a sketch of the fictitious magnetic field generated by the Weyl cones. This fictitious magnetic field contributes to the electric conductivity [14]. This effect is called the anomalous Hall effect. The effect is well-understood in the non-interacting case [15, 16]. We are interested in the changes of this magnetic field when the system is strongly interacting via AdS/CFT. This is our main point of interest. This is studied at zero temperature, zero chemical potential and relativistic scaling. We leave the generalization to future work. Moreover we compute the strongly interacting retarded single-particle Green's functions of this system at finite temperature, finite chemical potential and relativistic scaling. We analyze the associated spectral functions.

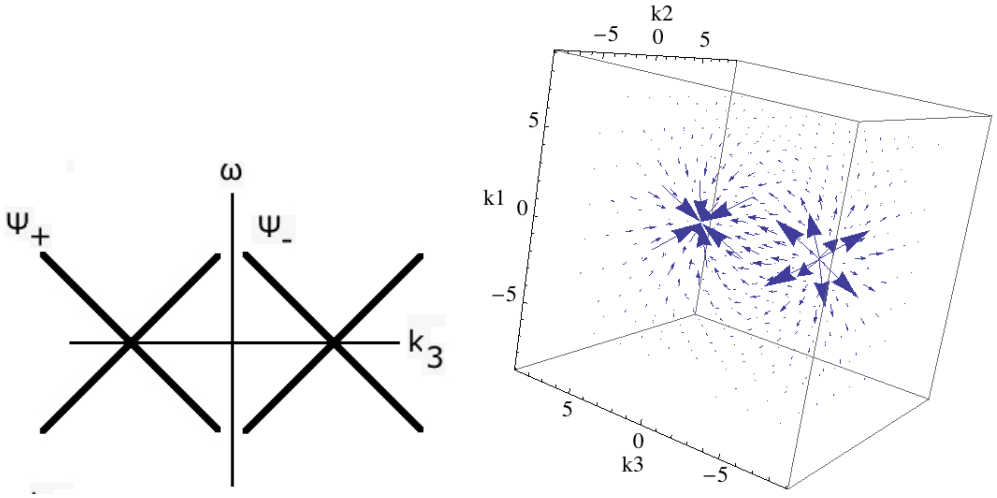

Figure 1.4: The first graph denotes a separation between chiral spinors. The fictitious magnetic field in momentum space is plotted in the second graph. The location of the monopoles corresponds to the location of the origins of the chiral cones.

conduction bands based on chiral two-component fermions that in the non-interacting limit satisfy the Weyl equation $\pm\vec{\sigma} \cdot \mathbf{k}\psi = E\psi$. Here, the $\pm$ denotes the chirality of the fermion.

1.0.1 Outline

In chapter 2 we develop the bulk theory. A black brane is constructed in the interior of the bulk and we break the relativistic scaling on the boundary. Using the holographic description proposed in [8, 9] we obtain a theory for one chiral spinor on the boundary. Furthermore, we add another fermion to the bulk such that there are two chiral spinors which form one Dirac spinor on the boundary. We expand the Dirac spinor in the boundary to a strongly interacting massive Dirac spinor theory. We calculate the corresponding retarded single-particle Green's functions and spectral functions.

Arriving to chapter 3 we add electric charge to the black brane such that we obtain a doped[2] theory on the boundary. We reevaluate the spectral function of the massive fermion obtained in chapter 2 now in presence of finite chemical potential.

In chapter 4 we revisit the massless Dirac fermion on the boundary. We break a specific symmetry by adding a suitable term to the action such that we obtain a model describing a strongly interacting Weyl semimetal. We calculate the corresponding retarded single-particle Green's functions and spectral functions, for doped and undoped cases.

We establish that breaking a particular symmetry in a Weyl semimetal generates the anomalous Hall effect in chapter 5. We compare the anomalous Hall effect in a non-interacting system to the case where we take the strong interactions via AdS/CFT into account. Finally, in chapter 6 we present conclusions, discussions and an outlook.

1.0.2 Notational conventions

The metric signature is $(-,+,+,...,+)$. The total amount of dimensions of the boundary theory is denoted by D. By $\mathbf{k}$ we denote a spatial vector. A latin index, i for example, denotes the components of $\mathbf{k}_i$ where i runs through the spatial dimensions. A Greek index, μ for example, denotes the components of $\mathbf{k}_\mu$ where μ runs through both spatial and temporal dimensions.

[2]Doping refers to having a finite chemical potential.

Chapter 2

Undoped Fermion Holography

In this chapter we start by engineering a gravity theory in the bulk which manifests itself as a Lifshitz theory on the boundary. This is needed because we want to obtain the possibility of non-relativistic scaling on the boundary. Moreover we introduce a massive fermion field in the bulk which needs boundary terms on the boundary to satisfy the variational principle. We do not take into account the back reaction on the metric tensor of this field. We introduce the boundary terms on a cut-off surface near the boundary at $r = r_0$, rather than at $r = \infty$.

Next, we place a dynamical term on the cut-off surface. This term corresponds to a non-interacting theory. After we make sure that the terms do not diverge in the limit $r_0 \to \infty$, we bring the cut-off surface to the boundary by taking $r_0 \to \infty$. This approach gives us a strongly interacting massless chiral fermion on the boundary. This chiral fermion obeys the sum rule (1.1) for a specific range of bulk fermion mass M. It is important to stress that the mass in the bulk should not be associated with mass on the boundary.

We add another fermion field to the bulk. Corresponding boundary terms and dynamical terms are introduced. Two chiral fermions on the boundary are obtained. Under particular conditions the chiral fermions form a single Dirac spinor. We study the spectral function of this fermion when we make it massive. This we do by adding a mass term to the boundary, which breaks the chiral symmetry.

In the first section we develop the bulk theory and set up the Dirac equation in the bulk. In the second section we acquire a massless chiral boundary action. In the third section we develop a massless Dirac spinor on the boundary. Finally, in the fourth section we study the case when adding a mass term to the boundary Dirac spinor.

2.1 Bulk background

2.1.1 Constructing a Lifshitz black brane

The need for a brane arises from requiring a planar topology on the boundary. It is more convenient to have a horizon with planar topology, rather than a spherical topology. We now develop the tools to obtain a black brane in the gravitational bulk.

General relativity teaches us [17] that any non-trivial tensor composed of products of solely the metric and its first and second derivatives, can be expressed in terms of the metric and the Riemann tensor. Therefore the Ricci scalar R is the unique scalar which takes into account derivatives of the

metric up to second order. From this notion the Einstein-Hilbert action is constructed,

$$S_{EH} = \int d^{D+1}x\sqrt{-g}\frac{1}{16\pi G_{D+1}}[R - \Lambda], \tag{2.1}$$

where D is the total number of dimensions of the theory on the boundary. The bulk has $D+1$ dimensions. The cosmological constant is denoted by Λ and g denotes the determinant of the metric, where $\sqrt{-g}$ represents a volume element of spacetime and is included to render the expression coordinate invariant. The Newton's constant of this theory[1] is denoted by G_{D+1}. Furthermore we work in natural units so $\hbar = c = 1$. The energy-momentum tensor is defined by taking variations with respect to $g^{\mu\nu}$ from the matter action S_M,

$$T_{\mu\nu} := -2\frac{1}{\sqrt{-g}}\frac{\delta S_M}{\delta g^{\mu\nu}}, \quad S_M := \int d^{D+1}\sqrt{-g}\mathcal{L}_M, \tag{2.2}$$

where $\mathcal{L}_M$ denotes the Lagrangian of some matter field. Using

$$\frac{\delta R}{\delta g^{\mu\nu}} = R_{\mu\nu}, \quad \frac{\delta\sqrt{-g}}{\delta g^{\mu\nu}} = -\frac{1}{2}\sqrt{-g}g_{\mu\nu}, \tag{2.3}$$

we apply the Euler-Lagrange equation to the Einstein-Hilbert action in the presence of matter. This yields Einstein's equations,

$$R_{\mu\nu} - \frac{1}{2}g_{\mu\nu} + \frac{1}{2}\Lambda g_{\mu\nu} = 8\pi G_{D+1}T_{\mu\nu}. \tag{2.4}$$

Vacuum solutions, i.e. $S_M = 0$, of Einstein's equations depend on the choice of the cosmological constant. When $\Lambda = 0$ we get just Minkowski space, when $\Lambda > 0$ we get de Sitter space and when $\Lambda < 0$ the solution is AdS. The metric of AdS in $D+1$ dimensions is given by

$$ds^2_{AdS} = \frac{\ell^2}{r^2}dr^2 - \frac{r^{2z}}{\ell^2}dt^2 + \frac{r^2}{\ell^2}d\vec{x}^2_{D-1}, \tag{2.5}$$

where ℓ is the AdS-radius. A special feature of AdS is that spatial infinity can be reached in finite time [17, 5]. This is a key feature when defining a notion of a boundary[2]. In equation (2.9) the r coordinate is identified as the holographic radial coordinate which corresponds with the extra dimension of the bulk with respect to the boundary theory. The boundary is at $r = \infty$. The scalings AdS obeys are

$$t \to \lambda t, \quad \vec{x} \to \lambda\vec{x}, \quad r \to \lambda^{-1}r. \tag{2.7}$$

The scalings in (2.7) correspond to relativistic scalings on the boundary theory. Because condensed matter systems are often non-relativistic it is important to include the option to also have non-relativistic scaling on the boundary. Anisotropic scalings are governed by

$$t \to \lambda t^z, \quad \vec{x} \to \lambda\vec{x}, \quad r \to \lambda^{-1}r, \tag{2.8}$$

[1]Newton's constant is defined in an equation that is the solution to the Poisson equation. The solutions to Poisson's equation depend on the dimensions of the problem and thus Newton's constant varies in different dimensions.

[2]When taking $\tilde{r} = \ell^2/r$ for AdS we obtain,

$$ds^2_{AdS} = \frac{\ell^2}{\tilde{r}^2}(d\tilde{r}^2 - dt^2 + d\vec{x}^2_{D-1}). \tag{2.6}$$

This expression makes it apparent that AdS is just "slices", with respect to the holographic radius r, of Minkowski space with a conformal factor in front, which scales such that these "slices" have the isometries of the conformal group.

where z, a real number, is called the dynamical exponent. The dynamical exponent governs the scaling on the boundary. A generalization of the AdS-metric which exhibits these scalings is the Lifshitz-metric. This metric is given by

$$ds^2_{Lif} = \frac{\ell^2}{r^2}dr^2 - \frac{r^{2z}}{\ell^{2z}}dt^2 + \frac{r^2}{\ell^2}d\vec{x}^2_{D-1}. \tag{2.9}$$

From now on the AdS-radius ℓ is put to unity. This is always possible through a suitable rescaling of coordinates. Notice that for $z = 1$ we obtain the AdS-metric.

Let us have a look at an example. In order to obtain a black brane for the Lifshitz metric from an action, we remember how the solution of a spherical symmetric Reissner-Nordström electric charged black hole is obtained, in $D = 3+1$-dimensions and for a static universe, i.e. $\Lambda = 0$. We add a Maxwell term to the bulk. This term is described by the usual electromagnetic anti-symmetric two-tensor F. This term is the considered matter field.

The spherical symmetry is taken into account using Killing vector fields together with the Lie derivative[3], $\mathcal{L}_v$, where $v \in \{\text{all Killing vector fields of appropriate symmetries}\}$. This puts constraints on $g_{\mu\nu}$ in the form of $\mathcal{L}_v(g_{\mu\nu}) = 0$ for all v. Summarizing the constraints,

$$\begin{cases} \mathcal{L}_M = -\frac{1}{4}F^2, \\ \Lambda = 0, \\ \mathcal{L}_v(g_{\mu\nu}) = 0, \end{cases} \tag{2.10}$$

we obtain a system of equations we have to solve. These equations come from Einstein's equations and the equations of motion of the matter fields,

$$\begin{cases} R_{\mu\nu} - \frac{1}{2}g_{\mu\nu} = 8\pi G_{D+1}(F_{\mu\rho}F^{\rho}_{\nu} - \frac{1}{4}g_{\mu\nu}F_{\rho\sigma}F^{\rho\sigma}), \\ D_\mu F^{\mu\nu} = 0, \\ \mathcal{L}_v(g_{\mu\nu}) = 0. \end{cases} \tag{2.11}$$

A strategy for solving (2.11) is to take a spherically symmetric ansatz for the metric tensor, thus solving the third constraint. The next step can be taking $A_i = 0$, since we are only interested in electric fields, and putting $A_0 = Q/r^2$. Here Q denotes electric charge. This choice solves the second equation in exchange for extra constraints on $g_{\mu\nu}$ due to the Christoffel symbols that appear in the covariant derivative D_μ. These steps immensely simplify the task of finding a solution to this system. Finally, it turns out [17] that the solution becomes,

$$ds^2_{RN} = \frac{1}{V^2(r,Q)}dr^2 - V^2(r,Q)dt^2 + r^2 d\Omega_2^2, \quad V^2(r,Q) = \left(1 - \frac{2GM}{r} + \frac{G_4 Q^2}{r^2}\right). \tag{2.12}$$

When putting $Q \to 0$ the Schwarzschild black hole solution is obtained. Notice that the electric constant ϵ_0 is put to unity. The factor V is called the emblackening factor. The black hole horizon radius r_h is defined as the largest real solution such that,

$$V(r_h) = 0. \tag{2.13}$$

[3]We mention this for completeness. It is not necessary to know the exact definition to appreciate this argument in this example. A good reference is [18].

When $r \to \infty$ we obtain Minkowski space, because $V \to 1$. This property is called asymptotic flatness. When instead of spherical symmetry S^2, the choice for planar symmetry $\mathbb{R}^2$ would be made, the solution would remain to be the same except for $d\Omega_2^2 \to d\vec{x}_2^2$. In this case the solution is called a black brane.

To obtain a suitable action which provides the metric (2.9) on the boundary, we have to apply the Reissner-Nordström approach, but in reversed order. The problem becomes what $\mathcal{L}_M$ we need to provide such that we obtain a system like (2.11) which is solved by a metric that becomes Lifshitz on the boundary, i.e. is asymptotically-Lifshitz. It turns out [6] that the following setup solves the problem,

$$\begin{aligned} \mathcal{L}_M =& \frac{1}{16\pi G_{D+1}}[-\frac{1}{2}(\partial\phi)^2 - \frac{1}{4}e^{\lambda_1}(F_1)^2], \quad \Lambda = -(D+z-1)(D+z-2), \\ e^{\lambda_1\phi} =& 2(z-1)(z+D-1)\frac{1}{f^2}r^{2(1-D)}, \quad (F_1)_{rt} = fr^{z+D-2}, \end{aligned} \tag{2.14}$$

where ϕ is a dilaton, a scalar field, and F is an anti-symmetric two-tensor as in electromagnetism. Some free parameter of the theory is f. This solution requires $D \geq 2$. Notice that the electric constant ϵ_0 is put to unity. An important remark is that the just-mentioned fields are not meant to have any direct physical interpretation. These fields just "feed" the right geometry and values such that we find the solution,

$$ds^2 = \frac{1}{r^2V^2(r)}dr^2 - V^2(r)r^{2z}dt^2 + r^2d\vec{x}_{D-1}^2, \quad V^2(r) = 1 - \left(\frac{r_h}{r}\right)^{D+z-1}, \tag{2.15}$$

which asymptotes to (2.9) when $r \to \infty$, as required. By r_h we denote the horizon of this particular black brane. Notice the absence of f in the solution.

2.1.2 Properties of the black brane

The bulk theory we adopt contains a Lifshitz black brane as described by (2.15). A black brane has a temperature. Due to the asymptotic Lifshitz metric the space has a boundary, because Lifshitz is generalization of AdS. Because of the boundedness of the bulk, the system can be in thermodynamical equilibrium with the black brane. Hence the temperature on the boundary equals the temperature T of the black brane, which is calculated by,

$$T = \frac{1}{4\pi}\left(\frac{\partial V^2}{\partial r}\right)\Big|_{r=r_h} r_h^{z+1}. \tag{2.16}$$

The expression for temperature is obtained by a Wick-rotation of the time-coordinate. We obtain a periodic coordinate. By demanding the absence of a conical singularity we rescale the periodicity and make the identification with temperature [5]. In the current setup,

$$T = \frac{D+z-1}{4\pi}(r_h)^z, \tag{2.17}$$

so $T = 0$ corresponds with having no black brane horizon[4].

It should be mentioned that the action in (2.14) has an issue for $z > 1$. It turns out that for $r \to \infty$, the dilation ϕ and the field F_1 diverge. But the metric has good asymptotic behavior and the

[4] A subtlety for $z \neq 1$ and $r_h = T = 0$, since geodesics are not well-defined when traveling through the singularity at $r = 0$. This subtlety can be solved by always considering an infinitesimal horizon.

fermions, which are introduced later, couple to none of these diverging fields. Since the metric and the fermions are the only quantities considered on the boundary, we assume that these divergences do not spoil the thermodynamic behavior on the boundary. Hence we are not considering renormalization of any of these terms.

Notice that when taking $z \to 1$ we get that $e^{\lambda_1 \phi} \to 0$[5], such that the dilaton and the gauge field F_1 decouple from the action and we end up with a regular Einstein-Hilbert action.

2.1.3 Bulk fermions

Being interested in a fermion systems on the boundary, it is instructive to highlight some properties of the Dirac equation. Let M represent the fermion mass and D_μ a covariant derivative. The classical Dirac equation becomes

$$(\not{D} - M)\Psi = 0, \tag{2.18}$$

where Ψ denotes the classical Dirac field and where $\not{D} := \gamma^\mu D_\mu$, $\overline{\Psi} := \Psi^\dagger \gamma^0$. The gammas represent elements of the Clifford Algebra, $\{\gamma^\mu, \gamma^\nu\} := \gamma^\mu\gamma^\nu + \gamma^\nu\gamma^\mu = 2\eta^{\mu\nu}$ in D dimensions. The gammas ensure

$$0 = (\not{D} \pm M)(\not{D} \mp M)\Psi = (\frac{1}{2}\{\gamma^\mu, \gamma^\nu\}D_\mu D_\nu - M^2)\Psi = (D^2 - M^2)\Psi, \tag{2.19}$$

meaning that Ψ also solves the Klein-Gordon equation and hence is a classical relativistic field, i.e. Lorentz invariance applies.

A virtue of the Clifford Algebra is that the representation of the elements in $D = 2n$, $n \in \mathbb{N}$, also represent the Clifford algebra in the $D = 2n + 1$ situation [19]. This property is convenient when relating the γ's on the boundary to the gamma matrices in the bulk. The gamma matrices in the bulk we denote by Γ. We are interested in $D = 4$. The explicit choice of representation when D is even is,

$$\Gamma^{\underline{r}} = \gamma^{D+1}, \quad \Gamma^{\underline{t}} = \gamma^0, \quad \Gamma^{\underline{i}} = \gamma^{\underline{i}}, \tag{2.20}$$

such that the spinors are related by,

$$\Psi = \frac{1}{2}(\mathbb{1}_D + \gamma^{D+1})\Psi + \frac{1}{2}(\mathbb{1}_D - \gamma^{D+1})\Psi := \Psi_R + \Psi_L = \begin{pmatrix} \Psi_+ \\ \Psi_- \end{pmatrix}. \tag{2.21}$$

The chiral spinors in the bulk are also the chiral spinors on the boundary[6]. The γ^{D+1} is the analogue of "usual" γ^5 in $D = 4$-dimensions. We work in the chiral, or Weyl, basis. For $D = 4$ we have explicitly,

$$\Gamma^{\underline{a}} = \begin{pmatrix} 0 & \overline{\sigma}^{\underline{a}} \\ \sigma^{\underline{a}} & 0 \end{pmatrix}, \quad \begin{array}{l} \sigma^{\underline{a}} = (\mathbb{1}_4, \vec{\sigma}), \\ \overline{\sigma}^{\underline{a}} = (-\mathbb{1}_4, \vec{\sigma}), \\ \vec{\sigma} = (\sigma^1, \sigma^2, \sigma^3), \end{array} \quad \underline{a} = \{\underline{t}, \underline{i}\}, \tag{2.22}$$

[5]The notation of "$\to$" rather than "$=$" is used because formally $e^{\lambda_1 \phi} \to 0$ is obtained by taking a limit.

[6]The explicit choice of representation used when D on the boundary is odd,

$$\Gamma^{\underline{r}} = \begin{pmatrix} \mathbb{1}_{\lfloor \frac{D}{2} \rfloor} & 0 \\ 0 & -\mathbb{1}_{\lfloor \frac{D}{2} \rfloor} \end{pmatrix}, \quad \Gamma^{\underline{t}} = \begin{pmatrix} \gamma^{\underline{0}} & 0 \\ 0 & \gamma^{\underline{0}} \end{pmatrix}, \quad \Gamma^{\underline{i}} = \begin{pmatrix} \gamma^{\underline{i}} & 0 \\ 0 & \gamma^{\underline{i}} \end{pmatrix}, \quad \Psi = \begin{pmatrix} \Psi_+ \\ \Psi_- \end{pmatrix},$$

where $\mathbb{1}_D$ denotes $D \times D$ unit matrix and $\lfloor . \rfloor$ denotes the entier (floor) function. Notice that the chiral components $\Psi_\pm$ in the bulk are Dirac spinors on the boundary. This is contrary to the case when D on the boundary is even, which is the case of our interest.

where the σ's denote Pauli matrices. Notice that when $M = 0$ we obtain

$$\sigma^{\underline{a}}\partial_{\underline{a}}\Psi_+ = 0, \quad \overline{\sigma}^{\underline{a}}\partial_{\underline{a}}\Psi_- = 0, \tag{2.23}$$

which are the Weyl equations. The spatial terms in front of the Ψ's represent spin-orbit couplings. So $\mathbf{k} \to -\mathbf{k}$ implies switching helicity and chirality. Before generalizing the metric to curved spacetime we present an example. Observe what happens when we change our metric sign convention,

$$\eta_{\mu\nu} \to -\eta_{\mu\nu}, \quad \begin{cases} \Rightarrow & (D^2 - M^2)\Psi = 0 \to (D^2 + M^2)\Psi = 0, \\ \Rightarrow & \{\gamma^\mu, \gamma^\nu\} = 2\eta^{\mu\nu} \to \{\gamma^\mu, \gamma^\nu\} = -2\eta^{\mu\nu}. \end{cases} \tag{2.24}$$

We require the Clifford algebra not to change. This is done by letting

$$\gamma^\mu \to \sqrt{-1}\gamma^\mu, \quad \Rightarrow \quad \{\gamma^\mu, \gamma^\nu\} = -2\eta^{\mu\nu} \to -\{\gamma^\mu, \gamma^\nu\} = -2\eta^{\mu\nu}, \tag{2.25}$$

such that the minus signs cancel. Notice that the Dirac equation picks up a relative i sign by this substitution. Hence

$$\eta_{\mu\nu} \to -\eta_{\mu\nu}, \quad \begin{cases} \Rightarrow & (D^2 - M^2)\Psi = 0 \to (D^2 + M^2)\Psi = 0, \\ \Rightarrow & (\not{D} \mp M)\Psi = 0 \to (i\not{D} \mp M)\Psi = 0, \\ \Rightarrow & 0 = (i\not{D} \mp M)(i\not{D} \pm M)\Psi = -(D^2 + M^2)\Psi. \end{cases} \tag{2.26}$$

This lesson is important for curved space. Up to this point we exclusively admitted the fermions to live in flat space. When $\eta_{\mu\nu} \to g_{\mu\nu}$, where $g_{\mu\nu}$ stands for a general metric tensor, it alters the Clifford algebra such that $\{\gamma^\mu, \gamma^\nu\} = 2g^{\mu\nu}$. Requiring that the Clifford algebra remains the same,

$$\eta_{\mu\nu} \to g_{\mu\nu}, \quad \Rightarrow \quad (\not{D} \mp M)\Psi = 0 \to (\gamma^{\underline{a}} e^\mu_{\underline{a}} D_\mu \mp M)\Psi = 0, \tag{2.27}$$

where $e^\mu_{\underline{a}}$ is called a vielbein and defined as $\eta_{\underline{ab}} = e^\mu_{\underline{a}} e^\nu_{\underline{b}} g_{\mu\nu}$[7]. The vielbein can be regarded to be the "square root" analogue of $\sqrt{-1}$ in the example where $\eta \to -\eta$. The underscored indices mean that they are coordinates in locally flat space.

This is not all that changes in curved spacetime. Since vielbeins depend on spacetime, the covariant derivative picks up a term

$$D_\mu \to D_\mu + \frac{1}{4}\Omega_{\mu\underline{ab}}\Gamma^{\underline{ab}}, \quad \Gamma^{\underline{ab}} := \frac{1}{2}\Gamma^{\underline{a}}\Gamma^{\underline{b}}, \quad \Omega_{\mu\underline{ab}} := e_{\nu\underline{a}}\partial_\mu e^\nu_{\underline{b}} + e_{\nu\underline{a}} e^\sigma e_{\underline{b}} \Gamma^\nu_{\sigma\mu}, \tag{2.28}$$

where the last Γ denotes a Christoffel symbol and Ω is called the spin-connection. The spin-connection Ω is defined [20] by the requirement that $D_\mu e^\nu_{\underline{a}} = 0$, which is called the tetrad postulate. This is equivalent to metric compatibility, i.e. $D_\mu g_{\sigma\nu} = 0$. Hence

$$0 = (\gamma^{\underline{a}} e^\mu_{\underline{a}} D_\mu \mp M)(\gamma^{\underline{a}} e^\mu_{\underline{a}} D_\mu \pm M)\Psi = (g^{\mu\nu} D_\mu D_\nu - M^2)\Psi = (D^2 - M^2)\Psi. \tag{2.29}$$

It is concluded that the Lagrangian of fermions in the bulk with a certain coupling constant g_f takes the form of

$$S_{\text{Dirac}} = i g_f \int d^{D+1}x \sqrt{-g}\overline{\Psi}(\gamma^{\underline{a}} e^\mu_{\underline{a}} D_\mu - M)\Psi, \quad D_\mu = \partial_\mu + \frac{1}{4}\Omega_{\mu\underline{ab}}\Gamma^{\underline{ab}}, \tag{2.30}$$

where the spacetime volume element $\sqrt{-g}$ is included to make the expression coordinate invariant.

[7] It should be noted that when looking at the bulk, $\underline{a}$ can also take the value $\underline{r}$.

2.2 From bulk to boundary: chiral spinor

2.2.1 Bulk fermions and boundary terms

We now construct the boundary action from the bulk action. The full bulk action under consideration is represented by,

$$S_{\text{full}} = S_{\text{Dirac}} + S_{\partial} + S_0. \tag{2.31}$$

The term S_{Dirac} is defined as (2.30). The term S_{∂} denotes a set of boundary terms at r_0 needed to satisfy $\delta S_{full} = 0$ together with boundary conditions on r. With S_0 a term at the cut-off surface is meant which generates the dynamical properties of the boundary fermion. The term S_0 is chosen to satisfy $\delta S_0 = 0$. All terms are fully specified during the calculation below. Applying the variational principle [21] leads to

$$\begin{aligned} 0 = \delta S_{\text{Dirac}} &= \text{term that vanishes due to E.O.M.} \\ &+ i\frac{g_f}{2}\int d^D x\sqrt{-h}\sqrt{-g^{rr}}\left(\overline{\Psi}_L\delta\Psi_R + \delta\overline{\Psi}_R\Psi_L - \overline{\Psi}_R\delta\Psi_L - \delta\overline{\Psi}_L\Psi_R\right)\Big|_{r=r_h}^{r=r_0}, \end{aligned} \tag{2.32}$$

where h is the determinant of the induced metric. Firstly observe that $\sqrt{-g^{rr}} \to 0$ as we approach the horizon r_h, such that we only need to worry about the behavior at the cut-off surface. Since the Dirac equation is a partial differential equation of first order, we can impose either $\delta\Psi_+ = 0$ or $\delta\Psi_- = 0$ when taking Dirichlet boundary conditions. The result is that we can make the remaining terms vanish if we define the boundary term S_{∂} to be,

$$S_{\partial} = \pm i\frac{g_f}{2}\int_{r=r_0} d^D x\sqrt{-h}\sqrt{-g^{rr}}(\overline{\Psi}_L\Psi_R + \overline{\Psi}_R\Psi_L), \quad \delta\Psi_{\pm} = 0, \tag{2.33}$$

where h is the determinant of the induced metric on the boundary. Now we have,

$$\delta\left(S_{\text{Dirac}} + S_{\partial}\right) = 0. \tag{2.34}$$

Without any loss of generality the case of $\delta\Psi_+ = 0$ is considered. A term like S_0 can be included on the cut-off surface as long as $\delta S_0 = 0$. Introduce

$$S_0 = iZ\int_{r=r0} d^D x\sqrt{-h}\overline{\Psi}_R\Gamma^{\underline{a}}e^{\mu}_{\underline{a}}D_{\mu}\Psi_R, \tag{2.35}$$

where Z is an arbitrary constant. This S_0 can be added since $\delta\Psi_R = (\delta\Psi_+, 0) = 0$. Notice that $\underline{a}$ runs through D dimensions. The added S_0 term renders the field Ψ_R dynamical on the cut-off surface. When D is even the $D_{\mu} \to \partial_{\mu}$ on the boundary, because the spin-connection vanishes. This is explicitly shown later on page 14.

We identify Ψ_+ on the boundary to be the source of Ψ_- in the bulk, because $\delta\Psi_+ = 0$. Using the bulk Dirac equation we obtain,

$$\Psi_- = -i\xi\Psi_+, \tag{2.36}$$

where we chose some suitable constants. We work out this proportionality ξ later. This expression is used to integrate out Ψ_- from the action. To obtain the retarded Green's function for Ψ_+ on the cut-off surface, we have to choose the second term $\overline{\Psi}_L\Psi_R$ in (2.33) and ignore the other one[8]. We also

[8]Choosing either of these terms is equivalent to choosing between an advanced or a retarded propagator. Choosing both gives neither.

multiply the term by a factor of two for conventional reasons. Thus

$$\delta\Psi_+ = 0, \quad \Rightarrow \quad S_\partial = ig_f \int_{r=r_0} d^D x\sqrt{-h}\sqrt{-g^{rr}}(\overline{\Psi}_R\Psi_L). \tag{2.37}$$

In the case where $\delta\Psi_- = 0$ we would end up with,

$$\delta\Psi_- = 0, \quad \Rightarrow \quad S_\partial = -ig_f \int_{r=r_0} d^D x\sqrt{-h}\sqrt{-g^{rr}}(\overline{\Psi}_L\Psi_R). \tag{2.38}$$

Using ξ we equate out Ψ_- from the action on the cut-off surface. This results in the following effective action for Ψ_+ on the boundary which is strongly interacting with a fermion in the bulk,

$$S_{\text{eff}} = S_0 + S_\partial = -\int_{r=r0} \frac{d^D k}{(2\pi)^D}\sqrt{-h}\Psi_+^\dagger(\mathbf{k},\omega)[-Z\sigma^{\underline{a}}e^\mu_{\underline{a}}\mathbf{k}_\mu + g_f\sqrt{g^{rr}}\ \xi(\mathbf{k},\omega)]\Psi_+(\mathbf{k},\omega), \tag{2.39}$$

where it is important to notice that this action for $D = 4$ has the structure of a 2×2 matrix rather than a 4×4 matrix. This corresponds with the fact that Ψ_+ is a chiral spinor. We transformed the action to a momentum space integral using a Fourier transformation.

2.2.2 Determining the proportionality ξ

Let us restrict to a boundary theory of $D = 4$ dimensions. Our goal is to compute the 2×2 matrix ξ such that in momentum space,

$$\Psi_- = -i\xi\Psi_+. \tag{2.40}$$

We assume $\mathbf{k} = (0, 0, k_3)$[9] and later on we rotate back to a general momentum. The virtue of this choice is that we only have to deal with the diagonal Pauli matrix σ^3. We obtain,

$$\xi\Psi_+ = \begin{pmatrix} \xi_+ & \\ & \xi_- \end{pmatrix}\Psi_+. \tag{2.41}$$

For the choice of $D = 4$ it holds that $\Psi \sim (u_+, d_+, u_-, d_-)$ and $\Psi_\pm := (u_\pm, d_\pm)$, which makes it possible to derive,

$$\xi_+ = i\frac{u_-}{u_+}, \quad \xi_- = i\frac{d_-}{d_+}. \tag{2.42}$$

To find the expressions above we have to start from the Dirac equation, find the relation between the components of the chiral spinors and construct the differential equation with respect to r which defines ξ. Recall,

$$(\not{D} - M)\Psi(x) = 0, \quad \begin{cases} \not{D} := \Gamma^{\underline{a}}e^\mu_{\underline{a}}D_\mu, \\ D_\mu := \partial_\mu + \frac{1}{4}(\omega_\mu)_{\underline{ab}}\Gamma^{\underline{ab}}. \end{cases} \tag{2.43}$$

Bearing in mind that V is still dependent on r, although this information is suppressed for notational convenience, it is straightforward to compute the non-vanishing vielbeins and other related expressions,

$$\begin{array}{l} e^r_{\underline{r}} = rV, \\ e^{\underline{t}}_{\underline{t}} = \frac{1}{r^z V}, \\ e^{\underline{i}}_{\underline{i}} = \frac{1}{r}, \end{array} \Rightarrow \quad \begin{array}{l} \frac{1}{4}(\omega_t)_{\underline{ab}}\Gamma^{\underline{a}}\Gamma^{\underline{b}} = -\frac{1}{2}rV\partial_r(r^z V)\Gamma^{\underline{tr}}, \\ \frac{1}{4}(\omega_i)_{\underline{ab}}\Gamma^{\underline{a}}\Gamma^{\underline{b}} = \frac{1}{2}rV\Gamma^{\underline{ir}}, \end{array} \Rightarrow \quad \begin{array}{l} D_r = \partial_r, \\ D_t = \partial_t - \frac{1}{2}rV\partial_r(r^z V)\Gamma^{\underline{t}}\Gamma^{\underline{r}}, \\ D_i = \partial_i + \frac{1}{2}rV\Gamma^i\Gamma^r. \end{array} \tag{2.44}$$

[9] Although there is no full Lorentz invariance for generic z, the spatial rotations hold true for any z. Hence we can always rotate the spatial momentum in the 3-direction.

This is where we can conclude that on the boundary the spin-connection vanishes. Using these explicit expressions and a plane wave decomposition,

$$\Psi(x) = e^{ix\cdot\mathbf{k}}\Psi(r) \tag{2.45}$$

together with $\Gamma^{\underline{t}}\Gamma^{\underline{t}}\Gamma^{\underline{r}} = -\Gamma^{\underline{r}}$ and $\Gamma^{\underline{i}}\Gamma^{\underline{i}}\Gamma^{\underline{r}} = \Gamma^{\underline{r}}$ the Dirac equation is expressed as,

$$\begin{aligned}
&(\not{D} - M)\Psi(x)\\
=&(\Gamma^{\underline{r}} rV\partial_r + \Gamma^{\underline{t}}(-i\omega - \frac{1}{2}rV\partial(r^zV)\Gamma^{\underline{t}})\frac{1}{r^zV} + \Gamma^{\underline{i}}(i\mathbf{k}_{\underline{i}} + (d-1)\frac{1}{2}rV\Gamma^{\underline{i}}\Gamma^{\underline{r}})\frac{1}{r} - \mathbb{1}_4 M)e^{ix\cdot\mathbf{k}}\Psi(r)\\
=&(\Gamma^{\underline{r}} rV\partial_r + \underbrace{\frac{i}{r}[\Gamma^t\frac{-\omega}{r^{z-1}V}] + \frac{i}{r}[\Gamma^{\underline{i}}\mathbf{k}_{\underline{i}}]}_{=:\,\frac{i}{r}\Gamma\cdot\tilde{\mathbf{k}}} + \frac{1}{2}\Gamma^{\underline{r}}\underbrace{[r^{1-z}\partial_r(r^zV) + (d-1)V]}_{=:\,p_z(r)} - \mathbb{1}_4 M)e^{ix\cdot\mathbf{k}}\Psi(r) = 0,
\end{aligned} \tag{2.46}$$

where,

$$\tilde{\mathbf{k}}^\mu := (-\tilde{\omega}, \mathbf{k}), \quad \tilde{\omega} := -\frac{\omega}{r^{z-1}V}. \tag{2.47}$$

From (2.46) it is possible to setup a differential equation relating different components of the Dirac field to each other, which leads to an expression for $\xi_\pm$. Before this is done, $p_z(r)$, which is the contribution of the spin-connection, is scaled out to simplify the differential equation,

$$\begin{aligned}
&\Psi(r) = e^{-\frac{1}{2}\int_r d\tilde{r}\frac{p_z(\tilde{r})}{\tilde{r}V(\tilde{r})}}\phi(r) = \frac{1}{\sqrt{r^{D-1+z}V(r)}}\phi(r),\\
\Rightarrow\quad &(\not{D} - M)\Psi(x)\\
&=(\Gamma^{\underline{r}} rV\partial_r[e^{-\frac{1}{2}\int_r d\tilde{r}\frac{p_z(\tilde{r})}{\tilde{r}V(\tilde{r})}}])\phi(r) + (\frac{1}{2}\Gamma^{\underline{r}}p_z(r))e^{-\frac{1}{2}\int_r d\tilde{r}\frac{p_z(\tilde{r})}{\tilde{r}V(\tilde{r})}}\phi(r) + e^{-\frac{1}{2}\int_r d\tilde{r}\frac{p_z(\tilde{r})}{\tilde{r}V(\tilde{r})}}(rV\Gamma^{\underline{r}}\partial_r + \frac{i}{r}\Gamma\cdot\tilde{\mathbf{k}} - \mathbb{1}_4 M)\phi(r)\\
\Rightarrow\quad &[rV\Gamma^{\underline{r}}\partial_r + \frac{i}{r}\Gamma\cdot\tilde{\mathbf{k}} - \mathbb{1}_4 M]\phi(r) = 0.
\end{aligned} \tag{2.48}$$

Expressing ϕ in chiral parts labeled with $\pm$ makes it possible to express the equation on the last line of (2.48) into,

$$\phi_\pm(r) = \mp\frac{i}{\tilde{\mathbf{k}}^2}(\gamma\cdot\tilde{\mathbf{k}})\mathcal{A}(\mp M)\phi_\mp(r), \quad \mathcal{A}(\mp M) := r(rV\partial_r \pm M). \tag{2.49}$$

This is the desired differential equation which relates the components of ϕ to each other. In the $D = 4$ case[10] the differential equation decouples to,

$$\begin{aligned}
i(\tilde{\omega} + k_3)u_+ &= \mathcal{A}(-M)u_-, \qquad i(\tilde{\omega} - k_3)d_+ = \mathcal{A}(-M)d_-,\\
i(\tilde{\omega} - k_3)u_- &= \mathcal{A}(M)u_+, \qquad i(\tilde{\omega} + k_3)d_- = \mathcal{A}(M)d_+,
\end{aligned} \tag{2.50}$$

while we continue letting $\mathbf{k} = (0, 0, k_3)$. The last step in the computation starts from equating $\frac{1}{i}r^2V\partial_r\xi_+ = r^2V\partial_r\frac{u_-}{u_+}$ and $\frac{1}{i}r^2V\partial_r\xi_- = r^2V\partial_r\frac{d_-}{d_+}$, with the aid of the identities of (2.50). This gives the desired expression for $\xi_\pm$,

$$r^2V\partial_r\xi_\pm(r,\omega,k_3) + 2Mr\xi_\pm(r,\tilde{\omega},k_3) = -\tilde{\omega}\mp k_3 + (-\tilde{\omega}\pm k_3)\xi_\pm^2(r,\tilde{\omega},k_3), \quad \tilde{\omega} = -\frac{\omega}{r^{z-1}V}. \tag{2.51}$$

[10]For D odd this is slightly more subtle. We find different chiral spinors related to each other instead of different spin-components.

Notice that this is a first order differential equation. We need a boundary condition to find a solution. We choose the boundary condition which corresponds with particles falling into the horizon. We compute this boundary condition by taking the two equations involving $u_\pm$ from (2.50). We insert a power law ansatz and take $r \to r_h$. This gives an expression for $u_\pm$. Using (2.42) we find that the infalling boundary conditions are,

$$\xi_\pm(r_h, k_3, \omega) = i. \tag{2.52}$$

The solution of ξ to equation (2.51) together with boundary condition (2.52) possesses certain symmetries. When $k_3 \to -k_3$, we observe a change in chirality,

$$\xi_\pm(r, -k_3, \omega) = \xi_\mp(r, k_3, \omega). \tag{2.53}$$

The switch regarding chirality can be understood by realizing that the helicity, as explained in (2.23), changes sign. Another symmetry is $(\omega, k) \to (-\omega, -k)$,

$$\xi_\pm(r, -k_3, -\omega) = -\xi^*_\pm(r, k_3, \omega), \tag{2.54}$$

where the asterisk denotes complex conjugation. This complex conjugate makes sure that the boundary condition (2.52) is met.

Finally we can also change the sign of the bulk mass M,

$$\xi_\pm(r, -M, k_3, \omega) = -\xi^{-1}_\pm(r, M, -k_3, \omega), \tag{2.55}$$

where ξ^{-1} denotes the inverse of ξ.

Because of the interest in the behavior of $\xi(r_0)$ when $r_0 \to \infty$, it is instructive to examine the asymptotic behavior in terms of r_0. Making a power law ansatz gives us [9]

$$\phi_\pm = r^{\pm M}(1 + ...)A_\pm + r^{\mp M-1}(1 + ...)B_\pm, \tag{2.56}$$

for the case that $\mathbf{k} \neq 0$, where ϕ is an asymptotic solution to (2.49) when $r \to \infty$. The dots denote terms of sub-leading orders of r. $A_\pm$ and $B_\pm$ are linearly related spinors. Recalling that $\Psi_- = -i\xi\Psi_+$, we thus see that

$$\xi = i\frac{\Psi_-}{\Psi_+} \sim i\frac{r^{-M}(1 + ...)}{r^{+M}(1 + ...)} \sim r^{-2M}, \tag{2.57}$$

for large r. This final conclusion holds for the $\mathbf{k} = 0$ case as well. Later on, when we explore which values for M are allowed, we see that there are some differences in the case when $\mathbf{k} = 0$.

Finally it is worth mentioning that only for $z = 1$ and temperature $T = 0$, we are able to obtain an analytic expression when solving (2.51) with (2.52), for generic k_3 and ω and allowed M[11]. The solution, for large values of r, takes the form

$$\xi_\pm(r, M, k_3, \omega) = r^{-2M}2^{-2M}\frac{\Gamma(\frac{1}{2} - M)}{\Gamma(\frac{1}{2} + M)}e^{-i\pi(M+\frac{1}{2})}\sqrt{\omega^2 - |k_3|^2}^{2M-1}(-\mathbb{1}_2\omega + \sigma^3 k_3). \tag{2.58}$$

Rotating to a general $\mathbf{k}$ is done by $k_3\sigma^3 \to \mathbf{k}_i\sigma^i$, obtaining

$$\xi_\pm(r, M, \mathbf{k}, \omega) = r^{-2M}2^{-2M}\frac{\Gamma(\frac{1}{2} - M)}{\Gamma(\frac{1}{2} + M)}e^{-i\pi(M+\frac{1}{2})}\sqrt{\omega^2 - |\mathbf{k}|^2}^{2M-1}(-\mathbb{1}_2\omega + \sigma^i \mathbf{k}_i). \tag{2.59}$$

The equations (2.52), (2.53), (2.54), (2.55) and (2.56) also hold for $k \to \mathbf{k}$ where $\mathbf{k}$ is a general vector due to rotational symmetry.

[11]Later in this chapter it turns out that in general $-\frac{1}{2} < M < \frac{1}{2}$ because of causality. There are other analytic solutions for ξ, for instance at $M = 0$ with $z = 2$ and general z for either ω or $\mathbf{k}$ equal to zero. These solutions are too restricted for general analysis in this thesis.

2.2.3 Renormalization and self-energy

Recall the obtained effective action on the cut-off surface with $D = 4$,

$$S_{\text{eff}} = -\int_{r=r0} \frac{d^4k}{(2\pi)^4}\sqrt{-h}\Psi_+^\dagger[-Z\sigma^{\underline{a}}e_{\underline{a}}^{\mu}\mathbf{k}_\mu + g_f\sqrt{g^{rr}}\xi]\Psi_+. \tag{2.60}$$

We explicitly calculate $\sqrt{-h}|_{r=r_0} = V(r_0)r_0^{z+3}$. We perform rescaling $\Psi_+ \to Z^{-1/2}r^{3/2}\Psi_+$ to obtain a canonically normalized action,

$$S_{\text{eff}} = -\int \frac{d^4k}{(2\pi)^4}\Psi_+^\dagger[V(r_0)(\omega - r_0^{z-1}\vec{\sigma}\cdot\mathbf{k}) + \frac{g_f}{Z}r_0^{1+z}V^2(r_0)\xi]\Psi_+, \tag{2.61}$$

where $V(r_0)$ is the emblackening factor of the black brane. The next step is to make sure that the effective action behaves properly on the boundary, i.e. when $r_0 \to \infty$. We already have that $V(r_0) \to 1$, which is easily obtained from its definition, (2.15). Let us take care of the term containing ξ by defining,

$$\Sigma(\mathbf{k},\omega) := -g\lim_{r_0\to\infty} r_0^{2M}\xi(r_0,\mathbf{k},\omega), \quad g := \frac{g_f}{Z}r_0^{1+z-2M}, \tag{2.62}$$

which is well-defined on the boundary as long as g_f/Z is defined to scale such that in a double scaling limit g remains finite as $r_0 \to \infty$,

$$r_0 \to \infty, \quad g_f \to 0, \quad g = constant. \tag{2.63}$$

Notice that we choose $g > 0$. This approach takes care of the ξ term on the boundary. As for the other term in (2.61), we observe divergent behavior for $z > 1$. In this case we have to renormalize this term. This renormalization has not been done explicitly. There are good reasons, dimensional analysis for instance [8], to expect to obtain,

$$\omega - r_0^{z-1}\sigma^i\mathbf{k}_i \to \omega - \frac{1}{\lambda}\sigma^i\mathbf{k}_i|\mathbf{k}|^{z-1}, \tag{2.64}$$

after a successful renormalization. We choose $\lambda = 1$. In general λ is believed to govern quantum phase transitions [9]. We do not go into that matter in this thesis.

When applying the regulations mentioned above we obtain a boundary effective action when taking $r_0 \to \infty$,

$$S_{\text{eff}} = -\int d^4k\Psi_+^\dagger(\omega - \sigma^i\mathbf{k}_i|\mathbf{k}|^{z-1} - \Sigma(\mathbf{k},\omega))\Psi_+ \tag{2.65}$$

The corresponding retarded propagator G_R for a chiral spinor strongly interacting via AdS/CFT is,

$$G_R(\mathbf{k},\omega) = -\left[\omega - \sigma^i\mathbf{k}_i|\mathbf{k}|^{z-1} - \Sigma(\mathbf{k},\omega)\right]^{-1}. \tag{2.66}$$

Now that the dust has settled we acquired a propagator with a dynamic term which can be toggled non-relativistic and a self-energy Σ which interacts with a chiral fermion in the bulk. In Figure 2.1 the holographic setup is illustrated.

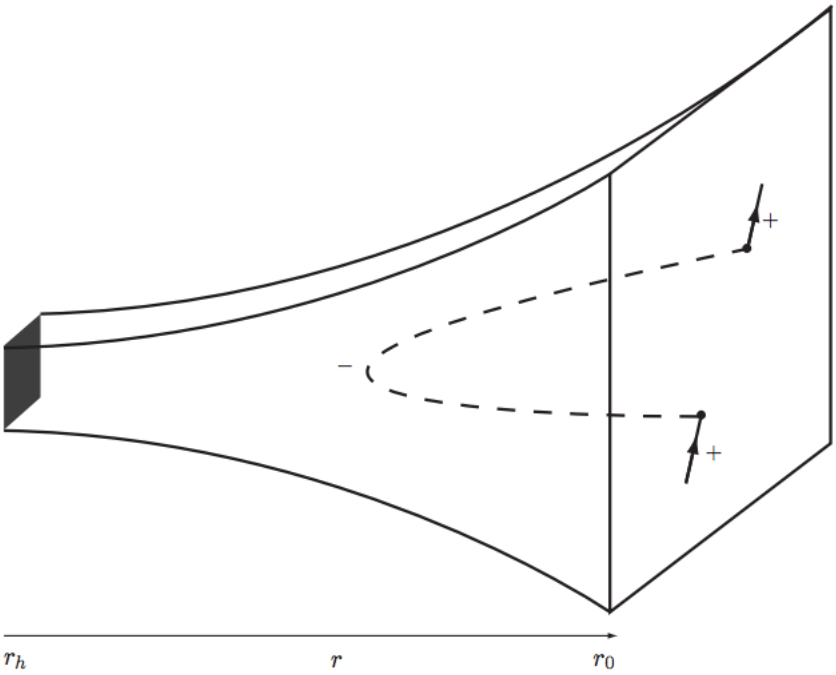

Figure 2.1: At r_h there is a black brane horizon and we have the cut-off surface at r_0. Equation (2.66) describes chiral fermion single-particle propagators on the boundary, $r_0 \to \infty$. The self-energy Σ arises from the fact that these chiral fermions interact with a fermion of opposite chirality that travels into the bulk, has classical interactions there, and comes back to the boundary. This Figure is taken from [9].

2.2.4 Sum rule

Now we study how to interpret G_R. We define the spectral function,

$$\rho(\mathbf{k},\omega) := \frac{1}{2\pi}\mathrm{Im}\{\mathrm{Tr}[G_R(\mathbf{k},\omega)]\}. \tag{2.67}$$

The $\frac{1}{2\pi}$ is chosen such that

$$\int_{-\infty}^{\infty} d\omega \rho(\mathbf{k},\omega) = 1. \tag{2.68}$$

This property is called the sum rule and is a direct result from elementary anti-commutation relations, i.e.

$$[\Psi_\alpha(\vec{x},t), \Psi^\dagger_{\alpha'}(\vec{x}',t)]_+ = \delta(\vec{x}-\vec{x}')\delta_{\alpha,\alpha'}, \tag{2.69}$$

where the α denotes the spin space and Ψ denotes fermionic single particle operators. It is important to stress that this sum rule only applies to retarded single-particle Green's functions. The beauty of the spectral function is that it is observable by Angle-Resolved Photoemission Spectroscopy (ARPES). The idea behind ARPES-experiments is that these experiments can probe spectral functions by firing photons with specific energy at a solid from different angles. Through the photoelectric effect the photons excite and sometimes kick out electrons. Of these electrons the energy and angle under which they leave the solid are measured. Using this information a profile of the dispersion relations can be obtained, which is also described by the spectral function.

The sum rule puts restrictions on the bulk mass M. When a propagator is analytic in the upper-half of the complex plane, it immediately implies,

$$\int_{-\infty}^{\infty} d\omega \mathrm{Tr}[G_R(\mathbf{k},\omega)] = 2\pi i, \tag{2.70}$$

by Cauchy's formula. It is the possible to close a contour in the upper half of the complex plane. For $z = 1$, it is shown that G_R is analytic in the upper-half of the complex plane if [8]

$$-\frac{1}{2} < M < \frac{1}{2}. \tag{2.71}$$

Hence the sum-rules also hold in this regime for M. For $z > 1$ we do not posses a generic analytic solution, as mentioned before, hence we have to check the sum rules numerically[12].

2.2.5 Spectral function

The spectral function we obtain from (2.66) is,

$$\rho(\mathbf{k},\omega) = -\frac{1}{2\pi}\mathrm{Im}\mathrm{Tr}[\frac{1}{\omega - \sigma^i \mathbf{k}_i |\mathbf{k}|^{z-1} - \Sigma(\mathbf{k},\omega)}]. \tag{2.72}$$

Using (2.59) for $z = 1$ and $T = 0$ we obtain,

$$\Sigma = \Sigma_\mu \sigma^\mu, \quad \Sigma_\mu = 2^{-2M}\frac{\Gamma(\frac{1}{2} - M)}{\Gamma(\frac{1}{2} + M)} e^{-i\pi(M+\frac{1}{2})}\mathbf{k}_\mu. \tag{2.73}$$

The function Σ_μ can be computed numerically for any value of z and T. We start by finding closed expressions for Σ_0 and Σ_3. Observe,

$$\begin{aligned}
\xi_\pm(k_3,\omega) &= \begin{pmatrix} \xi_+(k_3,\omega) & \\ & \xi_-(k_3,\omega) \end{pmatrix} = \begin{pmatrix} \xi_+(k_3,\omega) & \\ & \xi_+(-k_3,\omega) \end{pmatrix} \\
&= \begin{pmatrix} \frac{1}{2}(\xi_+(k_3,\omega) + \xi_+(-k_3,\omega)) & \\ \quad + \frac{1}{2}(\xi_+(k_3,\omega) - \xi_+(-k_3,\omega)) & \\ & \frac{1}{2}(\xi_+(k_3,\omega) + \xi_+(-k_3,\omega)) \\ & \quad - \frac{1}{2}(\xi_+(k_3,\omega) - \xi_+(-k_3,\omega)) \end{pmatrix} \\
&= \frac{1}{2}(\xi_+(k_3,\omega) + \xi_+(-k_3,\omega))\mathbb{1}_2 + \frac{1}{2}(\xi_+(k_3,\omega) - \xi_+(-k_3,\omega))\sigma_3 \\
&\sim \Sigma_0 \mathbb{1}_2 + \Sigma_3 \sigma_3.
\end{aligned} \tag{2.74}$$

Because we remain to have rotation symmetry we can therefore numerically obtain

$$\Sigma = \Sigma_\mu \sigma^\mu, \tag{2.75}$$

[12]This is where the exception of the restricted case $\mathbf{k} = 0$ should be noted. In this case $-\frac{z}{2} < M < \frac{z}{2}$. This result originates from the fact that the relation between the spinors A and B in (2.56) and the sub leading terms in the expansion, turn out to be different than when $\mathbf{k} \neq 0$.

for general $\mathbf{k}$, z and T. Take into account the following identity,

$$(a_\mu \sigma^\mu)(a_\nu \overline{\sigma}^\nu) = a^\mu a_\mu, \tag{2.76}$$

where a is some function. We conclude,

$$\boxed{\rho(\mathbf{k},\omega) = -\frac{1}{\pi}\mathrm{Im}[\frac{\omega + \Sigma_0}{(\omega+\Sigma_0)^2 - (\mathbf{k}_i|\mathbf{k}|^{z-1} + \Sigma_i)^2}]} \tag{2.77}$$

We have now reproduced the results of [8, 9].

2.3 Two chiral spinors make a Dirac spinor

We are interested in systems governed by a Dirac spinor rather than a chiral spinor. In this section a chiral spinor with opposite chirality is added to the boundary in addition to the one already developed. This is done by introducing another bulk field. For the second fermion we integrate out the opposite chiral spinor, Ψ_+ instead of Ψ_-. We now obtain two chiral spinors on the boundary. It possible to construct a Dirac fermion when the second bulk mass M_2 is tuned right. This enables us to create dispersion relations as in Figure 2.2.

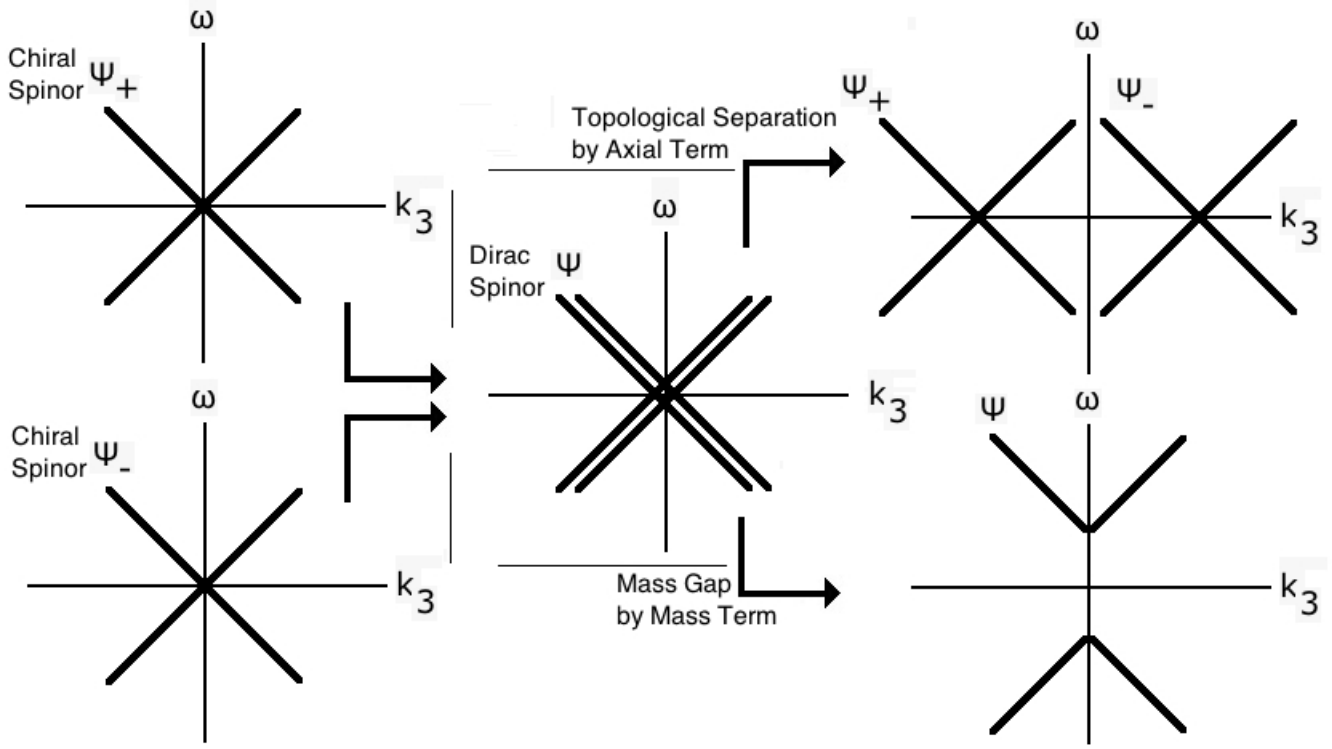

Figure 2.2: This Figure shows the dispersion relations of chiral spinors and Dirac spinors. It moreover sketches how we construct a Dirac spinor by combining two chiral spinors. An outlook to extensions of the model is also presented. In the chapters 2 and 3 we focus on the mass gap case. In chapter 4 and 5 we consider the topological separation case.

2.3.1 Adding another chiral spinor

We introduce an additional fermionic field to the bulk theory. We denote this field by Ψ_2. The bulk fermion Ψ_2 has bulk mass M_2. The goal is to integrate out $\Psi_{2,+}$, while keeping $\Psi_{2,-}$ on the boundary. We denote the original chiral spinor by $\Psi_{1,+}$. We apply the same steps as done for $\Psi_{1,+}$ but now the goal is to obtain $\delta\Psi_{2,-}=0$. We get,

$$S_{2,\partial}=-ig_f\int_{r=r_0}d^4x\sqrt{-h}\sqrt{g^{rr}}\overline{\Psi}_{2,L}\Psi_{2,R},\quad S_{2,0}=-iZ\int_{r=r0}d^4x\sqrt{-h}\overline{\Psi}_{2,L}\gamma^{\underline{a}}e^{\mu}_{\underline{a}}D_\mu\Psi_{2,L}. \tag{2.78}$$

The next step is inverting

$$\Psi_{2,-}=-i\xi_2\Psi_{2,+},\quad\Rightarrow\quad\Psi_{2,+}=i\xi_2^{-1}\Psi_{2,-}. \tag{2.79}$$

When adding the boundary term of the $\Psi_{1,+}$ case and the $\Psi_{2,-}$ we obtain

$$\begin{aligned}S_{1,\partial}+S_{2,\partial}=&-ig_f\int_{r=r_0}d^4x[\Psi_{1,+}(-i\xi_1)\Psi_+ +\Psi^\dagger_{2,-}(i\xi_2^{-1})\Psi_{2,-}]\\ =&-g_f\int_{r=r_0}d^4x\begin{pmatrix}\Psi_{1,+}\\ \Psi_{2,-}\end{pmatrix}^\dagger\begin{pmatrix}\xi_1 & \\ & -\xi_2^{-1}\end{pmatrix}\begin{pmatrix}\Psi_{1,+}\\ \Psi_{2,-}\end{pmatrix}\\ =&+g_f\int_{r=r_0}d^4x\begin{pmatrix}\Psi_{1,+}\\ \Psi_{2,-}\end{pmatrix}^\dagger\gamma^0\begin{pmatrix} & \xi_2^{-1}\\ \xi_1 & \end{pmatrix}\begin{pmatrix}\Psi_{1,+}\\ \Psi_{2,-}\end{pmatrix}\\ =&g_f\int_{r=r_0}d^4x\overline{\Psi}\xi\Psi,\end{aligned} \tag{2.80}$$

where

$$\Psi:=\begin{pmatrix}\Psi_{1,+}\\ \Psi_{2,-}\end{pmatrix},\quad\xi:=\begin{pmatrix} & \xi_2^{-1}\\ \xi_1 & \end{pmatrix}. \tag{2.81}$$

Here ξ is represented by a 4×4 matrix and Ψ is a Dirac spinor on the boundary. For the special value of $M_2=-M_1$ the symmetry of (2.55) implies $\xi_2^{-1}(k_3,\omega)=-\xi_1(-k_3,\omega)$, which has the consequence,

$$\begin{aligned}\xi=&\begin{pmatrix} & -\xi_1(-k_3,\omega)\\ \xi_1(k_3,\omega) & \end{pmatrix}\\ =&\begin{pmatrix} & & -\xi_+(-k_3,\omega) & \\ & & & -\xi_-(-k_3,\omega)\\ \xi_+(k_3,\omega) & & & \\ & \xi_-(-k_3,\omega) & & \end{pmatrix},\end{aligned} \tag{2.82}$$

using the chiral symmetry from (2.55) in the next step we continue,

$$\begin{aligned}=&\begin{pmatrix} & & -\xi_+(-k_3,\omega) & \\ & & & -\xi_+(k_3,\omega)\\ \xi_+(k_3,\omega) & & & \\ & \xi_+(-k_3,\omega) & & \end{pmatrix}\\ =&\begin{pmatrix} & & -\xi_S(k_3,\omega)+\xi_A(k_3,\omega) & \\ & & & -\xi_S(k_3,\omega)-\xi_A(k_3,\omega)\\ \xi_S(k_3,\omega)+\xi_A(k_3,\omega) & & & \\ & \xi_S(k_3,\omega)-\xi_A(k_3,\omega) & & \end{pmatrix}\\ =&\xi_S(k_3,\omega)\gamma^0+\xi_A(k_3,\omega)\gamma^3,\end{aligned} \tag{2.83}$$

where $\xi_S(k_3,\omega) := \frac{1}{2}(\xi_+(k_3,\omega) - \xi_+(-k_3,\omega))$ and $\xi_A(k_3,\omega) := \frac{1}{2}(\xi_+(k_3,\omega) + \xi_+(-k_3,\omega))$. Here the subscript A denotes anti-symmetry in ω and S denotes symmetry in ω. This can easily be understood using (2.54). In analogy with the rotation in spatial momentum in (2.59) and (2.74), we rotate the now explicitly in k_3 expressed ξ to a general expression,

$$\xi(\mathbf{k},\omega) = \xi_\mu(\mathbf{k},\omega)\gamma^\mu, \tag{2.84}$$

where ξ_μ is some function that can be calculated numerically. This is possible due to the conserved rotational symmetry of the momentum.

The total effective action obtained in the case of two spinors is,

$$\begin{aligned} S_{\text{eff}} =& S_{1,\partial} + S_{2,\partial} + S_{1,0} + S_{2,0} \\ =& \int_{r=r_0} \frac{d^4k}{(2\pi)^4}\sqrt{-h}\overline{\Psi}(\mathbf{k},\omega)[Z\gamma^{\underline{a}}e^{\mu}_{\underline{a}}\mathbf{k}_\mu - g_f\sqrt{g^{rr}}\xi(\mathbf{k},\omega)]\Psi(\mathbf{k},\omega), \end{aligned} \tag{2.85}$$

where the integral is transformed to momentum space. As a check of consistency it is obtained that when $\Psi_{2,-} \to 0$, the action in (2.60) is recovered.

In the next few lines we first normalize (2.85) and then renormalize the action. This happens in analogy to the single chiral case. For a canonical normalization, we perform $\Psi \to Z^{-1/2}r_0^{-3/2}$ to (2.85),

$$S_{\text{eff}} = \int \frac{d^4k}{(2\pi)^4}\overline{\Psi}(\mathbf{k},\omega)[V(r_0)(\gamma^0\omega - r_0^{z-1}\gamma^i\mathbf{k}_i) + \frac{g_f}{Z}r_0^{1+z}V^2(r_0)\xi(\mathbf{k},\omega)]\Psi(\mathbf{k},\omega). \tag{2.86}$$

Now we start regularizing the terms, one by one. We start with the term containing ξ. Because of the choice that $M_2 = -M_1$, it concluded that $\xi(r_0) \sim r_0^{-2M}$ as $r_0 \to \infty$. Defining

$$\Sigma(\mathbf{k},\omega) := -g\lim_{r_0\to\infty} r_0^{2M}\xi(r_0,\mathbf{k},\omega), \tag{2.87}$$

and demanding the same double scaling scheme as in (2.62), where $g > 0$, we make sure that the term consisting of ξ is well-defined on the boundary. The dynamical term, which needs renormalization for $z > 1$, is renormalized in the same fashion as done for (2.64),

$$\gamma^0\omega - r_0^{z-1}\gamma^i\mathbf{k}_i \to \gamma^0\omega - \frac{1}{\lambda}\gamma^i\mathbf{k}_i|\mathbf{k}|^{z-1}. \tag{2.88}$$

Thus when $r_0 \to \infty$ we obtain

$$S_{\text{eff}} = \int \frac{dk^4}{(2\pi)^4}\Psi^\dagger\gamma^0[\gamma^0\omega - \frac{1}{\lambda}\gamma^i\mathbf{k}_i|\mathbf{k}|^{z-1} - \Sigma(\mathbf{k},\omega)]\Psi, \tag{2.89}$$

where we continue to take $\lambda = 1$. When letting $\xi_{2,-} \to 0$, we obtain the regular action for Ψ_+, (2.65). We will use the following identity,

$$\gamma^0(a\gamma^0 - b_i\gamma^i)(a\gamma^0 - b_i\gamma^i)\gamma^0 = -(a^2 - b_i^2), \tag{2.90}$$

where the coefficients denote arbitrary functions. The function Σ_μ is still numerical obtainable using (2.74), (2.83) and (2.84). We establish,

$$\Sigma = \Sigma_\mu\gamma^\mu, \tag{2.91}$$

where for zero temperature $T = 0$ and $z = 1$ we still have in analogy to (2.73),

$$\Sigma_\mu = 2^{-2M}\frac{\Gamma(\frac{1}{2}-M)}{\Gamma(\frac{1}{2}+M)}e^{-i\pi(M+\frac{1}{2})}\mathbf{k}_\mu. \tag{2.92}$$

It is concluded that for (2.89) using (2.90),

$$G_R = -\frac{(\omega+\Sigma_0)\mathbb{1}_4 - (\mathbf{k}_i+\Sigma_i)\gamma^i\gamma^0}{(\omega+\Sigma_0)^2 - (\mathbf{k}_i|\mathbf{k}|^{z-1}+\Sigma_i)^2}. \tag{2.93}$$

Using equation (2.67), but now times an extra factor $\frac{1}{2}$ because our matrix is now 4×4 instead of 2×2, the corresponding spectral function is,

$$\boxed{\rho(\mathbf{k},\omega) = -\frac{1}{\pi}\mathrm{Im}\left[\frac{\omega+\Sigma_0}{(\omega+\Sigma_0)^2 - (\mathbf{k}_i|\mathbf{k}|^{z-1}+\Sigma_i)^2}\right]} \tag{2.94}$$

Some plots of spectral functions (2.94) are presented in Figure 2.3. Because we have rotational symmetry for the momentum we choose the total momentum to be in one direction when making the plots.

2.4 Massive Dirac spinor

When adding a mass term on the boundary which couples the different chiralities we obtain a mass gap. We are interested in inducing a mass gap in a system because this is a start towards describing atoms at unitarity, for instance.

2.4.1 Gaining mass

Before any renormalization has been done we add the following term to the cut-off surface,

$$S_m = Z\int_{r=r_0} d^4x\sqrt{-h}\overline{\Psi}[-i\tilde{m}]\Psi. \tag{2.95}$$

It is clear that,

$$\begin{aligned}\delta S_m \sim&\delta(\Psi^\dagger_{2,-}\Psi_+ - \Psi^\dagger_+\Psi_{2,-})\\ =&\Psi^\dagger_{2,-}\delta\Psi_+ + \delta(\Psi^\dagger_{2,-})\Psi_+ - \Psi^\dagger_+\delta\Psi_{2,-} - \delta(\Psi^\dagger_+)\Psi_{2,-}\\ =&0,\end{aligned} \tag{2.96}$$

which means that this term does not obstruct the bulk, hence it can be freely added. The canonical normalization, $\Psi \to Z^{-1/2}r_0^{3/2}$, implies that

$$S_m = Z\int\frac{d^4k}{(2\pi)^4}\overline{\Psi}[-V(r_0)r_0^z i\tilde{m}]\Psi. \tag{2.97}$$

Now define

$$m := \tilde{m}r^z, \tag{2.98}$$

such that in some double scaling limit of $r_0 \to \infty$, m becomes a positive constant. This term behaves well on the boundary, thus taking $r_0 \to \infty$ delivers,

$$\begin{aligned} S_m &= \int \frac{d^4k}{(2\pi)^4} \Psi^\dagger \gamma^0 [-im\mathbb{1}_4]\Psi, \\ \Rightarrow \quad S_{\text{eff}} &= \int \frac{d^4k}{(2\pi)^4} \Psi^\dagger \gamma^0 [\gamma^0\omega - \frac{1}{\lambda}\gamma^i \mathbf{k}_i |\mathbf{k}|^{z-1} - \Sigma(\mathbf{k},\omega) - im\mathbb{1}_4]\Psi. \end{aligned} \tag{2.99}$$

Take into account,

$$\gamma^0((a\gamma^0 - b_i\gamma^i) - c\mathbb{1}_4)((a\gamma^0 - b_i\gamma^i) + c\mathbb{1}_4)\gamma^0 = (a^2 - b^2 + c^2), \tag{2.100}$$

where a, b_i and c are complex functions. The retarded propagator corresponding to (2.99) obtained using (2.100) is,

$$G_R = -\frac{(\omega + \Sigma_0)\mathbb{1}_4 + (\mathbf{k}_i|\mathbf{k}|^{z-1} + \Sigma_i)\gamma^i\gamma^0 + im\gamma^0}{(\omega + \Sigma_0)^2 - (\mathbf{k}_i|\mathbf{k}|^{z-1} + \Sigma_i)^2 - m^2}. \tag{2.101}$$

Using equation (2.67), times an extra factor $\frac{1}{2}$ since our matrix is now 4×4 instead of 2×2, the corresponding spectral function is,

$$\boxed{\rho(\mathbf{k},\omega) = -\frac{1}{\pi}\text{Im}\left[\frac{\omega + \Sigma_0}{(\omega + \Sigma_0)^2 - (\mathbf{k}_i|\mathbf{k}|^{z-1} + \Sigma_i)^2 - m^2}\right]} \tag{2.102}$$

With a vanishing mass m, (2.94) is restored. See Figure 2.4 for plots of $z = 1$. For plots with $z = 2$ see Figure 2.5. Comparing the different dynamical exponents we clearly observe the differences in scaling of the spectral functions arise.

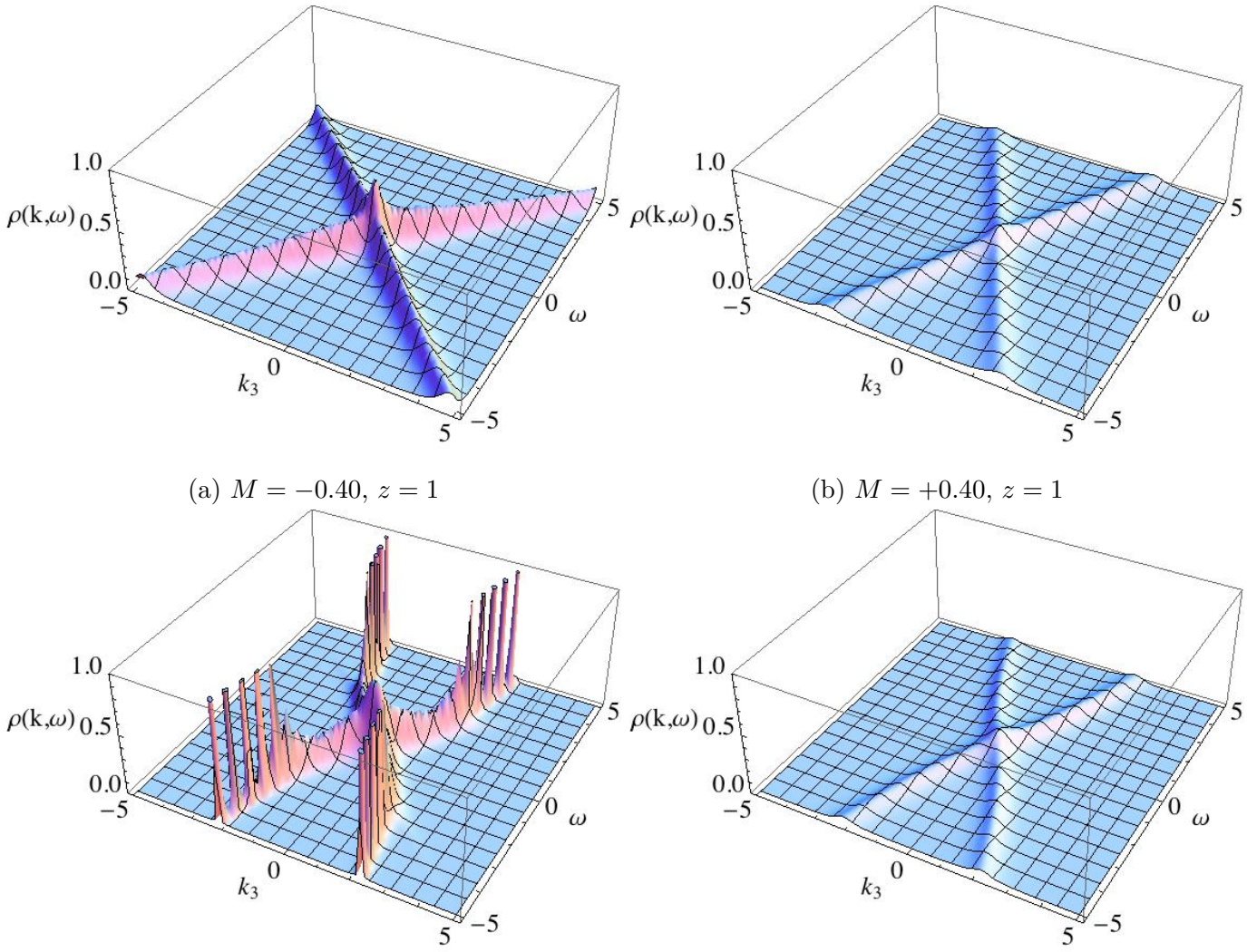

(a) $M = -0.40$, $z = 1$

(b) $M = +0.40$, $z = 1$

(c) $M = -0.40$, $z = 2$

(d) $M = +0.40$, $z = 2$

Figure 2.3: The plots correspond to the spectral function (2.94). When only taking into account the k_3 and ω axes we obtain the dispersion relations. The width of peaks at fixed momentum carries information about the possible existence of quasi-particles. The broader these peaks are, the less well-defined the quasi-particles are because their lifetime becomes shorter. The height of the graph is related to the distribution of the fermions. The spikes in (c) are due to the numerics. The spikes should be a smooth surface. All plots are obtained for $T = 1$. The larger T, the broader the peaks at fixed momentum become [9]. Moreover we put $g = 1$ from now on. The effect of increasing or decreasing g does not change any qualitative properties.

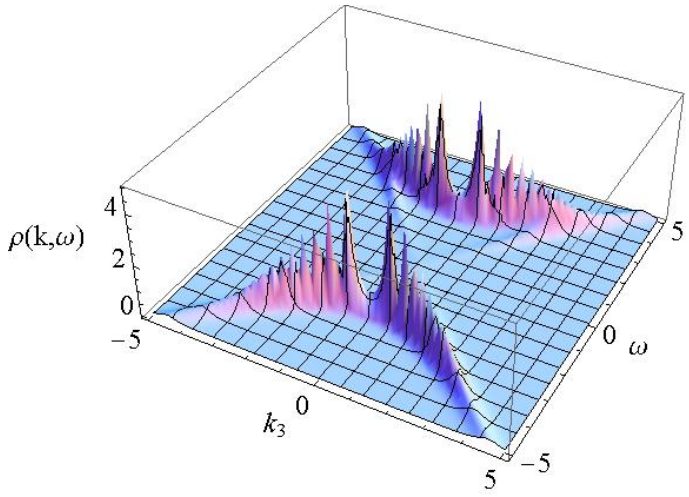

(a) $M = -0.40$, $z = 1$

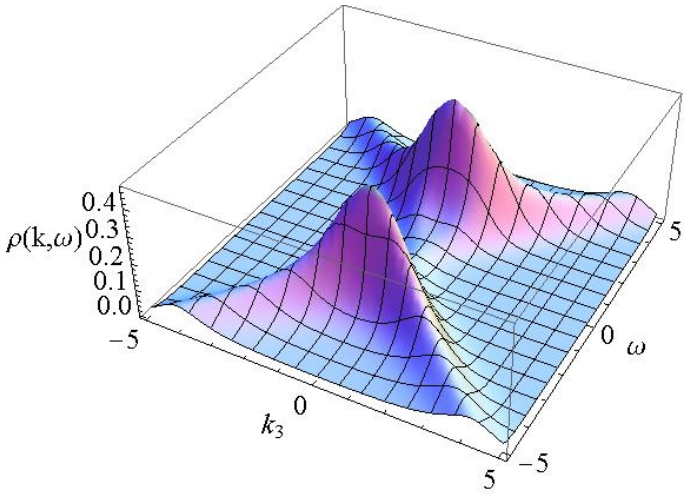

(b) $M = -0.20$, $z = 1$

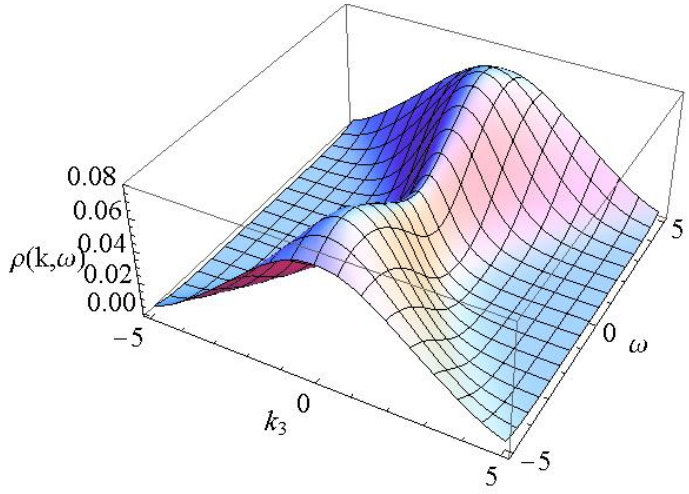

(c) $M = +0.20$, $z = 1$

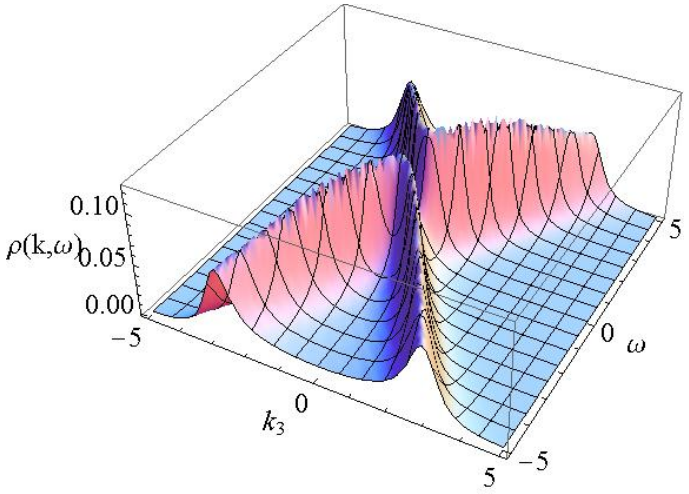

(d) $M = +0.40$, $z = 1$

Figure 2.4: The spectral functions for (2.102) are plotted for $m = 2$ and $T = 1$. Notice that there remain some non-vanishing contributions near origin. We chose different ranges for the z-axes because we are interested in the qualitative behavior. For non-zero m the correct dynamical exponent z is recovered at high energies. We observe that for low energy the spectral function does not correspond to the implied scaling by the dynamical exponent z. Moreover it is observed that for negative M the distribution seems to be pushed away from the origin in contrast to the case for positive M, where the distribution seems to be pulled towards the origin. These effects are all manifestations of the self-energy. The spikes in (a) are due to numerics. It should represent a smooth arc with a bump in the middle.

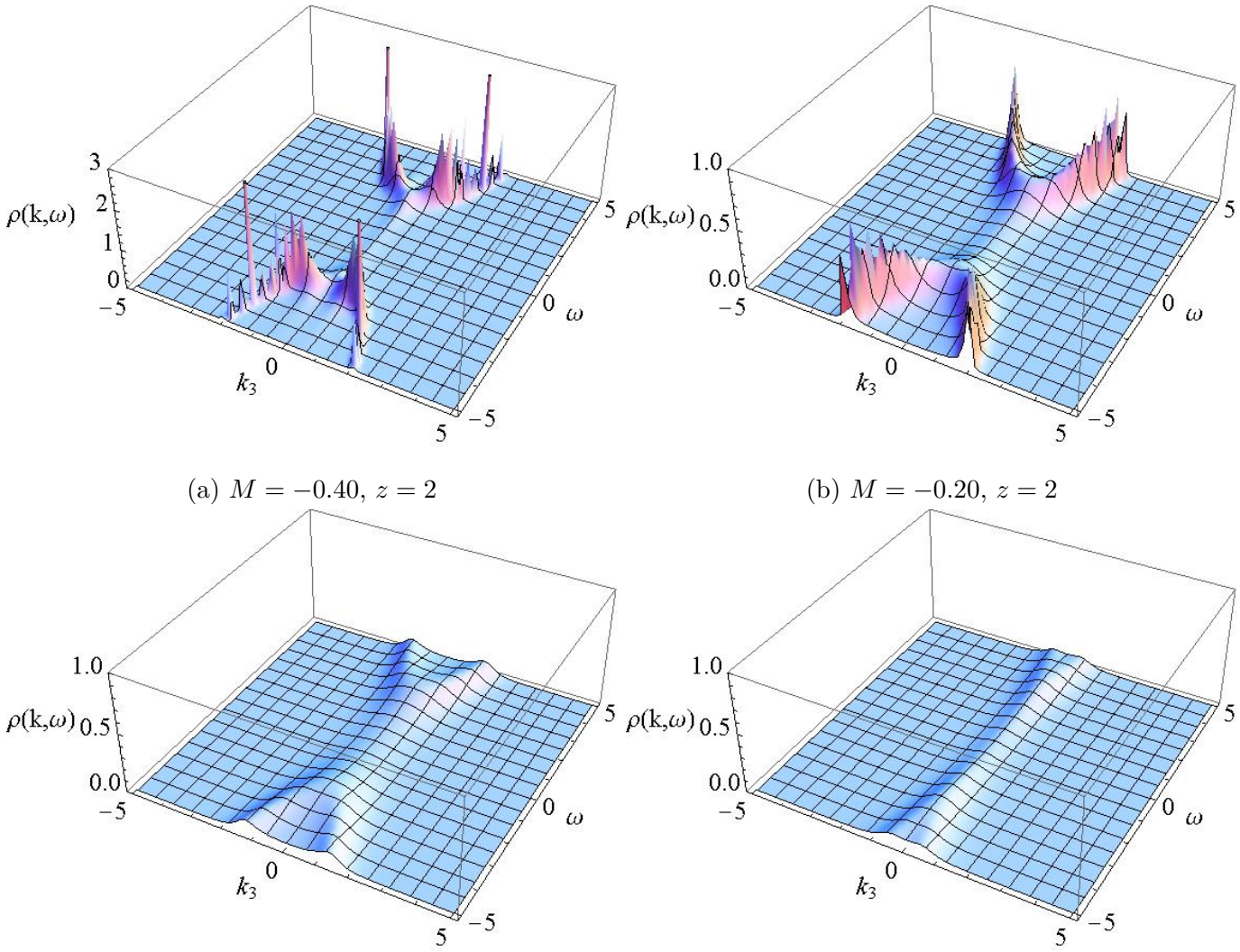

(a) $M = -0.40$, $z = 2$

(b) $M = -0.20$, $z = 2$

(c) $M = +0.20$, $z = 2$

(d) $M = +0.40$, $z = 2$

Figure 2.5: The spectral functions for (2.102) are plotted. We take $m = 2$ and $T = 1$. We observe the same behavior as discussed in Figure(2.4).

Chapter 3

Doping Fermion Holography

Now that certain dispersion relations emerge on the boundary, the next step is identifying a way to add a chemical potential μ.

When the entropy and volume of a system are fixed in thermodynamics, we define

$$\mu := \frac{dU}{dN}, \tag{3.1}$$

where U is the internal energy of the system and N the number of particles. Therefore we can say that the chemical potential μ is the amount of energy needed when adding a particle to a system. Hence adding a finite chemical potential breaks particle-hole symmetry. When considering fermions, the higher the value of μ the bigger the Fermi-sea gets.

In general non-interacting dispersion relations are characterized by,

$$\omega = \epsilon_{\mathbf{k}} - \mu, \tag{3.2}$$

where $\epsilon_{\mathbf{k}}$ is the energy of some quasi-particle, for instance. The boundary systems considered until now are identified with system at $\mu = 0$. Hence we have dispersion relations characterized by

$$\omega = \epsilon_{\mathbf{k}}. \tag{3.3}$$

This motivates for searching for a transformation such that

$$\begin{aligned} &\omega = \epsilon_{\mathbf{k}}, \\ &\omega \to \omega + \mu, \end{aligned} \quad \Rightarrow \quad \omega = \epsilon_{\mathbf{k}} - \mu. \tag{3.4}$$

The way to obtain such a relation sounds less obvious than it turns out to be. Namely, to introduce a chemical potential on the boundary, the black brane in the bulk should be charged electrically with some charge Q_B. Once the brane is charged with charge Q_B we charge the fermions in the bulk with q_f. The covariant derivative obtains a minimal coupling term. The fields couple. Thus,

$$D_\nu \to D_\nu - iq_f A_\nu, \tag{3.5}$$

where A_ν denotes the electric potential for $\nu = 0$, for which the strength depends on Q_B. Concentrating on the electric field, we choose $A_i = 0$. Transform (3.5) to momentum space we get,

$$\begin{aligned} &\mathbf{k} \to \mathbf{k} \\ &\omega \to \omega + q_f A_0. \end{aligned} \tag{3.6}$$

The obtained equation in the bulk has the desired structure, since a shift in ω occurs. The last step remaining is identifying μ on the boundary as

$$\mu := \lim_{r_0 \to \infty} q_f A_0(r_0). \tag{3.7}$$

In the first section of this chapter the matter fields in the bulk are "updated" such that they are able to hatch a charged black brane solution. Furthermore quantities relevant to the boundary theory are identified.

In the second section the self-energy Σ is reevaluated, in the presence of the charged black brane. The spectral functions of the massive boundary theory are obtained including doping. Corresponding plots are presented and analyzed.

3.1 Charging a black brane

3.1.1 Adding charged matter

Recall the example of a charged Reissner-Nordström black hole, initiated on page 9. There it is established that the metric tensor of the Schwarzschild black hole and the Reissner-Nordström black hole are geometrically the same and only differ in the emblackening factor V. Moreover, the emblackening factor V, which in the case of Reissner-Nordström depends on charge Q and radius r, coincides with the emblackening factor of the Schwarzschild black hole when $Q \to 0$.

The same as mentioned for the black hole case can be done by altering the matter term $\mathcal{L}_M$ in (2.14), such that the geometry of the metric tensor as formulated in (2.15) is obtained, with a slight alteration of the emblackening factor V. Hence,

$$ds^2 = \frac{1}{rV^2(r,Q_B)}dr^2 - V^2(r,Q_B)r^{2z}dt^2 + r^2 d\vec{x}^2_{D-1}, \tag{3.8}$$

where $V(r,Q_B)$ explicitly depends on the total charge Q_B of the black brane. The emblackening factor $V(r,Q_B)$ should be constructed such that $\lim_{Q_B\to 0} V(r,Q_B) \to V(r)$, where $V(r)$ denotes the emblackening factor of the uncharged black brane. This construction secures the asymptotic behavior of the metric tensor.

The following setup solves the problem of finding a charged Lifshitz black brane metric tensor [6] and satisfies the equations of motion generated by the matter fields,

$$\begin{aligned}
\mathcal{L}_M =& \frac{1}{16\pi G_{D+1}}[-\frac{1}{2}(\partial\phi)^2 - \frac{1}{4}e^{\lambda_1}(F_1)^2 - \frac{1}{4}e^{\lambda_2}(F_2)^2], \quad \Lambda = -\frac{(D+z-1)(D+z-2)}{\ell^2}, \\
e^{\lambda_1\phi} =& \ell^{-2z}2(z-1)(z+D-1)\frac{1}{f^2}r^{2(1-D)}, \quad (F_1)_{rt} = f r^{z+D-2}, \\
(F_2)_{rt} =& \rho_2\left[\frac{1}{2(D+z-1)(z-1)}\ell^{2z}f^2\right]^{\frac{\lambda_2}{\lambda_1}} r^{-(z+D-2)}, \quad \lambda_1 = -\sqrt{2\frac{D-1}{z-1}}, \quad \lambda_2 = \sqrt{2\frac{z-1}{D-1}}.
\end{aligned} \tag{3.9}$$

Here f is some free parameter and ρ_2 is related to the total charge on the brane. The ρ_2 should be thought of as a charge density of the brane. Notice that we restored the Lifshitz radius ℓ. Before discussing this solution further, the resulting emblackening factor is presented,

$$V^2(r,\rho_2) = 1 - r_m r^{1-D-z} + \rho_2^2\left[\frac{1}{2(D+z-1)(z-1)}\ell^{2z}f^2\right]^{\frac{\lambda_2}{\lambda_1}} \frac{\ell^{2z}}{2(D-1)(D+z-3)} r^{-2(z+D-2)}, \tag{3.10}$$

where r_m is an integration constant. Before analyzing and discussing this emblackening factor, we will first simplify this function in the next subsection.

The equations in (3.9) and (3.10) solve the problem of finding a charged Lifshitz black brane. Notice that $\mathcal{L}_M$ in (3.9) only has one extra term with respect to (2.14). This term is $e^{\lambda_2\phi}F_2^2$, where F_2 is a anti-symmetric two-tensor and ϕ is a dilaton scalar field. This extra term is analogous to the Maxwell term, F^2, added in the Reissner-Nordström black hole action. The added term induces charge on the brane. The dilaton is present to generalize the relativistic $z = 1$ case to arbitrary $z \geq 1$.

It is immediately clear from (3.9) that this extra term does not have divergent properties on the boundary for any z. This is important because in contrast to the other field F_1, the field F_2 does couple to the fermions.

Recall from the uncharged black brane (page 11) that when $z \to 1$ we obtain $e^{\lambda_1\phi} \to 0$ and thus the extra fields decouple. The coupling with the F_2 field does not vanish at $z \to 1$ but becomes a non-zero constant,

$$e^{\lambda_2\phi} = (e^{\lambda_1\phi})^{\frac{\lambda_2}{\lambda_1}} = (e^{\lambda_1\phi})^{-2\frac{z-1}{D-1}} \to \text{constant}. \tag{3.11}$$

When $z \to 1$ it is also noted that,

$$(F_2)_{rt} \sim \rho_2 r^{-(D-1)}, \tag{3.12}$$

which exhibits the proper radial scaling behavior of an electric field in $D+1$ dimensions[1]. By integration of $(F_2)_{rt} = \partial_r A_{2,t}$ we find

$$A_{2,t} = -\rho_2 \left[\frac{1}{2(d+z-1)(z-1)}\ell^{2z}f^2\right]^{\frac{\lambda_2}{\lambda_1}} \frac{1}{d+z-3}(r^{3-d-z} - r_h^{3-d-z}), \tag{3.13}$$

where the integration constant is fixed such that $A_{2,t}$ vanishes at r_h, the horizon of the black brane.

3.1.2 A matter of units

The present goal is to identify the quantities which lead to non-zero chemical potential on the boundary and to simplify emblackening factor V. To identify quantities natural constants have to be reinserted to identify the correct quantities. The first issue raised is that the Maxwell term F_2^2 in $\mathcal{L}_M$ in (3.9) has the gravitational Newton's constant G_{D+1}, rather than μ_0, the permittivity of the vacuum. This choice of constants is possible due to the fact that both classical electric and gravity forces are described by solving Poisson's equation. Both G_{D+1} and μ_0 are defined via these equations. We choose $D = 4$ and let $\hat{m}$ be a mass such that

$$G_5\frac{\hat{m}^2}{r^3} = F_z = F_E = \frac{1}{16\pi\epsilon_0}\frac{e^2}{r^3} = c^2\frac{\mu_0}{16\pi}\frac{e^2}{r^3}, \quad \Rightarrow \quad \frac{1}{G_5} = 16\pi\frac{\hat{m}^2}{e^2c^2}\frac{1}{\mu_0}, \tag{3.14}$$

where e is the elementary charge. We now know how G_5 is related to μ_0. Restoring c in the following term of the action reveals

$$\overbrace{\int d^{4+1}x \frac{c^3}{16\pi G_5}\frac{F^2}{4}}^{=\text{ dimension of }\hbar} = \overbrace{\int d^{4+1}x \underbrace{\frac{1}{16\pi}\frac{1}{G_5}\frac{e^2c^2}{\hat{m}^2c}}_{=\frac{1}{\mu_0 c}}\underbrace{\frac{1}{4}(\frac{\hat{m}c}{e}F)^2}_{=\frac{1}{4}(F^{SI})^2}}^{=\text{ dimension of }\hbar}, \quad \Rightarrow \quad F_{rt} = \frac{e}{c\hat{m}}F_{rt}^{SI}, \quad A_t = \frac{e}{c\hat{m}}A_t^{SI}, \tag{3.15}$$

[1] As a check, remember that in D+1=4, the regular case, $F \sim E \sim r^{-2}$ is the normal radial dependence of electromagnetism.

where with the superscripted SI quantities of regular (SI-)units are denoted. Hence we have a conversion factor for the electric field. We calculate the total charge on the brane Q_2 by calculating the conserved current of F_2,[2]

$$Q_2 = V_{D-1}\frac{1}{16\pi G_5}\rho_2\ell^{z-1} = \overbrace{\underbrace{\frac{1}{16\pi G_5}\left(\frac{e}{\hat{m}}\right)^2}_{=\epsilon_0}\underbrace{c^2\frac{\hat{m}}{e}\rho_2 r^{-(D-z)}e^{-\lambda_2\phi}}_{=[E^{SI}]}\underbrace{r^{D-z}e^{\lambda_2\phi}\ell^{z-1}V_{D-1}}_{=[L^{D-1}]=[S_D]}}^{=[Q^{SI}]}\times\frac{\hat{m}}{e}\frac{1}{c^2}, \tag{3.16}$$

where V_n is a dimensionless volume factor. By identification of Gauss' law in the last line above, we may conclude that

$$Qc^2\frac{e}{\hat{m}} = Q^{SI}. \tag{3.17}$$

Now define $Q_f^{SI} := \hat{q}_f e$, where e denotes the elementary charge of an electron such that $\hat{q}_f$ is dimensionless. Fermions with charge on the boundary coupled to the electric field of the black brane through minimal coupling implies,

$$\hbar D_t = \hbar\partial_t - icQ_f^{SI}A_{2,t}^{SI}, \tag{3.18}$$

therefore,

$$\mu := c(\hat{q}_f e)A^{SI}(\infty) = c^2\hat{m}\hat{q}_f\rho_2\frac{1}{D+z-3}r_h^{3-D-z}\left[\frac{1}{2(D+z-1)(z-1)}\ell^{2z}f^2\right]^{\frac{\lambda_2}{\lambda_1}}. \tag{3.19}$$

In contrary to the other quantities we defined,

$$\mu = \mu^{SI}, \tag{3.20}$$

which denotes that μ is expressed in SI units. In addition we can also express ρ_2 in terms of the total charge on the brane. Using (3.16), (3.17) and $\hat{Q}_B e = Q_2^{SI}$, such that $\hat{Q}_B$ is dimensionless we find,

$$\rho_2 = \frac{16\pi}{V_{D-1}}G_5\ell^{1-z}Q_2 = \frac{16\pi}{V_{D-1}}G_5\ell^{1-z}\frac{\hat{m}}{c^2}\hat{Q}_B. \tag{3.21}$$

Define the following dimensionless rescaling factors,

$$\begin{aligned} q_f &= \hat{q}_f\overbrace{\left[\left(\frac{f\ell^{z+D-1}}{\sqrt{2(D+z-1)(z-1)}}\right)^{\frac{\lambda_2}{\lambda_1}}\frac{16\pi}{V_{D-1}}\sqrt{\frac{1}{2(D-1)(D+z-3)}}\frac{\hat{m}G_5\ell^{2-D}}{c^2}\right]}^{\text{dimensionless}}\overbrace{\left[\frac{c^4}{G_5}\ell^{D-2}\frac{1}{\frac{\hbar c}{\ell}}\right]}^{\text{dimensionless}}\left(\frac{V_{D-1}}{16\pi}2(D-1)\right) \\ Q_B &= \hat{Q}_B\underbrace{\left[\left(\frac{f\ell^{z+D-1}}{\sqrt{2(D+z-1)(z-1)}}\right)^{\frac{\lambda_2}{\lambda_1}}\frac{16\pi}{V_{D-1}}\sqrt{\frac{1}{2(D-1)(D+z-3)}}\frac{\hat{m}G_5\ell^{2-D}}{c^2}\right]}_{\text{dimensionless}}. \end{aligned} \tag{3.22}$$

[2]In the case of Reissner-Nordström the total charge Q' that is calculated via (3.16) naturally coincides with the Q in the Maxwell field F, $Q' = Q$. We formulated the charge on the brane in terms of some charge density, hence we still have to do this step to calculate the total charge.

It is important to highlight that both rescaling factors depend on f the same way and moreover it turns out that this rescaling completely removes f from all expressions on the boundary. Introduce another rescaling,

$$r \to r\ell, \quad r_h \to r_h\ell, \tag{3.23}$$

such that r and r_h are dimensionless. This is convenient when checking whether quantities have the right dimensions. Using the rescaling factors it is obtained that

$$\mu = \frac{\hbar c}{\ell} Q_B q_f r_h^{3-D-z}, \tag{3.24}$$

and

$$V^2 = 1 - \left(\frac{r_m}{r}\right)^{D+z-1} + Q_B^2 \left(\frac{1}{r}\right)^{2(D+z-2)}, \tag{3.25}$$

where r_m is a dimensionless integration constant. This emblackening factor, in contrast to the uncharged emblackening factor, has more than one solutions for the r_h and moreover it is not solvable analytically for $D = 4$ and non-trivial values of r_m.

The temperature is obtained using the formula for temperature (2.17), but this time with restored units,

$$T = \frac{\hbar c}{k_B} \frac{1}{4\pi\ell} r_h^{z+1} \partial_r V^2 \Big|_{r=r_h}, \tag{3.26}$$

where k_B is Boltzmann's constant. Hence

$$T = \frac{\hbar c}{k_B} \frac{1}{4\pi\ell} r_h^z \left[(D+z-1) - (D+z-3) Q_B^2 r_h^{-2(D+z-2)}\right], \tag{3.27}$$

where r_m was eliminated using $V(r_h) = 0$,

$$r_m^{D+z-1} = r_h^{D+z-1} \left[1 + Q_B^2 r_h^{-2(D+z-2)}\right]. \tag{3.28}$$

A sign of warning has to be given for the case that T vanishes. When this happens, it can occur that $V'(r)|_{r=r_h} = 0$, although r_h is not zero. If that happens the black brane is extremal, i.e. has a double zero at the horizon. This has the result that when $T = 0$, the entropy S which is proportional to the area of the black brane [5] is non-zero. This might be a point of caution when matching this model to a real physical system.

Putting together (3.17), (3.18) and (3.19) we find,

$$A_{2,t}(r) = A_{2,t}(\infty)\left[1 - \left(\frac{r}{r_h}\right)^{3-D-z}\right] \Rightarrow \quad \hbar D_t = \hbar\partial_t - i\mu\left[1 - \left(\frac{r}{r_h}\right)^{3-D-z}\right] \tag{3.29}$$

Looking at (3.25) and (3.24) we see that q_f and Q_B are the only remaining extra parameters when going from a neutral black brane to a charged black brane. Notice that $Q_B \to -Q_B$ if and only if $q_f \to -q_f$. This is a symmetry of the system.

3.2 The doped boundary action

3.2.1 Self-energy revisited

The self-energy, which depends on ξ, changes due to the addition of a non-zero chemical potential. Looking back at how (2.51) is derived we see that only two changes matter. Firstly the fact that the

emblackening factor V now is more complex. This does not effect the derivation but only the solution to the differential equation changes. The second change is the fact that the covariant derivative picks up an extra term,

$$\not{D} = \gamma^{\underline{a}} e^{\mu}_{\underline{a}} D_\mu = \Gamma^{\underline{a}} e^{\mu}_{\underline{a}} (\partial_\mu - iq_f A_{2,\mu} + \frac{1}{4}\Omega_{\mu \underline{ab}} \Gamma^{\underline{ab}}). \tag{3.30}$$

This last term only shifts the value of ω which again only changes the final differential equation. This induces a redefinition of $\tilde{\omega}$. Hence, using (3.28),

$$r^2 V \partial_r \xi_\pm + 2Mr\xi_\pm = -\tilde{\omega} \mp k_3 + (-\tilde{\omega} \pm k_3)\xi_\pm^2, \quad \tilde{\omega} = -\frac{\hbar\omega + \mu(1 - (r/r_h)^{3-D-z})}{r^{z-1}V} \frac{\ell}{\hbar c}. \tag{3.31}$$

This equation summarizes that the only changes are a redefinition of $\tilde{\omega}$ and an altered emblackening factor V. It should come as no surprise, taking into account what we learned from the undoped equivalent of this equation, that this equation is not analytically solvable for general k, M and ω, when $\mu \neq 0$.

It is also important to notice that adding chemical potential does not change the leading order of the asymptotic power law solution, (2.56). This means that

$$\Sigma = \lim_{r_0 \to \infty} -g r_0^{2M} \xi(r_0, \mathbf{k}, \omega), \tag{3.32}$$

remains well-defined for the same composition choices for g as defined in (2.62). Moreover, this does not change the derivation of the boundary condition.

3.2.2 Doped massive spinor

Now we look at the effect of an added finite chemical potential to (2.99), the massive boundary theory. The things that change are $\omega \to \omega + \mu$ and the self-energy Σ. Applying this straightforward generalization implies that the retarded propagator and thus the spectral function (2.102) for any z become,

$$\boxed{\rho(\mathbf{k}, \omega) = -\frac{1}{\pi} \mathrm{Im} \left[\frac{\omega + \mu + \Sigma_0}{(\omega + \mu + \Sigma_0)^2 - (\mathbf{k}_i |\mathbf{k}|^{z-1} + \Sigma_i)^2 - m^2} \right]} \tag{3.33}$$

where Σs in general are obtained numerically using (2.84). Plots of (3.33) are shown in (3.1). The effect of μ is that the peaks get translated and there appears to be more weight on the valence band. Recall that the height of the graphs is related to the distribution of the fermions.

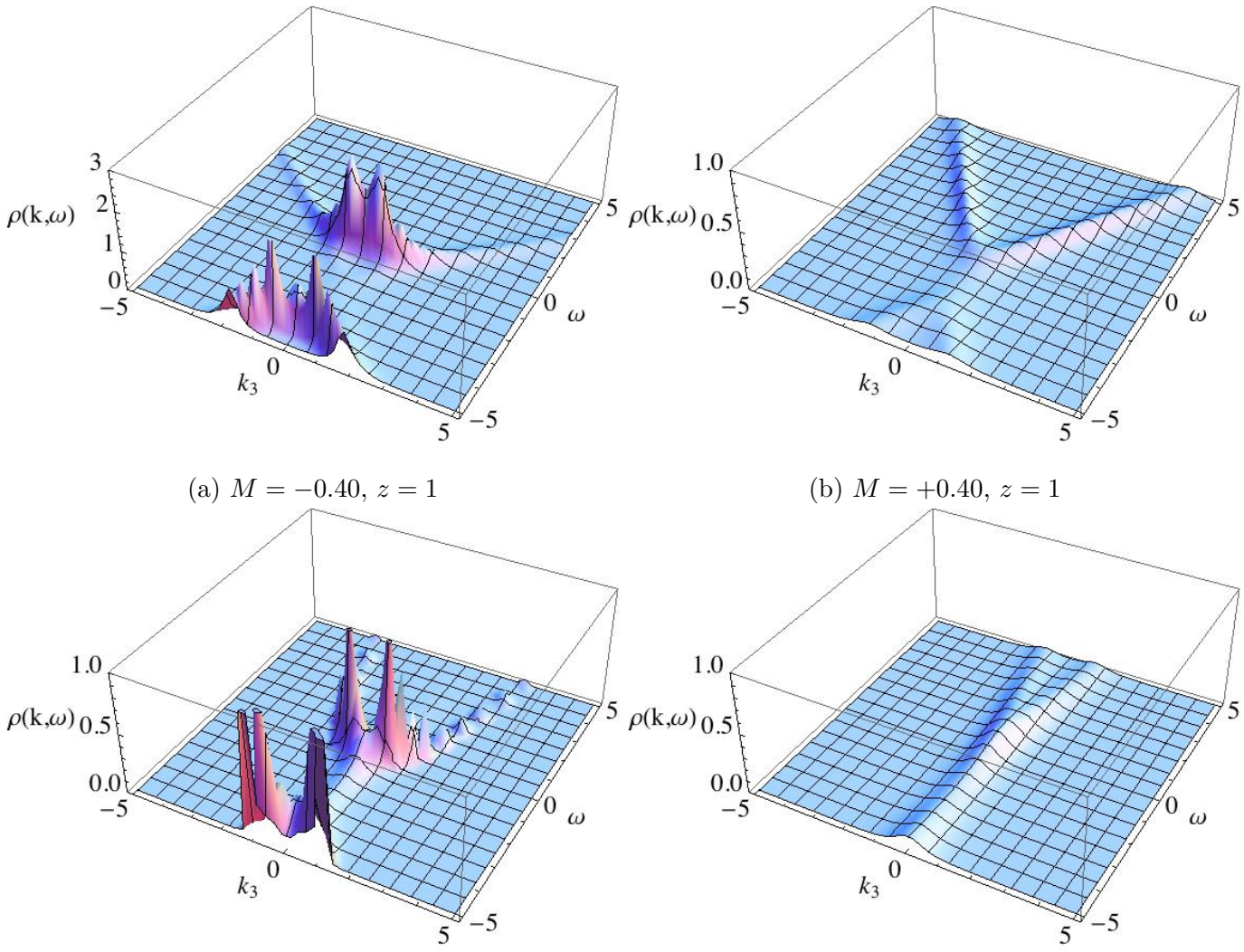

(a) $M = -0.40$, $z = 1$

(b) $M = +0.40$, $z = 1$

(c) $M = -0.40$, $z = 2$

(d) $M = +0.40$, $z = 2$

Figure 3.1: These are the spectral functions obtained using (3.33). We chose $T = 1$, $m = 2$ and $\mu = 2.5$. Compare these results with the results of Figure 2.4 and 2.5. Not only did the peaks get shifted, also the heights change. There is more weight on the valence bands. The ranges of the plots are different, because we are only interested in the qualitative changes of adding chemical potential. The spikes are due to the numerics.

Chapter 4

Weyl Semimetals

In this chapter we break a particular symmetry in a massless Dirac spinor theory. Recall that a Dirac spinor is composed of two chiral spinors. Breaking a particular symmetry changes the dispersion relation described by one Dirac cone into the dispersion relation described by two chiral cones with some separation in between, as sketched earlier in Figure 1.3. For $z = 1$ and $\mu = 0$ the chiral cones describe a Weyl semimetal in the low energy limit. When breaking the particular symmetry this system exhibits a topological effect that induces a fictitious magnetic field. This particular effect is studied in chapter 5.

We start by explicitly inducing a separation between two chiral cones. We study the corresponding undoped spectral functions at $z = 1$. We conclude by considering the case where $\mu \neq 0$.

4.1 Making a separation

Similar to when adding the mass term to create a mass gap, as is sketched in Figure 1.4, now a term that lifts the degeneracy of the dispersion relation of the chiral spinors is considered. On the boundary we obtain explicitly[1] ,

$$S_5 = \int \frac{d^4k}{(2\pi)^4} \Psi^\dagger \gamma^0 [-\Delta \mathbf{k}_\mu \gamma^\mu \gamma^5] \Psi, \quad \Delta \mathbf{k}_\mu := (\Delta\omega, \Delta k_1, \Delta k_2, \Delta k_3), \tag{4.1}$$

where the terms with a "Δ" are constants, which are chosen to be positive for the sake of simplicity. $\Delta\omega$ is added for completeness, but is chosen to be vanishing. If the "γ^5" is excluded, the extra term would have the exact same structure as the dynamical part of action (2.89). The extra term would just shift the peaks of the spectral function on the k-axes in the same direction[2].

Now take $\gamma^5 = \mathrm{diag}(\mathbb{1}_2, -\mathbb{1}_2)$ into account. The matrix γ^5 makes sure that the shift in momentum space that is done to one chiral spinor, is done to the other chiral spinor but in the reversed direction. This has as a consequence that the peaks of the spectral function are shifted away from each other on the k-axes creating a separation. See Figure 2.2. This separation is shown to yield non-trivial effects in chapter 5. Now consider the effective action when we include S_5,

$$S_{\text{eff}} = \int \frac{dk^4}{(2\pi)^4} \Psi^\dagger \gamma^0 [\gamma^0 \omega - \frac{1}{\lambda} \gamma^i \mathbf{k}_i |\mathbf{k}|^{z-1} - \Sigma(\mathbf{k}, \omega) - \Delta \mathbf{k}_\mu \gamma^\mu \gamma^5] \Psi. \tag{4.2}$$

[1] We have taken exactly the same steps as in the case for the mass term m to obtain this term. Starting from $S_5 = \int_{r=r_0} d^4x \Psi^\dagger \gamma^0 [-\tilde{\Delta \mathbf{k}}_\mu \gamma^\mu \gamma^5] \Psi$, on which the exact same normalization is applied and an analogous double scaling limit is taken which renders the term well-defined on the boundary, resulting in (4.1). Also it is clear that $\delta S_5 = 0$.

[2] Take note that when $\Delta\omega \neq 0$ there would also be a relative shift on the ω-axes.

The goal is to compute the corresponding G_R. Because there is still chiral symmetry, the different chiralities do not couple. Hence the G_R^{-1} is diagonal with respect to the different chiralities. We can find G_R for each chiral spinor and then stack them in a diagonal matrix to find the total propagator. To make this more concrete suppose,

$$\begin{aligned} G_R^{-1} =&\gamma^0(a\gamma^0 - b_i\gamma^i + c_0\gamma^0\gamma^5 - c_i\gamma^i\gamma^5) \\ =&- a\mathbb{1}_4 - b_i\gamma^0\gamma^i - c_0\gamma^5 - c_i\gamma^0\gamma^i\gamma^5 \\ =&a\begin{pmatrix} -\mathbb{1}_2 & \\ & -\mathbb{1}_2 \end{pmatrix} + b_i\begin{pmatrix} +\sigma^i & \\ & -\sigma^i \end{pmatrix} + c_0\begin{pmatrix} -\mathbb{1}_2 & \\ & +\mathbb{1}_2 \end{pmatrix} + c_i\begin{pmatrix} +\sigma^i & \\ & +\sigma^i \end{pmatrix}, \end{aligned} \tag{4.3}$$

which is diagonal with respect to chiral spinors. All coefficients represent functions. Equation (4.3) can be inverted using,

$$((-a \mp c_0)\mathbb{1}_2 + (c_i \pm b_i)\sigma^i)((-a \mp c_0)\mathbb{1}_2 - (c_i \pm b_i)\sigma^i) = (-a \mp c_0)^2 - (\pm b_i + c_i)^2, \tag{4.4}$$

where the upper signs corresponds to Ψ_+ and the down signs correspond to Ψ_-. Thus

$$G_R = -\begin{pmatrix} \frac{(a+c_0)\mathbb{1}_2+(b_i+c_i)\sigma^i}{(a+c_0)^2-(b_i+c_i)^2} & \\ & \frac{(a-c_0)\mathbb{1}_2+(b_i-c_i)\sigma^i}{(a-c_0)^2-(b_i-c_i)^2} \end{pmatrix}. \tag{4.5}$$

The retarded operator corresponding to (4.2) is

$$G_R = -\begin{pmatrix} \frac{(\omega+\Sigma_0+\Delta\omega)\mathbb{1}_2+(\mathbf{k}_i+\Sigma_i+\Delta\mathbf{k}_i)\sigma^i}{(\omega+\Sigma_0+\Delta\omega)^2-(\mathbf{k}_i+\Sigma_i+\Delta\mathbf{k}_i)^2} & \\ & \frac{(\omega+\Sigma_0-\Delta\omega)\mathbb{1}_2+(\mathbf{k}_i+\Sigma_i-\Delta\mathbf{k}_i)\sigma^i}{(\omega+\Sigma_0-\Delta\omega)^2-(\mathbf{k}_i+\Sigma_i-\Delta\mathbf{k}_i)^2} \end{pmatrix}, \tag{4.6}$$

where we again use $\Sigma = \Sigma_\mu\gamma^\mu$. Compare both terms in G_R. Pay attention to the relative minus signs, this is the manifestation of γ^5. The spectral function according to the obtained action is expressed as,

$$\boxed{\rho(\mathbf{k},\omega) = -\frac{1}{2\pi}\mathrm{Im}\left[\frac{\omega+\Sigma_0+\Delta\omega}{(\omega+\Sigma_0+\Delta\omega)^2-(\mathbf{k}_i+\Sigma_i+\Delta\mathbf{k}_i)^2} + \frac{\omega+\Sigma_0-\Delta\omega}{(\omega+\Sigma_0-\Delta\omega)^2-(\mathbf{k}_i+\Sigma_i-\Delta\mathbf{k}_i)^2}\right]} \tag{4.7}$$

where it is clear that when $\Delta\mathbf{k}_\mu = 0$ the expression is consistent with (2.94). Some plots are shown in Figure 4.1. An important observation is that for $M > 0$ the separation also depends on M.

4.2 Doped separation

Adding chemical potential to the boundary system result in a change of (4.7). The self-energy Σ now depends on the new solution of ξ and the ω gets shifted by μ. We are only interested in the $z = 1$ case. In addition taking $\Delta\omega = 0$,

$$\boxed{\rho(\mathbf{k},\omega) = -\frac{1}{2\pi}\mathrm{Im}\left[\frac{\omega+\mu+\Sigma_0}{(\omega+\mu+\Sigma_0)^2-(\mathbf{k}_i+\Sigma_i+\Delta\mathbf{k}_i)^2} + \frac{\omega+\mu+\Sigma_0}{(\omega+\mu+\Sigma_0)^2-(\mathbf{k}_i+\Sigma_i-\Delta\mathbf{k}_i)^2}\right]} \tag{4.8}$$

where Σ_μ is obtained numerically. Plotting (4.8) in Figure 4.2 we observe that there is more weight on the valence band and that the peaks of the dispersion relations got shifted. We from now on only consider zero chemical potential in this system.

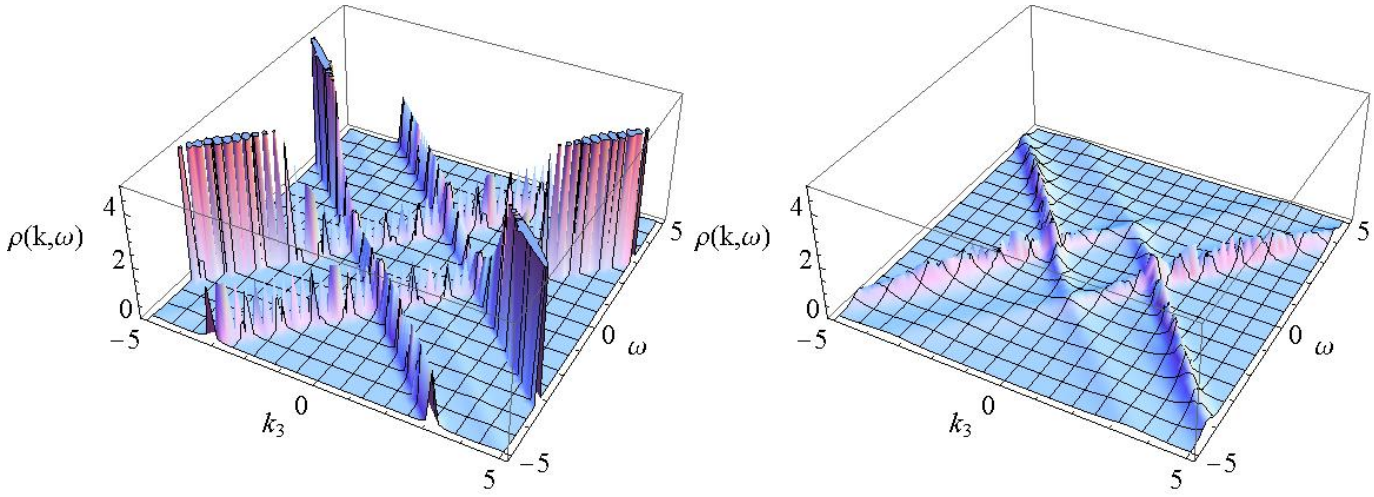

(e) $M = -0.40$

(f) $M = -0.20$

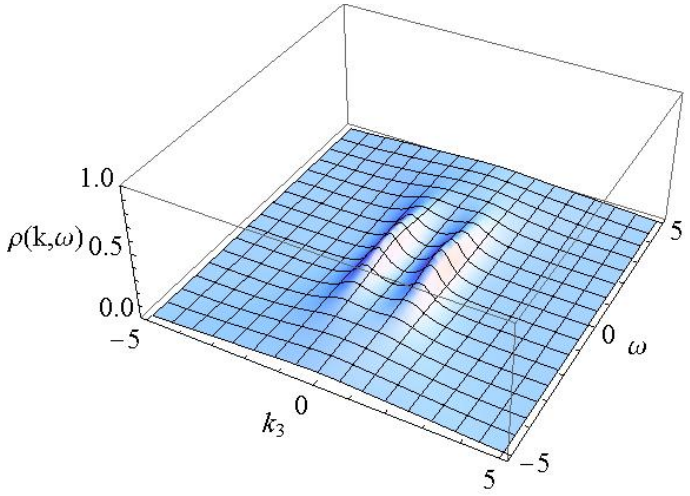

(g) $M = +0.20$

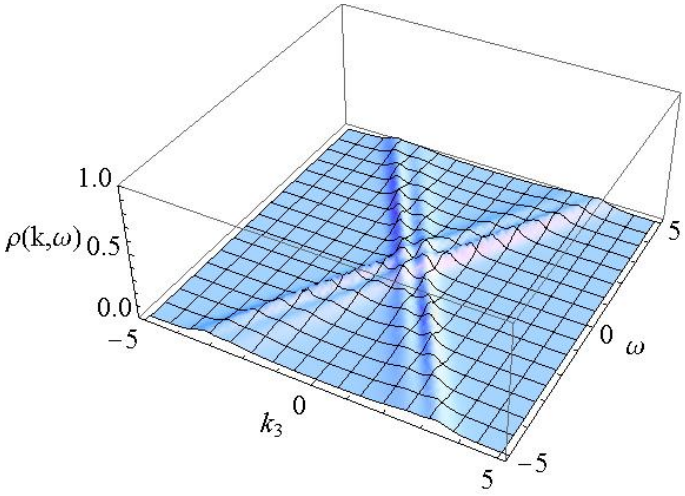

(h) $M = +0.40$

Figure 4.1: The spectral functions for (4.7) are plotted. We chose $\Delta k_3 = 2$ and $T = 1$. In contrary to the massive spinor we do not get scalings which do not obey the dynamical exponent z. An important feature is that for positive M the cones obtain a different separation depending on the value of M, without changing $\Delta k_3 = 2$. For negative M the separation seems to remain the same. This is an effect of the self-energy. The spikes are due to numerics and should be smoothened out.

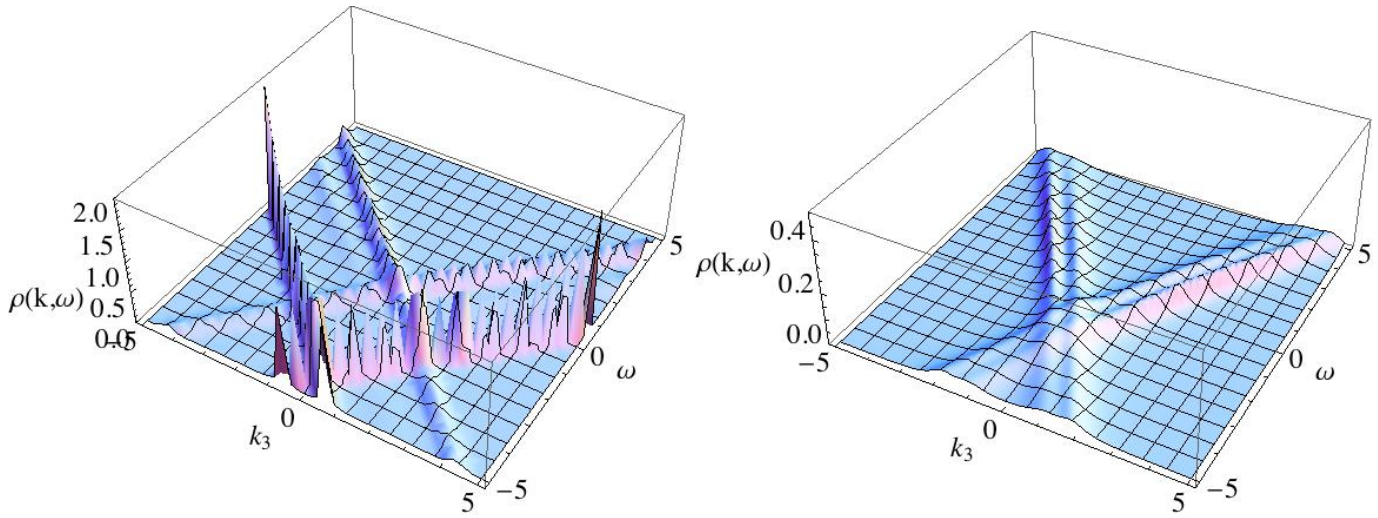

(a) $M = -0.40$, $z = 1$ (b) $M = +0.40$, $z = 1$

Figure 4.2: These spectral functions are obtained using (4.8). We chose $T = 1$, $\mu = 2.5$ and $\Delta k_3 = 2$. Compare these results to Figure 4.1. Not only did the peaks of the dispersion relation get shifted, also the heights change. There is more weight on the valence bands. The ranges of the plots are different, because we are only interested in the qualitative changes of adding chemical potential.

Chapter 5

Anomalous Hall Effect

In this chapter we work exclusively with the chiral boundary action with the topological separation term. We take $z = 1$ and restrict ourselves to the undoped case, $\mu = 0$. A solid with the resulting spectral function is a Weyl semimetal [10, 9].

The particular dispersion created by a non-zero separation generates a non-trivial Berry curvature. The Berry curvature behaves as a magnetic field in momentum space which gives rise to the anomalous Hall effect. This effect can be directly expressed in terms of the anomalous Hall conductivity. We are interested in the changes of the anomalous Hall effect when we add the holographic self-energy to the system [15, 12].

In the first section we give an overview of the Berry curvature and the anomalous Hall effect. In addition to that we obtain an expression for the conductivity via linear response for the non-interacting case. Furthermore, we calculate the anomalous Hall effect via the chiral anomaly. Using the action formalism we find out that the symmetry which is broken by this separation is the time-reversal symmetry.

In the second section we include the self-energy in the calculation of the anomalous Hall effect and compare results to the non-interacting anomalous Hall effect.

5.1 Anomalous Hall effect in the non-interacting case

5.1.1 Berry curvature

We sketch how to establish the Berry connection. In this section about Berry curvature we let $\mathbf{k}$ be a set of parameters which depend on time, i.e. $\mathbf{k} = \mathbf{k}(t)$. Let H be a Hamiltonian which fully depends on $\mathbf{k}$,

$$H(\mathbf{k})|n, \mathbf{k}\rangle = \epsilon_n(\mathbf{k})|n, \mathbf{k}\rangle, \tag{5.1}$$

where $\epsilon_n(\mathbf{k})$ is the energy corresponding to the eigenstates $|n, \mathbf{k}\rangle$. The quantum adiabatic theorem states [14] that when a system initially is in an eigenstate of H, it continues to stay an eigenstate throughout the evolution of time. This can be translated into

$$|\Psi_n(t)\rangle = e^{iC_n(t)} \exp\left[-\frac{i}{\hbar}\int_0^t dt' \epsilon(\mathbf{k}(t'))\right] |n, \mathbf{k}(t)\rangle, \tag{5.2}$$

which in combination with multiplying the left hand side of the time-dependent Schrödinger equation with $\langle n, \mathbf{k}(t)|$,

$$\langle n, \mathbf{k}(t)|i\hbar\partial_t|\Psi_n(t)\rangle = \langle n, \mathbf{k}(t)|H(\mathbf{k}(t))|\Psi_n(t)\rangle, \tag{5.3}$$

implies,

$$C_n = \int_\gamma d\mathbf{k} \cdot \mathbf{a}_n(\mathbf{k}(t)), \quad \mathbf{a}_n := i\langle n, \mathbf{k}|\vec{\nabla}_{\mathbf{k}}|n, \mathbf{k}\rangle, \tag{5.4}$$

where γ is some path through parameter space $\mathbf{k}$ and C_n is a phase factor. The a_n is called the Berry connection. The phase factor can gauged to zero since a_n is gauge dependent,

$$|n, \mathbf{k}\rangle \to e^{i\phi(\mathbf{k})}|n, \mathbf{k}\rangle \Rightarrow \quad \mathbf{a}_n(\mathbf{k}) \to \mathbf{a}_n(\mathbf{k}) - \vec{\nabla}_{\mathbf{k}}\phi(\mathbf{k}), \quad C_n \to C_n + \phi[\mathbf{k}(t_{\text{begin}})] - \phi[\mathbf{k}(t_{\text{end}})]. \tag{5.5}$$

However, if γ is a closed path the situation changes. For this purpose, let $\mathbf{k}(t_{\text{begin}}) = \mathbf{k}(t_{\text{end}})$. Then

$$\phi[\mathbf{k}(t_{\text{begin}})] - \phi[\mathbf{k}(t_{\text{end}})] = m2\pi, \tag{5.6}$$

where m is an integer. So we conclude from (5.2) we obtain that any gauge dependence drops out, rendering a_n to be gauge independent, hence observable. In this particular case C_n (5.4) is called the Berry phase. We define the Berry curvature to be

$$\mathbf{b}_n(\mathbf{k}) := \vec{\nabla}_{\mathbf{k}} \times \mathbf{a}_n, \tag{5.7}$$

where it is used that the parameter space is three-dimensional, $\mathbf{k} = (k_1, k_2, k_3)$. The Berry curvature can be viewed as a magnetic field in momentum space, sourced by the Berry phase, which takes the place of an analogous vector potential. By construction it is true that under (5.5) the Berry curvature remains gauge invariant.

5.1.2 Anomalous Hall effect

In 1889 Edwin H. Hall discovered [15] that when a current carrying conductor is placed in a magnetic field, the Lorentz force makes the electrons go to one side of the conductor. This effect is now called the Hall effect. Later Hall found out that the effect was much stronger in ferromagnetic iron. This effect is called the Anomalous Hall effect. The Anomalous Hall effect contributes to the off-diagonal terms of the conductivity tensor σ_{ij}. The tensor σ_{ij} is defined as the proportionality constant between the current in a certain direction and an applied electric field,

$$J_i := \sigma_{ij} E^j. \tag{5.8}$$

We considering the contributions of the anomalous Hall effect to σ_{12} with $\Delta k_1 = \Delta k_2 = 0$, where 1 and 2 are chosen without any loss of generality. We develop the following formula using the theory of linear response in the DC limit[1] [23],

$$\sigma^{ij} = -\epsilon^{ij\ell}\frac{e^2}{\hbar}\int \frac{d^3k}{(2\pi)^3}\sum_n n_f(\epsilon_n(\mathbf{k}))(\mathbf{b}_n)_\ell. \tag{5.9}$$

Notice that $\sigma^{ij} = 0$ if $\mathbf{b}_n = 0$.

[1]DC stands for Direct Current. Because we are interested in the dissipative part we take the real part of the tensor σ_{ij}. In addition we are interested in first taking $\mathbf{k} \to 0$ and then $\omega \to 0$ which corresponds with taking the DC limit.

5.1.3 Theory of linear response

Let us consider a Hamiltonian H_0 which has eigenstates and energies,

$$H_0(\mathbf{k})|n,\mathbf{k}\rangle = \epsilon_n(\mathbf{k})|n,\mathbf{k}\rangle. \tag{5.10}$$

In linear response theory we study how a system changes when a weak external field is applied. Put differently, let us introduce some quantum observable A. We want to find out the change of $\langle A\rangle$, the expectation value of A, to linear order in some small perturbation of the Hamiltonian, denoted by H'.

To make the statement of perturbation more precise, consider a system in thermodynamic equilibrium. The system before perturbation is described by,

$$\langle A(\mathbf{k})\rangle_0 = \frac{1}{Z_0(\mathbf{k})}\mathrm{Tr}[\rho_0(\mathbf{k})A(\mathbf{k})] = \frac{1}{Z_0(\mathbf{k})}\sum_n \langle n,\mathbf{k}|A(\mathbf{k})|n,\mathbf{k}\rangle \exp[-\beta\epsilon_n(\mathbf{k})], \tag{5.11}$$

$$\rho_0(\mathbf{k}) = \exp[-\beta H_0(\mathbf{k})] = \sum_n |n,\mathbf{k}\rangle\langle n,\mathbf{k}| \exp[-\beta\epsilon_n(\mathbf{k})], \quad Z_0(\mathbf{k}) = \mathrm{Tr}\left[\rho_0(\mathbf{k})\right]. \tag{5.12}$$

We denote $\rho_0(\mathbf{k})/Z_0(\mathbf{k})$ as the Boltzmann distribution. Here β denotes inverse temperature. Now suppose we switch on a perturbation to the Hamiltonian $H'(\mathbf{k},t)$ at $t = t_0$, i.e.,

$$H(\mathbf{k},t) = H_0(\mathbf{k}) + H'(\mathbf{k},t)\theta(t-t_0), \tag{5.13}$$

such that the equations in (5.11) and (5.12) become

$$\langle A(\mathbf{k},t)\rangle = \frac{1}{Z_0(\mathbf{k})}\mathrm{Tr}[\rho(\mathbf{k},t)A(\mathbf{k})] = \frac{1}{Z_0(\mathbf{k})}\sum_n \langle n,\mathbf{k},t|A(\mathbf{k})|n,\mathbf{k},t\rangle \exp[-\beta\epsilon_n(\mathbf{k})], \tag{5.14}$$

$$\rho(\mathbf{k},t) = \sum_n |n,\mathbf{k},t\rangle\langle n,\mathbf{k},t| \exp[-\beta\epsilon_n(\mathbf{k})]. \tag{5.15}$$

The states are now time dependent and are governed by the new Hamiltonian. The time dependence of the states is given by the Schrödinger equation, i.e.,

$$i\hbar\partial_t|n,\mathbf{k},t\rangle = H(\mathbf{k},t)|n,\mathbf{k},t\rangle, \tag{5.16}$$

so recall that in the interaction picture [22],

$$|n,\mathbf{k},t\rangle = e^{-\frac{i}{\hbar}H_0 t}U(t,t_0)e^{\frac{i}{\hbar}H_0 t}|n,\mathbf{k},t_0\rangle, \tag{5.17}$$

where the time operator is given by $U(t,t_0) = 1 - i\int_{t_0}^{t} dt' H'(\mathbf{k},t')$, which is up to linear order in H'. Expressing (5.14) as in (5.17) shows,

$$\begin{aligned}\langle A(\mathbf{k},t)\rangle =& \langle A(\mathbf{k})\rangle_0 - i\int_{t_0}^{t} dt' \frac{1}{Z_0(\mathbf{k})}\sum_n \exp[-\beta\epsilon_n(\mathbf{k})]\langle n,\mathbf{k},t_0|A(\mathbf{k},t)H'(\mathbf{k},t') - H'(\mathbf{k},t')A(\mathbf{k},t)|n,\mathbf{k},t_0\rangle \\ =& \langle A(\mathbf{k})\rangle_0 - i\int_{t_0}^{t} dt' \langle[A(\mathbf{k},t),H'(\mathbf{k},t')]\rangle_0.\end{aligned} \tag{5.18}$$

Consider equation (5.18). It is important to notice that the non-equilibrium quantity $\langle A(\mathbf{k},t)\rangle$ is expressed in terms of thermal equilibrium, $\langle..\rangle_0$. Define,

$$\delta\langle A(\mathbf{k},t)\rangle := \langle A(\mathbf{k},t)\rangle - \langle A(\mathbf{k})\rangle_0 = -i\int_{t_0}^{\infty} dt'\theta(t-t')\langle[A(\mathbf{k},t),H'(\mathbf{k},t')]\rangle_0, \tag{5.19}$$

which expresses the linear response to a pertubation H'. The Heaviside step function θ enters the expression because we change the integration boundaries. This formula is known as the Kubo formula.

5.1.4 Kubo formula for conductivity

We consider a system of charged particles of a single species with elementary charge e, which are subjected to a small external electric field $\mathbf{E}_{ext}$. This field induces a current which has a linear response coefficient. Put in a formula,

$$\mathbf{J}_e^i(\mathbf{r},t) = \int dt' \int d\mathbf{r}' \sum_j \sigma^{ij}(\mathbf{r},\mathbf{r}',t,t')\mathbf{E}_{ext}^j(\mathbf{r}',t'), \tag{5.20}$$

where σ^{ij} is the conductivity tensor. The $\mathbf{J}_e$ stands for the electric current. Within linear response, we know that the conductivity tensor is a property of the equilibrium system and therefore it is time-translation invariant, i.e. $\sigma(t,t') = \sigma(t-t')$. Performing a Fourier transform we obtain,

$$\mathbf{J}_e^i(\mathbf{r},\omega) = \int d\mathbf{r}' \sum_j \sigma^{ij}(\mathbf{r},\mathbf{r}',\omega)\mathbf{E}_{ext}^j(\mathbf{r}',\omega). \tag{5.21}$$

The electric field $\mathbf{E}_{ext}$ is given by an external electric potential ϕ_{ext} and an external vector potential $\mathbf{A}_{ext}$ [22],

$$\mathbf{E}(\mathbf{r},t) = -\nabla_{\mathbf{r}}\phi_{ext}(\mathbf{r},t) - \partial_t \mathbf{A}_{ext}(\mathbf{r},t). \tag{5.22}$$

Therefore, the perturbation of the Hamiltonian due to the electric field up to linear order takes the form [23],

$$H'(t) = -e\int d\mathbf{r}\rho(\mathbf{r})\phi_{ext}(\mathbf{r},t) + e\int d\mathbf{r}\mathbf{J}(\mathbf{r})\cdot\mathbf{A}_{ext}(\mathbf{r},t), \tag{5.23}$$

where the first term, which depends on the electric potential, can be put to zero with a suitable gauge choice. The $\rho(\mathbf{r})$ denotes the particle density operator. Here $\mathbf{J}$ denotes the current density operator. The operator $\mathbf{J}$ is related to $\mathbf{J}_e$ through $\mathbf{J}_e = -e\langle\mathbf{J}\rangle$. We let $\mathbf{A}_0$ denote the vector potential before $\mathbf{A}_{ext}$ is applied and let $\mathbf{A}$ denote the total vector potential,

$$\mathbf{A} = \mathbf{A}_0 + \mathbf{A}_{ext}. \tag{5.24}$$

From the quantization of the electromagnetic field [23] we obtain the decomposition of $\mathbf{J}$,

$$\mathbf{J}(\mathbf{r}) = \mathbf{J}_{para}(\mathbf{r}) + \frac{e}{m}\mathbf{A}(\mathbf{r})\rho(\mathbf{r}), \tag{5.25}$$

where e denotes the elementary charge, m denotes particle mass, $\rho(\mathbf{r})$ again is the particle density operator and $\mathbf{J}_{para}$ is the paramagnetic contribution to the current density operator. Equivalently to $\mathbf{J}$ we define $\mathbf{J}_0$ to be,

$$\mathbf{J}_0(\mathbf{r}) = \mathbf{J}_{para}(\mathbf{r}) + \frac{e}{m}\mathbf{A}_0(\mathbf{r})\rho(\mathbf{r}), \tag{5.26}$$

such that we can express,

$$\mathbf{J}(\mathbf{r}) = \mathbf{J}_0(\mathbf{r}) + \frac{e}{m}\mathbf{A}_{ext}(\mathbf{r})\rho(\mathbf{r}). \tag{5.27}$$

When $\mathbf{A}_{ext} \to 0$ then $\mathbf{J} \to \mathbf{J}_0$. Regarding $H'(t)$ as defined in (5.23) only up to first order in $\mathbf{A}_{ext}$ and with a suitable choice of gauge we obtain,

$$H'(t) = e\int d\mathbf{r}\mathbf{J}_0(\mathbf{r})\cdot\mathbf{A}_{ext}(\mathbf{r},t). \tag{5.28}$$

Performing a Fourier transform (5.28) becomes,

$$H'(\omega) = \frac{e}{i\omega}\int d\mathbf{r}\mathbf{J}_0(\mathbf{r})\cdot\mathbf{E}(\mathbf{r},\omega). \tag{5.29}$$

Calculating the expectation value of (5.27) we find,

$$\mathbf{J}_e = -e\langle\mathbf{J}(\mathbf{r})\rangle = -e\langle\mathbf{J}_0(\mathbf{r})\rangle - e\langle\frac{e}{m}\mathbf{A}_{ext}(\mathbf{r})\rho(\mathbf{r})\rangle. \tag{5.30}$$

The second term is not important for us because it only contributes to the diagonal part[2] of the conductivity tensor σ. For the first term, since the equilibrium state does not carry any current, we conclude that $\delta\langle\mathbf{J}_0\rangle = \langle\mathbf{J}_0\rangle$. Therefore using (5.19) we calculate,

$$\begin{aligned}
&\langle(\mathbf{J}_0(\mathbf{r},\omega))_\alpha\rangle = \delta\langle(\mathbf{J}_0(\mathbf{r},\omega))_\alpha\rangle = \int d\mathbf{r}'\sum_\beta \Pi^R_{\alpha\beta}(\mathbf{r},\mathbf{r}',\omega)\frac{e}{i\omega}E^\beta(\mathbf{r}',\omega),\\
&\Pi^R_{\alpha\beta}(\mathbf{r},\mathbf{r}',t-t') = -i\theta(t-t')\langle[\mathbf{J}^\alpha_0(\mathbf{r},t),\mathbf{J}^\beta_0(\mathbf{r}',t')]\rangle_0.
\end{aligned} \tag{5.31}$$

Using (5.21) and (5.31) we can conclude,

$$\sigma_{\alpha\beta}(\mathbf{r},\mathbf{r}',\omega) = \frac{ie^2}{\omega}\Pi^R_{\alpha\beta}(\mathbf{r},\mathbf{r}',\omega). \tag{5.32}$$

Let it be stressed that this formula only takes into account the off-diagonal part. We are interested in finding the real part[3] of the conductivity in the DC limit,

$$\sigma_{\alpha\beta} := \mathrm{Re}\left[\sigma_{\alpha\beta}(0,0)\right] = -e^2\frac{1}{\omega}\lim_{\omega^+\to 0+i0}\lim_{\mathbf{q}\to 0}\mathrm{Im}\left[\Pi^R_{\alpha\beta}(\mathbf{q},\omega^+)\right]. \tag{5.33}$$

We assume that Π is isotropic, in addition to time-translation invariant. This choice is justified later. Taking the Fourier transform of both space and time of (5.31) we arrive at

$$\begin{aligned}
\Pi^R_{\alpha\beta}(\mathbf{q},\omega^+) &= \int_{-\infty}^{\infty} d(t-t')\int_{-\infty}^{\infty} d^3(\mathbf{r}-\mathbf{r}')\Pi^R_{\alpha\beta}(\mathbf{r}-\mathbf{r}',t-t')e^{-i(\mathbf{r}-\mathbf{r}')\mathbf{q}}e^{-i(t-t')\omega^+}\\
&= -i\int_{-\infty}^{\infty} d(t-t')\theta(t-t')\langle[\mathbf{J}^\alpha_0(\mathbf{q},t),\mathbf{J}^\beta_0(-\mathbf{q},t')]\rangle_0 e^{-i(t-t')\omega^+}.
\end{aligned} \tag{5.34}$$

Taking the $\mathbf{q}\to 0$ limit of the retarded propagator Π^R,

$$\Pi^R_{\alpha\beta}(\omega^+) = \lim_{\mathbf{q}\to 0}\Pi^R_{\alpha\beta}(\mathbf{q},\omega^+) = -i\int_{-\infty}^{\infty} d(t-t')\theta(t-t')\langle[\mathbf{J}^\alpha_0(t),\mathbf{J}^\beta_0(t')]\rangle_0 e^{-i(t-t')\omega^+} \tag{5.35}$$

where $\omega^+ := \omega + i\epsilon$, ensuring that Π is analytic in the upper half of the complex plane. The next step is inserting several complete basises $\int d\mathbf{k}_j\sum_{l_j}|l_j,\mathbf{k}_j\rangle\langle l_j,\mathbf{k}_j|$. Notice that therefore in the following

[2]For this term we use that to linear order in $\mathbf{A}_{ext}$ the expectation value can be evaluated in the equilibrium state [23],

$$\langle\frac{e}{m}\mathbf{A}_{ext}(\mathbf{r})\rho(\mathbf{r})\rangle \approx \frac{e}{m}\mathbf{A}_{ext}(\mathbf{r},\omega)\langle\rho(\mathbf{r})\rangle_0 = \frac{e}{i\omega m}\langle\rho(\mathbf{r})\rangle_0\mathbf{E}_{ext}(\mathbf{r},\omega)$$

[3]Taking the real part makes sure we look at the dissipative part of the conductivity [23].

derivation the subscript does not necessarily denote an entry. We expand $\hat{A}(t) := e^{\frac{i}{\hbar}H_0 t}\hat{A}_0 e^{-\frac{i}{\hbar}H_0 t}$ such that,

$$\begin{aligned}
\Pi^R_{\alpha\beta}(\omega^+) =& -i\int_0^\infty d(t-t')\{ \\
&\int \frac{d^3\mathbf{k}}{(2\pi)^3}\sum_n \langle n,\mathbf{k}|\frac{\rho_0(H_0(\mathbf{k}))}{Z_0(\mathbf{k})}\int \frac{d^3\mathbf{k}_1}{(2\pi)^3}\sum_{n_1}|n_1,\mathbf{k}_1\rangle\langle n_1,\mathbf{k}_1|e^{\frac{i}{\hbar}H_0 t}\int \frac{d^3\mathbf{k}_2}{(2\pi)^3}\sum_{n_2}|n_2,\mathbf{k}_2\rangle \\
&\langle n_2,\mathbf{k}_2|\mathbf{J}_0^\alpha\int \frac{d^3\mathbf{k}_3}{(2\pi)^3}\sum_{n_3}|n_3,\mathbf{k}_3\rangle\langle n_3,\mathbf{k}_3|e^{-\frac{i}{\hbar}H_0 t}\int \frac{d^3\mathbf{k}_4}{(2\pi)^3}\sum_{n_4}|n_4,\mathbf{k}_4\rangle\langle n_4,\mathbf{k}_4|e^{\frac{i}{\hbar}H_0 t'}\int \frac{d^3\mathbf{k}_5}{(2\pi)^3}\sum_{n_5}|n_5,\mathbf{k}_5\rangle \\
&\langle n_5,\mathbf{k}_5|\mathbf{J}_0^\beta\int \frac{d^3\mathbf{k}_6}{(2\pi)^3}\sum_{n_6}|n_6,\mathbf{k}_6\rangle\langle n_6,\mathbf{k}_6|e^{-\frac{i}{\hbar}H_0 t'}|n,\mathbf{k}\rangle \\
&-\begin{pmatrix}\mathbf{J}_0^\alpha \leftrightarrow \mathbf{J}_0^\beta \\ t\leftrightarrow t'\end{pmatrix}\}e^{-i(t-t')\omega^+} \\
=& -i\int \frac{d^3\mathbf{k}}{(2\pi)^3}\int_0^\infty d(t-t')\{\sum_{n\neq m}[n_f(\epsilon_n(\mathbf{k}))-n_f(\epsilon_m(\mathbf{k}))]e^{\frac{i}{\hbar}(\epsilon_n(\mathbf{k})-\epsilon_m(\mathbf{k})-\hbar\omega^+)(t-t')}\mathbf{J}^\alpha_{0nm}(\mathbf{k})\mathbf{J}^\beta_{0mn}(\mathbf{k})\} \\
=& -\hbar\int \frac{d^3\mathbf{k}}{(2\pi)^3}\sum_{n\neq m}[n_f(\epsilon_n(\mathbf{k}))-n_f(\epsilon_m(\mathbf{k}))]\frac{1}{\epsilon_n(\mathbf{k})-\epsilon_m(\mathbf{k})-\hbar\omega^+}\mathbf{J}^\alpha_{0nm}(\mathbf{k})\mathbf{J}^\beta_{0mn}(\mathbf{k}),
\end{aligned} \tag{5.36}$$

where $\rho_0/Z_0 = n_f$ is the Fermi-Dirac distribution. Because we are interested in describing a fermionic system we let ρ_0/Z_0 denote the Fermi-Dirac distribution rather than the Boltzmann distribution. A complete derivation is presented in [24]. Putting (5.33) and (5.36) together we find,

$$\begin{aligned}
\sigma_{\alpha\beta} =& -e^2\lim_{\omega^+\to 0+i0}\left\{-\frac{1}{\omega^+}\mathrm{Im}\left[\hbar\int\frac{d^3\mathbf{k}}{(2\pi)^3}\sum_{n\neq m}[n_f(\epsilon_n(\mathbf{k}))-n_f(\epsilon_m(\mathbf{k}))]\frac{1}{\epsilon_n(\mathbf{k})-\epsilon_m(\mathbf{k})-\hbar\omega^+}\mathbf{J}^\alpha_{0nm}(\mathbf{k})\mathbf{J}^\beta_{0mn}(\mathbf{k})\right]\right\} \\
=&\hbar e^2\int\frac{d^3\mathbf{k}}{(2\pi)^3}\sum_{n\neq m}[n_f(\epsilon_n(\mathbf{k}))-n_f(\epsilon_m(\mathbf{k}))]\frac{1}{(\epsilon_n(\mathbf{k})-\epsilon_m(\mathbf{k}))^2}\mathrm{Im}[\mathbf{J}^\alpha_{0nm}(\mathbf{k})\mathbf{J}^\beta_{0mn}(\mathbf{k})],
\end{aligned} \tag{5.37}$$

where[4] the current is given by $\mathbf{J}_0^\alpha := \partial_{\mathbf{k}_\alpha}H$.

5.1.5 Conductivity of the anomalous Hall effect

We are interested in the DC conductivity corresponding to the following Hamiltonian,

$$H(\mathbf{k}) = \gamma^0\gamma^i\mathbf{k}_i + \Delta\mathbf{k}_\mu\gamma^0\gamma^\mu\gamma^5, \tag{5.38}$$

which corresponds to the action in (4.2), without consideration of the self-energy term. This Hamiltonian is invariant under differences in time and space, hence we can use the derivation from the last

[4]We used $\mathrm{Im}\left[\Pi^R(0)\right] = 0$. This is obtained from the fact that a retarded propagator defined as (5.35) has an odd imaginary part [5],

$$\mathrm{Im}\left[\Pi^R(\omega)\right] = -\mathrm{Im}\left[\Pi^R(-\omega)\right].$$

Therefore,

$$\lim_{\omega\to 0}\mathrm{Im}\left[\frac{\Pi(\omega)}{\omega}\right] = \lim_{\omega\to 0}\mathrm{Im}\left[\frac{\Pi(\omega)-\Pi(0)}{\omega}\right] = \mathrm{Im}\left[\Pi'(\omega)\right]|_{\omega=0}.$$

section. Let $v_i := \frac{1}{\hbar}\mathbf{J}_0^i = \partial_{\mathbf{k}_i} H$. Thus the DC conductivity is given by

$$\sigma_{ij} = \frac{e^2}{\hbar}\int \frac{d^3\mathbf{k}}{(2\pi)^3}\sum_{n\neq m}\left[n_f(\epsilon_n(\mathbf{k})) - n_f(\epsilon_m(\mathbf{k}))\right]\mathrm{Im}\left[\frac{\langle n,\mathbf{k}|v_i(\mathbf{k})|m,\mathbf{k}\rangle\langle m,\mathbf{k}|v_j(\mathbf{k})|n,\mathbf{k}\rangle}{(\epsilon_n(\mathbf{k})-\epsilon_m(\mathbf{k}))^2}\right]. \tag{5.39}$$

Observe that,

$$\begin{aligned}\langle n,\mathbf{k}|\partial_{k_i}(H(\mathbf{k}))|m,\mathbf{k}\rangle =& \langle n,\mathbf{k}|\partial_{k_i}(H(\mathbf{k})|m,\mathbf{k}\rangle) - \langle n,\mathbf{k}|H(\mathbf{k})\partial_{k_i}(|m,\mathbf{k}\rangle)\\ =& \langle n,\mathbf{k}|\partial_{k_i}(\epsilon_m(\mathbf{k})|m,\mathbf{k}\rangle) - \epsilon_n(\mathbf{k})\langle n,\mathbf{k}|\partial_{k_i}(|m,\mathbf{k}\rangle)\\ =& \partial_{k_i}(\epsilon_m(\mathbf{k}))\langle n,\mathbf{k}|m,\mathbf{k}\rangle + \epsilon_m(\mathbf{k})\langle n,\mathbf{k}|\partial_{k_i}(|m,\mathbf{k}\rangle) - \epsilon_n(\mathbf{k})\langle n,\mathbf{k}|\partial_{k_i}(|m,\mathbf{k}\rangle).\end{aligned} \tag{5.40}$$

Hence,

$$\langle n,\mathbf{k}|\partial_{k_i}|m,\mathbf{k}\rangle = \frac{\langle n,\mathbf{k}|\partial_{k_i}(H(\mathbf{k}))|m,\mathbf{k}\rangle}{\epsilon_n(\mathbf{k})-\epsilon_m(\mathbf{k})}, \tag{5.41}$$

where we assumed $n \neq m$, which is the case we are considering. In the equation above, the operator works on the object right of the operator. It is useful to define $\overleftarrow{\partial}$ for a derivative working on the object on the left of the operator. We apply the same approach as in (5.40) to establish,

$$\langle n,\mathbf{k}|\overleftarrow{\partial_{k_i}}|m,\mathbf{k}\rangle = \frac{\langle n,\mathbf{k}|(H(\mathbf{k}))\overleftarrow{\partial_{k_i}}|m,\mathbf{k}\rangle}{\epsilon_m(\mathbf{k})-\epsilon_n(\mathbf{k})} = \frac{\langle n,\mathbf{k}|\overrightarrow{\partial_{k_i}}(H(\mathbf{k}))|m,\mathbf{k}\rangle}{\epsilon_m(\mathbf{k})-\epsilon_n(\mathbf{k})} = -\langle n,\mathbf{k}|\overrightarrow{\partial_{k_i}}|m,\mathbf{k}\rangle. \tag{5.42}$$

We are now ready to simplify (5.39),

$$\begin{aligned}\sigma_{ij} \sim& \sum_{n\neq m}[n_f(\epsilon_n(\mathbf{k})) - n_f(\epsilon_m(\mathbf{k}))]\mathrm{Im}\left\{\frac{\langle n,\mathbf{k}|v_i(\mathbf{k})|m,\mathbf{k}\rangle\langle m,\mathbf{k}|v_j(\mathbf{k})|n,\mathbf{k}\rangle}{(\epsilon_n(\mathbf{k})-\epsilon_m(\mathbf{k}))^2}\right\}\\ =& \sum_{n\neq m}(n_f(\epsilon_n(\mathbf{k})) - n_f(\epsilon_m(\mathbf{k})))\mathrm{Im}\left\{\langle n,\mathbf{k}|\overleftarrow{\partial_{k_i}}|m,\mathbf{k}\rangle\langle m,\mathbf{k}|\overrightarrow{\partial_{k_j}}|n,\mathbf{k}\rangle\right\}\\ =& \frac{-1}{2i}\sum_{n\neq m} n_f(\epsilon_n(\mathbf{k}))\left(\langle n,\mathbf{k}|\overleftarrow{\partial_{k_i}}|m,\mathbf{k}\rangle\langle m,\mathbf{k}|\overrightarrow{\partial_{k_j}}|n,\mathbf{k}\rangle - \langle m,\mathbf{k}|\overleftarrow{\partial_{k_i}}|n,\mathbf{k}\rangle\langle n,\mathbf{k}|\overrightarrow{\partial_{k_j}}|m,\mathbf{k}\rangle\right)\\ & - \left(n_f(\epsilon_n(\mathbf{k})) \leftrightarrow n_f(\epsilon_m(\mathbf{k}))\right)\\ =& \frac{-1}{2i}\left\{\sum_n n_f(\epsilon_n(\mathbf{k}))\left(\langle n,\mathbf{k}|\overleftarrow{\partial_{k_i}}\overrightarrow{\partial_{k_j}} - \overleftarrow{\partial_{k_j}}\overrightarrow{\partial_{k_i}}|n,\mathbf{k}\rangle\right) + \sum_m n_f(\epsilon_m(\mathbf{k}))\left(\langle m,\mathbf{k}|\overleftarrow{\partial_{k_i}}\overrightarrow{\partial_{k_j}} - \overleftarrow{\partial_{k_j}}\overrightarrow{\partial_{k_i}}|m,\mathbf{k}\rangle\right)\right\}\\ =& \frac{-1}{i}\sum_n n_f(\epsilon_n(\mathbf{k}))\left(\overrightarrow{\partial_{k_i}}\langle n,\mathbf{k}|\overrightarrow{\partial_{k_j}}|n,\mathbf{k}\rangle - \overrightarrow{\partial_{k_j}}\langle n,\mathbf{k}|\overrightarrow{\partial_{k_i}}|n,\mathbf{k}\rangle\right)\\ =& -\sum_n n_f(\epsilon_n(\mathbf{k}))\epsilon_{ijk}(\nabla_{\mathbf{k}}\times\vec{a}_n)_k, \qquad \vec{a}_n := \langle n,\mathbf{k}|\vec{\nabla}_{\mathbf{k}}|n,\mathbf{k}\rangle,\end{aligned} \tag{5.43}$$

where ϵ_{ijk} is the Levi-Civita symbol. Using what we established we can express (5.39) as

$$\sigma^{ij} = -\frac{e^2}{\hbar}\epsilon^{ij\ell}\int\frac{d^3\mathbf{k}}{(2\pi)^3}\sum_n n_f(\epsilon_n(\mathbf{k}))(\vec{\nabla}_{\mathbf{k}}\times\vec{a}_n)_\ell = -\frac{e^2}{\hbar}\epsilon^{ij\ell}\int\frac{d^3\mathbf{k}}{(2\pi)^3}\sum_n n_f(\epsilon_n(\mathbf{k}))(\mathbf{b}_n)_\ell. \tag{5.44}$$

5.1.6 Hamiltonian formalism

Now we solve (5.44). The first step is calculating $\mathbf{b}_n$ and $\epsilon_n(\mathbf{k})$ for all four eigenfunctions, i.e. solve,

$$H(\mathbf{k})|n,\mathbf{k}\rangle = \epsilon_n(\mathbf{k})|n,\mathbf{k}\rangle, \quad \mathbf{b}_n := \vec{\nabla}_{\mathbf{k}} \times \mathbf{a}_n, \quad \mathbf{a}_n := i\langle n,\mathbf{k}|\vec{\nabla}_{\mathbf{k}}|n,\mathbf{k}\rangle, \quad n \in \{1,2,3,4\}, \tag{5.45}$$

with the Hamiltonian given in (5.38). We obtain,

n	$\epsilon_n(\mathbf{k})$	$\mathbf{b}_n$
1	$-\lvert\mathbf{k}-\Delta\mathbf{k}\rvert - \Delta\omega$	$+\frac{\mathbf{k}-\Delta\mathbf{k}}{2\lvert\mathbf{k}-\Delta\mathbf{k}\rvert^3}$
2	$+\lvert\mathbf{k}-\Delta\mathbf{k}\rvert - \Delta\omega$	$-\frac{\mathbf{k}-\delta\mathbf{k}}{2\lvert\mathbf{k}-\Delta\mathbf{k}\rvert^3}$
3	$-\lvert\mathbf{k}+\Delta\mathbf{k}\rvert + \Delta\omega$	$-\frac{\mathbf{k}+\Delta\mathbf{k}}{2\lvert\mathbf{k}+\Delta\mathbf{k}\rvert^3}$
4	$+\lvert\mathbf{k}+\Delta\mathbf{k}\rvert + \Delta\omega$	$+\frac{\mathbf{k}+\Delta\mathbf{k}}{2\lvert\mathbf{k}+\Delta\mathbf{k}\rvert^3}$

From now on we put $\Delta\omega = 0$ and take temperature to be zero, $T = 0$, so $n_f(\epsilon_n(\mathbf{k})) = \theta(-\epsilon_n(\mathbf{k}))$. Clearly the $n = 2, 4$ cases do no contribute to σ^{ij} since $\theta(-|\mathbf{k}|) = 0$. Another way to see this is that only the valence bands contribute. Taking into account that $\theta(+|\mathbf{k}|) = 1$,

$$\sigma^{ij} = -\epsilon^{ij\ell}\frac{e^2}{\hbar}\int \frac{d^3\mathbf{k}}{(2\pi)^3}[\mathbf{b}_{1,\ell} + \mathbf{b}_{3,\ell}] = -\epsilon^{ij\ell}\frac{e^2}{\hbar}\int \frac{d^3\mathbf{k}}{(2\pi)^3}\left[\frac{1}{2}\frac{(\mathbf{k}-\Delta\mathbf{k})_\ell}{|\mathbf{k}-\Delta\mathbf{k}|^3} - (\Delta\mathbf{k} \to -\Delta\mathbf{k})\right]. \tag{5.46}$$

The Berry curvature, $\mathbf{b}_1 + \mathbf{b}_3$, is visualized in Figure 5.1. When considering the total integral it is

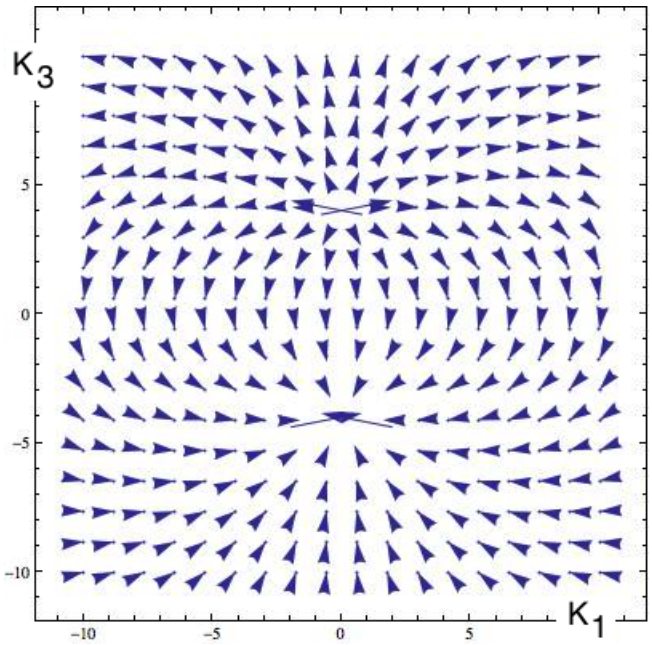

Figure 5.1: Plotted is the magnetic field generated by the Berry curvature in equation (5.47). Due to cylindrical symmetry we can consider the following intersection without any generality. The horizontal axes denote k_1 and the vertical axes k_3. The value for Δk_3 is 5. A three-dimensional version of this plot was presented in the introduction as Figure 1.4.

important to notice that for the ℓth component of the integrand it is allowed to choose the Δk_i and

Δk_j in the integrand to be vanishing. It is allowed to consider σ^{12} without any loss of generality. Thus we can consider solving,

$$\sigma^{12} = -\frac{e^2}{\hbar}\int \frac{d^3\mathbf{k}}{(2\pi)^3}\left[\frac{1}{2}\frac{(k_3-\Delta k_3)}{(k_1^2+k_2^2+(k_3-\Delta k_3))^{3/2}} - \frac{1}{2}\frac{(k_3+\Delta k_3)}{(k_1^2+k_2^2+(k_3+\Delta k_3))^{3/2}}\right]. \tag{5.47}$$

The details of solving (5.47) are discussed and evaluated in appendix A. Transforming to cylindrical coordinates implies,

$$\begin{aligned} k_1 &\to r\cos(\phi), \\ k_2 &\to r\sin(\phi), \\ k_3 &\to h. \end{aligned} \tag{5.48}$$

For the measures,

$$\int_{-\infty}^{\infty} dk_3 \int_{-\infty}^{\infty} dk_2 \int_{-\infty}^{\infty} dk_1 \to \int_{-\infty}^{\infty} h \int_0^{2\pi} d\phi \int_0^{\infty} dr[r], \tag{5.49}$$

where $[r]$ denotes the Jacobian. Notice that the order of k_1 and k_2 with respect to k_3 does not change, also in new coordinates. This new choice of coordinates only "mixes" the k_1 and k_2, which commute anyway. We can now conclude that this is an allowed choice of coordinates, as long as we perform the integral over h as the last one. The integral is independent of ϕ, as we see,

$$\begin{aligned} \sigma^{12} =& -\frac{e^2}{\hbar}\frac{1}{(2\pi)^3}\int_{-\infty}^{\infty} dh \int_0^{2\pi} d\phi \int_0^{\infty} dr[r]\left[\frac{1}{2}\frac{h-\Delta k_3}{(r^2+(h-\Delta k_3)^2)^{3/2}} - \frac{1}{2}\frac{h+\Delta k_3}{(r^2+(h+\Delta k_3)^2)^{3/2}}\right] \\ =& -\frac{e^2}{\hbar}\frac{1}{(2\pi)^3}\int_{-\infty}^{\infty} dh[2\pi] \int_0^{\infty} dr[r]\left[\frac{1}{2}\frac{h-\Delta k_3}{(r^2+(h-\Delta k_3)^2)^{3/2}} - \frac{1}{2}\frac{h+\Delta k_3}{(r^2+(h+\Delta k_3)^2)^{3/2}}\right] \\ =& -\frac{e^2}{\hbar}\frac{1}{2}\frac{1}{(2\pi)^2}\int_{-\infty}^{\infty} dh\left[\frac{h-\Delta k_3}{|h-\Delta k_3|} - \frac{h+\Delta k_3}{|h+\Delta k_3|}\right] \\ =& -\frac{e^2}{\hbar}\frac{1}{2}\frac{1}{(2\pi)^2}\int_{-\infty}^{\infty} dh[\mathrm{sign}(h-\Delta k_3) - \mathrm{sign}(h+\Delta k_3)] \\ =& -\frac{e^2}{\hbar}\frac{1}{2}\frac{1}{(2\pi)^2}\int_{-\Delta k_3}^{\Delta k_3} dh[-2] \\ =& \frac{e^2}{\hbar}\frac{1}{2\pi^2}\Delta k_3. \end{aligned} \tag{5.50}$$

Hence we find,

$$\sigma^{ij} = \frac{e^2}{\hbar}\epsilon^{ij\ell}\frac{1}{2\pi^2}\Delta\mathbf{k}_\ell. \tag{5.51}$$

5.1.7 Action formalism and chiral anomaly

Consider,

$$S = \int d^4x\overline{\Psi}[i\gamma^\mu(\partial_\mu - iA_\mu) - \Delta\mathbf{k}_\mu\gamma^\mu\gamma^5]\Psi, \tag{5.52}$$

where A_μ indicates the external applied electric field. This is analogous to the external electric field applied in the derivation using linear response. It is important to stress that the fermionic fields Ψ and $\overline{\Psi}$ are dynamical. When performing an infinitesimal chiral rotation, $\Psi \to \exp(i\Delta k_\mu x^\mu\gamma^5)\Psi$ and $\overline{\Psi} \to \overline{\Psi}\exp(i\Delta k_\mu x^\mu\gamma^5)$, we do not only render,

$$S = \int d^4x\overline{\Psi}[i\gamma^\mu(\partial_\mu - iA_\mu) - \Delta\mathbf{k}_\mu\gamma^\mu\gamma^5]\Psi \to \int d^4x\overline{\Psi}[i\gamma^\mu(\partial_\mu - iA_\mu)]\Psi, \tag{5.53}$$

but we get a non-trivial contribution from the integration measures of the dynamical fields Ψ and $\overline{\Psi}$,

$$\int D\overline{\Psi}D\Psi \rightarrow \int D\overline{\Psi}D\Psi|\text{Jacobian}|. \tag{5.54}$$

The non-triviality is a result of the action having different symmetries than the path integral measures. All information about the axial "γ^5" term is captured in the Jacobian, which can be evaluated using the Heat Kernel regularization trick [11, 10]. The effective action we obtain,

$$S_{\text{eff}} = \frac{e^2}{16\pi^2}\int d^4x \Delta\mathbf{k}_\mu \mathbf{x}^\mu \epsilon^{\mu\nu\alpha\beta} F_{\mu\nu}F_{\alpha\beta}. \tag{5.55}$$

Notice that the new term captures all information about the axial term, because it originates from the Jacobian. If the fields Ψ and $\overline{\Psi}$ would not have been dynamical, but classical instead, the new term would be absent. The transformation would have had a conserved current j_5 instead. Making the fields dynamical, which corresponds to making the theory semi-classical or quantum, "suddenly" renders j_5 to be non-conserved. This is what is called the chiral anomaly. The new term is a topological field theory, i.e. this term is metric independent, since it does not couple to $g_{\mu\nu}$ in any way.

Computing the currents of the "anomalous" term associated with A_μ we obtain,

$$j_\nu = \frac{e^2}{2\pi^2}\Delta\mathbf{k}_i \epsilon^{i\nu\alpha\beta}\partial_\alpha A_\beta, \tag{5.56}$$

and

$$j_\nu = -\frac{e^2}{2\pi^2}\Delta\mathbf{k}_0 \epsilon^{0\nu\alpha\beta}\partial_\alpha A_\beta. \tag{5.57}$$

From (5.56) it is concluded that,

$$\mathbf{J}_e = \frac{e^2}{2\pi^2}\Delta\mathbf{k}\times\mathbf{E}_{ext}, \tag{5.58}$$

which enables us, by comparing this equation with the definition of the conductivity tensor and restoring dimensions to obtain (5.51).

The following table, borrowed from [11], summarizes transformation properties of the various fermion bilinears under C, P and T. Here C stands for the inversion of charge, P stands for the inversion of parity and T stands for the inversion of time.

	$\overline{\Psi}\Psi$	$i\overline{\Psi}\gamma^5\Psi$	$\overline{\Psi}\gamma^\mu\Psi$	$\overline{\Psi}\gamma^\mu\gamma^5\Psi$	∂_μ
P	$+1$	-1	$(-1)^\mu$	$-(-1)^\mu$	$(-1)^\mu$
T	$+1$	-1	$(-1)^\mu$	$(-1)^\mu$	$-(-1)^\mu$
C	$+1$	$+1$	-1	$+1$	$+1$

Where $(-1)^\mu = 1$ when $\mu = 0$ and $(-1)^\mu = -1$ when $\mu = i$. The term $\Psi^\dagger\gamma^0\Delta\mathbf{k}_\mu\gamma^\mu\gamma^5\Psi$ picks up a minus sign under T, when $\mu = i$. This means that this term breaks time-reversal symmetry. When $\mu = 0$ the terms picks up a minus sign under P. This means that it is not symmetric under space-reversal. Thus it is said that for the anomalous Hall effect it is needed to break time-reversal symmetry [12][5].

[5]QCD allows a CP-symmetry breaking term, but there have been no measurements showing the existence of such a particle. Denote $\theta := \Delta_\mu x^\mu$ to be a field. This θ arises from Peccei-Quinn theory[16] as proposal for a particle that breaks CP-symmetry. This particle is called an Axion.

5.2 Anomalous Hall effect in the interacting case

5.2.1 Revisiting the Berry curvature

We now turn to the big question: "How do interactions change the magnetic field induced by the Berry curvature?". We add the holographic self-energy $\Sigma(\omega, \mathbf{k})$ to the action,

$$S = \int \frac{dk^4}{(2\pi)^4} \Psi^\dagger \gamma^0 [\gamma^0 \omega - \gamma^i \mathbf{k}_i - \Sigma(\mathbf{k}, \omega) - \Delta \mathbf{k}_i \gamma^i \gamma^5] \Psi, \tag{5.59}$$

which is the action as posed in (4.2). This self-energy, which explicitly depends on ω, changes the dispersion relations. The magnetic field in momentum space receives corrections from the self-energy. The Berry curvature gets an additional contribution in addition to the magnetic field, a term which can be identified as an electric field in momentum space. In the non-interacting case we considered eigenfunctions of the Hamiltonian. When adding a self-energy we consider the eigenfunctions of the Hermitian part of the inverse retarded propagator denoted by $G^{-1}_{H,R}$ [13]. This is equivalent to adding the real part of the self-energy to the non-interacting Hamiltonian. The on-shell energy $\epsilon_n(\mathbf{k})$ is obtained from solving,

$$G^{-1}_{R,H}(\mathbf{k}, \omega)\big|_{\omega = \epsilon_n(\mathbf{k})} = 0. \tag{5.60}$$

The conductivity, when including a self-energy, is calculated via [13],

$$\sigma^{ij}_\Sigma = \epsilon^{ij\ell} \frac{e^2}{\hbar} \int \frac{d^3\mathbf{k}}{(2\pi)^3} \sum_n n_f(\epsilon_n(\mathbf{k}))[(\mathbf{b}_{\Sigma,n})_\ell - (\mathcal{E}_n \times \vec{\nabla}_k \epsilon_n(\mathbf{k}))_\ell], \tag{5.61}$$

where,

$$\mathbf{b}_{\Sigma,n} := \vec{\nabla}_\mathbf{k} \times \mathbf{a}_n, \quad \mathbf{a}_n := i\langle n, \mathbf{k}|\vec{\nabla}_\mathbf{k}|n, \mathbf{k}\rangle, \tag{5.62}$$

which, in contrast to (5.45) might depend on ω, because we now consider eigenstates of $G^{-1}_{H,R}$. The electric field $\mathcal{E}_n$ is defined as,

$$\mathcal{E}_n := i(\partial_\omega \langle n, \mathbf{k}|\vec{\nabla}_k|n, \mathbf{k}\rangle - \vec{\nabla}_k \langle n, \mathbf{k}|\partial_\omega|n, \mathbf{k}\rangle). \tag{5.63}$$

All expressions in (5.61) are evaluated on-shell, i.e. $\omega = \epsilon_n(\mathbf{k})$. Since we want to examine the effect of the self-energy, we want to compare its effect on the magnetic field in momentum space. Thus we are not doing any calculations on the electric field. We neglect this part of the conductivity from now on and leave the consideration of this term to future work.

We return to the matter of the eigenfunctions of $G^{-1}_{R,H}$. We need to calculate

$$G^{-1}_{R,H} = \frac{1}{2}[(G^{-1}_R)^\dagger + G^{-1}_R], \tag{5.64}$$

where G^{-1}_R is obtained from (5.59),

$$G^{-1}_R = \gamma^0[\gamma^0 \omega - \mathbf{k}_i \gamma^i - \Sigma(\mathbf{k}, \omega) - \Delta \mathbf{k}_i \gamma^i \gamma^5]. \tag{5.65}$$

After establishing the following identities,

$$(\gamma^0\gamma^\mu)^\dagger = (\gamma^0\gamma^\mu\gamma^0)(\gamma^0\gamma^0\gamma^0) = \gamma^0\gamma^\mu, \quad (\gamma^0\gamma^\mu\gamma^5)^\dagger = (\gamma^5)^\dagger(\gamma^0\gamma^\mu)^\dagger = \gamma^5\gamma^0\gamma^\mu = \gamma^0\gamma^\mu\gamma^5, \tag{5.66}$$

we conclude

$$\begin{aligned} G_{R,H}^{-1} =& -\gamma^0\omega\mathbb{1}_4 - \mathbf{k}_i\gamma^0\gamma^i - \frac{1}{2}\gamma^0(\Sigma(\mathbf{k},\omega)^\dagger + \Sigma(\mathbf{k},\omega)) - \Delta\mathbf{k}_i\gamma^0\gamma^i\gamma^5 \\ =& \Sigma(\mathbf{k},\omega)\mathbf{k}_\mu\gamma^0\gamma^\mu - \mathbf{k}_\mu\gamma^0\gamma^\mu - \Delta\mathbf{k}_i\gamma^0\gamma^i\gamma^5, \end{aligned} \tag{5.67}$$

where using (2.59) we redefined Σ in the second line,

$$\Sigma(\mathbf{k},\omega) = g2^{-2M}\frac{\Gamma(\frac{1}{2}-M)}{\Gamma(\frac{1}{2}+M)}\mathrm{Re}\left[e^{-i\pi(M+\frac{1}{2})}\left(\sqrt{\omega^2-|\mathbf{k}|^2}\right)^{2M-1}\right]. \tag{5.68}$$

To determine the on-shell energy $\epsilon_n(\mathbf{k})$ we are required to solve (5.60). Solving this expression analytically yields a very complicated expression, if solveable at all. Thus we take $\epsilon_n(\mathbf{k})$ to be the energy from the case without self-energy, as an approximation. This is a preliminary approach which might be justified in a low-energy regime. Finding the eigenfunctions of $G_{R,H}^{-1}$ makes it possible to determine $\mathbf{b}_{\Sigma,n}$ via (5.62),

n	$\epsilon_n(\mathbf{k})$	$(\mathbf{b}_n)_3$	$(\mathbf{b}_{\Sigma,n})_3$
1	$-\lvert\mathbf{k}-\Delta\mathbf{k}\rvert$	$+\frac{1}{2}\frac{k_3-\Delta k_3}{(k_1^2+k_2^2+(k_3-\Delta k_3)^2)^{3/2}}$	$+\frac{1}{2}\frac{(1-\Sigma)[(k_3+\Delta k_3)-(2k_3+\Delta k_3)\Sigma+k_3\Sigma^2-\Delta k_3(k_2\partial_{k_2}\Sigma+k_1\partial_{k_1}\Sigma)]}{(k_1^2+k_2^2+(k_3+\Delta k_3)^2-2(k_1^2+k_2^2+k_3(k_3+\Delta k_3))\Sigma+(k_1^2+k_2^2+k_3^2)\Sigma^2)^{3/2}}$
2	$+\lvert\mathbf{k}-\Delta\mathbf{k}\rvert$	$-$“ ”	$-$“ ”
3	$-\lvert\mathbf{k}+\Delta\mathbf{k}\rvert$	$-(\Delta k_3\to-\Delta k_3)$	$-(\Delta k_3\to-\Delta k_3)$
4	$+\lvert\mathbf{k}+\Delta\mathbf{k}\rvert$	$+(\Delta k_3\to-\Delta k_3)$	$+(\Delta k_3\to-\Delta k_3)$

We are only interested in the 3-component at $\Delta k_1 = \Delta k_2 = 0$. When considering the 1 and 2 components in cylindrical coordinates these terms turn out to depend linearly on $\cos[\theta]$ or $\sin[\theta]$. Therefore, it is checked that when considering σ^{13} or σ^{23} they instantly vanish because of the integration, just like in the non-interacting case. The third column describes the case without Σ and the fourth column describes the 3-component when taking Σ into account. It is immediately clear that when $\Sigma\to 0$, not only $\mathcal{E}_n\to 0$, but also[6] $\mathbf{b}_{\Sigma,n}\to-\mathbf{b}_n$. Inserting the last into (5.61) exactly gives us (5.44). Hence it is checked that

$$\Sigma\to 0 \quad\Rightarrow\quad \sigma_\Sigma^{ij}\to\sigma^{ij}. \tag{5.69}$$

5.2.2 Obtaining the effects of holographic self-energy

It is instructive to explicitly evaluate $\Sigma(\mathbf{k},\omega)$ using the approximated energy,

$$\begin{aligned} \Sigma(\mathbf{k},\omega)|_{\omega=\epsilon_n} =& \Sigma(\mathbf{k},\pm\Delta k_3) \\ =& g2^{-2M}\frac{\Gamma(\frac{1}{2}-M)}{\Gamma(\frac{1}{2}+M)}\mathrm{Re}\left[e^{-i\pi(M+\frac{1}{2})}\left(\sqrt{k_1^2+k_2^2+(k_3\pm\Delta k_3)^2-|\mathbf{k}|^2}\right)^{2M-1}\right] \\ =& c_{M,g}\mathrm{Re}\left[e^{-i\pi(M+\frac{1}{2})}\left(\sqrt{(k_3\pm\Delta k_3)^2-k_3^2}\right)^{2M-1}\right], \end{aligned} \tag{5.70}$$

where $c_{M,g} := g2^{-2M}\frac{\Gamma(\frac{1}{2}-M)}{\Gamma(\frac{1}{2}+M)}$. It is important to notice that in our approximation the self-energy does not depend on k_1 or k_2. Hence,

$$\partial_{k_1}(\Sigma(\mathbf{k},\omega)|_{\omega=\epsilon_n}) = \partial_{k_2}(\Sigma(\mathbf{k},\omega)|_{\omega=\epsilon_n}) = 0. \tag{5.71}$$

[6]The minus sign corresponds to the minus sign when applying a Legendre transformation when switching from the Hamiltonian approach to the Action of Lagrangian formalism.

This also means that Σ is independent of r and ϕ when turning to cylindrical coordinates. Another important identity of Σ in cylindrical coordinates is,

$$\begin{aligned}\Sigma(h,\Delta k_3) =& c_{M,g}\mathrm{Re}\left[e^{-i\pi(M+\frac{1}{2})}\left(\sqrt{(h+\Delta k_3)^2-h^2}\right)^{2M-1}\right]\\ =& c_{M,g}\mathrm{Re}\left[e^{-i\pi(M+\frac{1}{2})}\left(\sqrt{((-h)-\Delta k_3)^2-(-h)^2}\right)^{2M-1}\right]\\ =& \Sigma(-h,-\Delta k_3).\end{aligned} \tag{5.72}$$

Now we make the first step towards calculating σ_Σ^{12},

$$\sigma_\Sigma^{12} = \frac{e^2}{\hbar}\int \frac{d^3k}{(2\pi)^3}\left[(\mathbf{b}_{\Sigma,1})_3 + (\mathbf{b}_{\Sigma,3})_3\right]. \tag{5.73}$$

In Figure 5.2 the magnetic field of (5.73) in momentum space is plotted. Finally, using the table on page 52 we compute,

$$\begin{aligned}\sigma_\Sigma^{12} =& \frac{e^2}{\hbar}\int \frac{d^3k}{(2\pi)^3}[(\mathbf{b}_{\Sigma,1})_3 + (\mathbf{b}_{\Sigma,3})_3]\\ =& \frac{e^2}{\hbar}\frac{1}{(2\pi)^3}\int_{-\infty}^{\infty} dh\int_0^{2\pi} d\phi\int_0^{\infty} dr[r][(\mathbf{b}_{\Sigma,1})_3(r,h,\phi) - (\Delta k_3\to -\Delta k_3)]\\ =& \frac{e^2}{\hbar}\frac{1}{(2\pi)^3}\int_{-\infty}^{\infty} dh[2\pi]\int_0^{\infty} dr[r]\\ &\times\left[+\frac{1}{2}\frac{(1-\Sigma(h,-\Delta k_3))(h+\Delta k_3-(2h+\Delta k_3)\Sigma(h,-\Delta k_3)+h(\Sigma(h,-\Delta k_3))^2)}{(r^2+(h+\Delta k_3)^2-2(r^2+h(h+\Delta k_3))\Sigma(h,-\Delta k_3)+(h^2+r^2)(\Sigma(h,-\Delta k_3))^2)^{3/2}} - (\Delta k_3\to -\Delta k_3)\right]\\ =& \frac{e^2}{\hbar}\frac{1}{(2\pi)^2}\int_{-\infty}^{\infty} dh\\ &\times\left[-\frac{1}{2}\frac{h+\Delta k_3-h\Sigma(h,-\Delta k_3)}{\sqrt{\Delta k_3^2+2h\Delta k_3(1-\Sigma(h,-\Delta k_3))+(h^2+r^2)(1-\Sigma(h,-\Delta k_3))^2}} - (\Delta k_3\to -\Delta k_3)\right]\Bigg|_{r=0}^{r=\infty}\\ =& \frac{e^2}{\hbar}\frac{1}{(2\pi)^2}\int_{-\infty}^{\infty} dh\left[0+\frac{1}{2}\frac{h+\Delta k_3-h\Sigma(h,-\Delta k_3)}{|h+\Delta k_3-h\Sigma(h,-\Delta k_3)|} - (\Delta k_3\to -\Delta k_3)\right]\\ =& \frac{1}{2}\frac{e^2}{\hbar}\frac{1}{(2\pi)^2}\int_{-\infty}^{\infty} dh\left[\frac{h+\Delta k_3-h\Sigma(h,-\Delta k_3)}{|h+\Delta k_3-h\Sigma(h,-\Delta k_3)|} - \frac{h-\Delta k_3-h\Sigma(h,+\Delta k_3)}{|h-\Delta k_3-h\Sigma(h,+\Delta k_3)|}\right]\\ =& \frac{1}{2}\frac{e^2}{\hbar}\frac{1}{(2\pi)^2}\int_{-\infty}^{\infty} dh(\mathrm{sign}[h+\Delta k_3-h\Sigma(h,-\Delta k_3)] + \mathrm{sign}[(-h)+\Delta k_3-(-h)\Sigma(-h,-\Delta k_3)]).\end{aligned} \tag{5.74}$$

The last step has to be done numerically and is presented in Figure 5.3.

The different behaviors for $M<0$ and $M>0$ originate from the fact that in the last line of (5.74) the arguments in the sign-functions behave different depending on the sign of M. Recall that for a sign-function it is only important where the argument changes sign, i.e. where the argument equals zero. In Figure 5.4 we plot the arguments and observe that when $M<0$ for small values of Δk_3 the zero solution, where the function equals zero, becomes very large. This behavior is what causes the sign functions in the last line of (5.74) to assign a divergent value near $\Delta k_3 = 0$. This does not occur for $M>0$. For $M>0$ the value of the zero solution goes to zero as Δk_3 goes to zero.

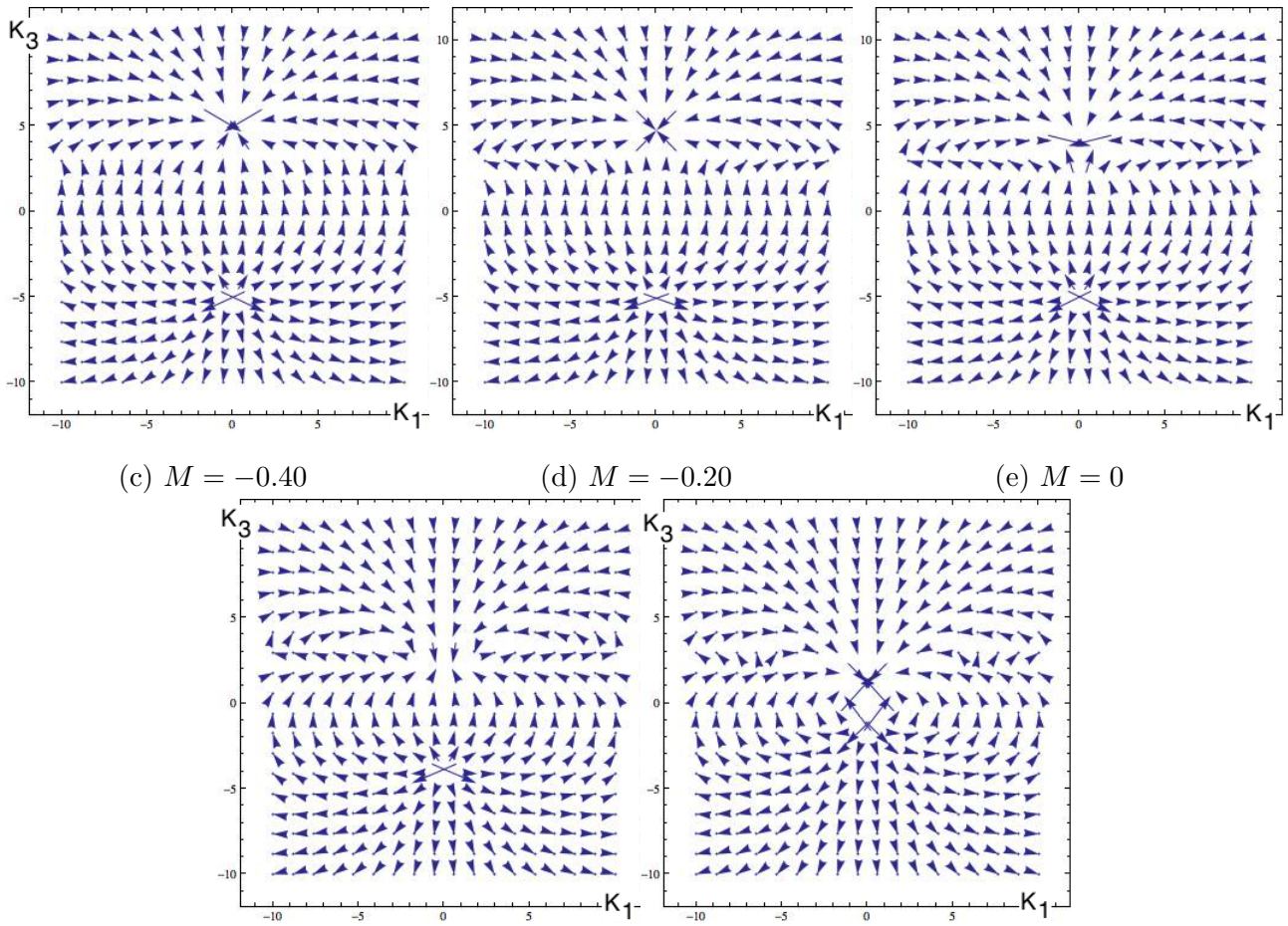

(c) $M = -0.40$ (d) $M = -0.20$ (e) $M = 0$

(f) $M = +0.20$ (g) $M = +0.40$

Figure 5.2: We plotted the Berry curvature of (5.73). Due to cylindrical symmetry we can consider the following intersection without any generality. The horizontal axes denote k_1 and the vertical axes k_3. The value for Δk_3 is 5. Compare this to Figure 5.1. When looking carefully there is a horizontal line at the height of the upper-singularity in each plot where the vectors behave odd. This behavior is accounted to a jump in the value of the k_1 component. This occurs because the k_1 component depends on the derivative of Σ in k_3, which contrary to the other derivatives in (5.71) does not vanish but makes a jump. Notice that for positive values of M the poles shift toward eachother.

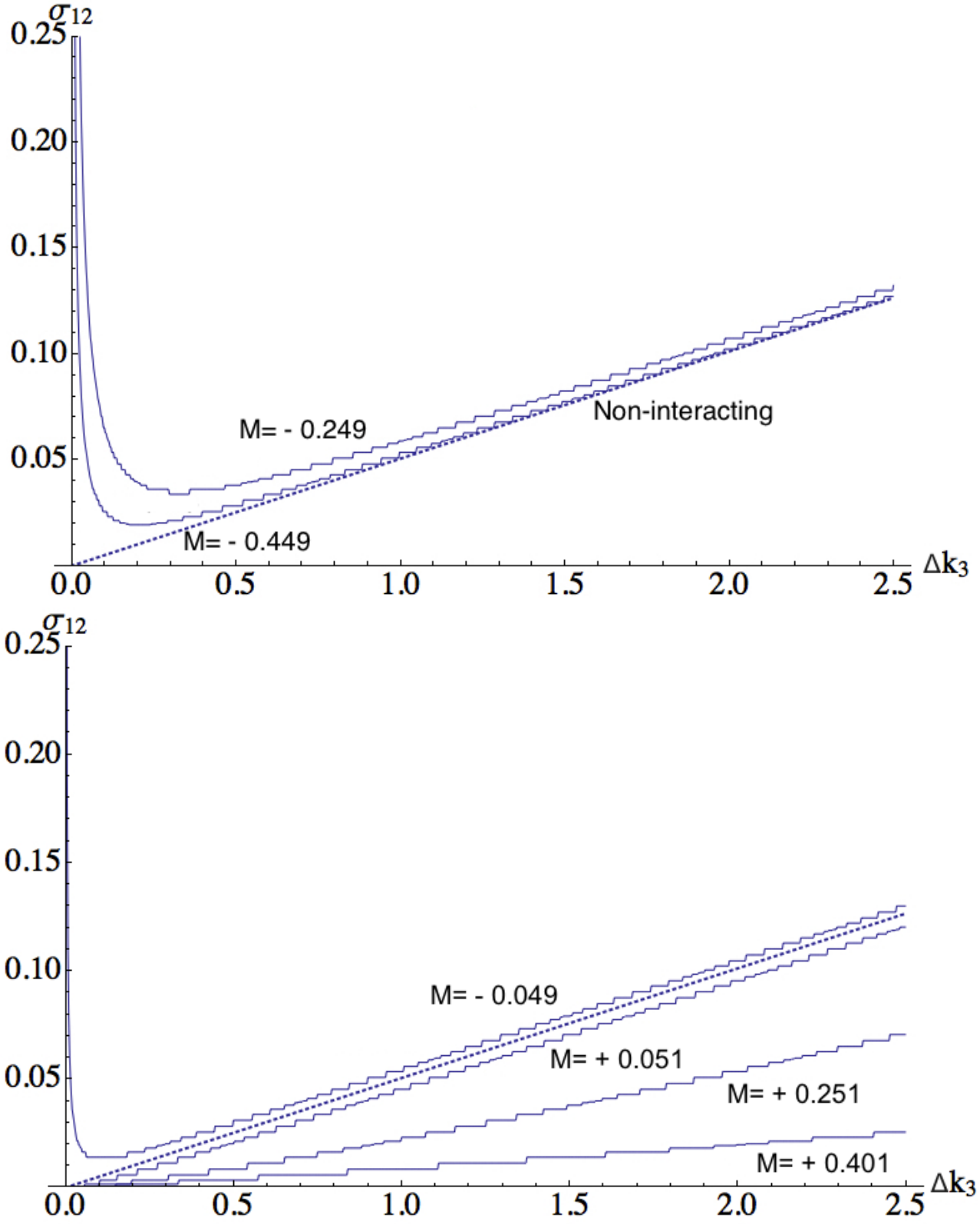

Figure 5.3: This Figure shows the contributions of the interactions to σ_{12}, when only taking into account the magnetic field in momentum space. The σ_{12} is expressed in units of $e^2/\hbar$. The dashed lines denote the conductivity for the non-interacting system, (A.8). The plateaus are an artifact of the numerics. The point $\Delta k_3 = 0$ is not well-defined. However, for negative values of M the plots seem divergent near Δk_3.

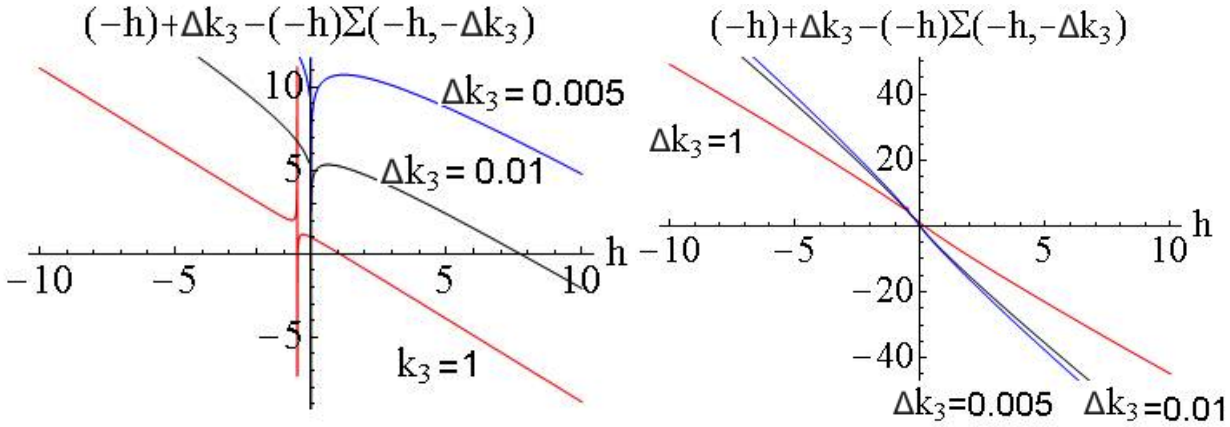

(a) $M = -0.40$ (b) $M = +0.40$

Figure 5.4: Recall the definition of Σ from (5.72). We plot the behavior for the function $(-h) + \Delta k_3 - (-h)\Sigma(-h, -\Delta k_3)$, for small Δk_3. This function is the argument of the sign function in the last line of (5.74). The function has leading order 1 in h and only real coefficients. Apart from the divergences, the function only has one real zero, intersection with horizontal axes. This ensures us that outside this range the function does not become zero. In Figure A.2 in the appendix we plotted how the sign-function argument works.

Chapter 6

Conclusions, Discussion and Outlook

The goal of this research is to investigate the effect of strong interactions via AdS/CFT on a massive Dirac spinor and Weyl semimetals. Our main goal is the study of the effect of the anomalous Hall effect on the conductivity when switching on interactions.

In chapter 2 the massive spinor case was studied. We obtained spectral function (2.102). Non-trivial behavior of the spectral function is found when using bulk mass M as a parameter for the holographic self-energy, Figure 2.4 and 2.5. Different features were observed depending on the sign of M, such as a different distribution. Moreover we added a chemical potential in chapter 3, resulting in equation (3.33). Using the dynamical exponent z we can break relativistic invariance, Figure 3.1. For $z > 1$ the problem still remains that there is a need of a holographic renormalization [8]. Further research on this model could consist of probing the dependence of the Fermi-surfaces on λ (which we put to unity in this thesis), M, m, T and μ and construct corresponding phase diagrams. In addition, it would be interesting to study the spectral functions when $-M_1 \neq M_2$, such that (2.55) does not apply to the chiral spinors.

In chapter 4 we developed the model for Weyl semimetals with the possibility to induce a separation in momentum space between the chiral cones and the possibility to take into account chemical potential. In chapter 5 we computed the changes in the contribution of the fictitious magnetic field in momentum space to the conductivity σ when adding the holographic self-energy to the system, (5.74). This computation of the interacting case is evaluated using an approximation of the on-shell energy using the solution to the dispersion relation of the non-interacting system (5.45). Switching on interactions in this approximation we found characteristic changes to the conductivity for $M < 0$ and $M > 0$, Figure 5.3. When $M = 0$ the self-energy vanishes because the product in the argument of Re[..] becomes purely imaginary (5.72).

It is possible that the singular behavior for negative values of M is an artifact of the approximated on-shell energy. The behavior of positive values of M is in line with the common observation in all related spectral function plots and Figure 5.2 that the separation also depends on M when M is positive. For further research it is interesting to have a look at the validity of the approximation and to calculate the actual on-shell energy for the interacting case. In addition it would be important tot calculate $\mathcal{E}$, the electric field in momentum-space (5.63), which we discarded. This quantity is meaningful because the total conductivity due to the intrinsic contribution of the anomalous Hall effect can be computed when including it to the Berry curvature [13]. Another generalization would be to probe the temperature dependence, the case when $T \neq 0$.

Although we developed Weyl semimetals taking into account doping (4.8) in chapter 4, we did not consider this possibility in the calculations of the conductivity for doping. In [16] it is calculated using

questionable regularizations that for the non-interacting Weyl semimetal the $\mu = 0$ case coincides with $\mu \neq 0$. This remains to be shown using our adopted integral formalism, developed on page 63 in the appendix. The interacting case with finite chemical potential would be another extension of what we did in this thesis. In addition, the effect of letting $\Delta\omega \neq 0$ (4.1) shifts the dispersion relations in a non-trivial way, which could be taken into account. A beginning has been made in [10].

Non-zero chemical potential and finite temperature altogether with taking into account $\mathcal{E}$ would be a promising experimental benchmark since this intrinsic contribution is independent of the scattering amplitude and impurities and therefore possibly therefore traceable via experiment [15, 14]. Moreover, for full understanding the diagonal parts of the conductivity should be computed.

There are other ways to compute the conductivity due to the anomalous Hall effect in the interacting case. A way could be a calculation via Feynman diagrams and Ward-identities [22]. Applying this approach we get a direct expression for the conductivity in terms of the products of (derivatives of) the retarded Green's function. We have an explicit expression for this Green's functions (4.6). Another way that could be considered is using the action formalism [10] and the chiral anomaly to compute the conserved currents and the conductivity tensor. This last approach could also be used to show that in the non-interacting case $\mu = 0$ coincides with $\mu \neq 0$ by calculating that μ does not couple to the conserved current of the applied electric field.

In conclusion, the results obtained in this thesis are promising but there is still work to be done. For instance, how big is the contribution of $\mathcal{E}$ and how valid is the approximation of the solution of the dispersion relation of the interacting case? Furthermore, this thesis illustrates some intriguing features of a holographic self-energy, such as the effect of the bulk fermion mass M on the theory on the boundary. Although the results are still far away from verification, the suggested paths for further study, when comprehended, should be able to produce exciting new predictions.

Bibliography

[1] J. Maldacena, *The large N limit of superconformal field theories and supergravity*, Abd. Theor. Math. Phys. **2**, 231 (1998), [Int. J. Theory. Phys. **38**, 1113 (1999)].

[2] E. Witten, *Anti-de Sitter space and holography*, Abd. Theor. Math. Phys. **2**, 253 (1998).

[3] S. Gubser, I. Klebanov, A. Polyakov, *Gauge theory correlators from noncritical string theory*, Phys. Lett. B **428** (1998) 105.

[4] J. McGreevy, *Holographic duality with a view toward many-body physics*, [arXiv:0909.0518v3 [hep-th]].

[5] S. Hartnoll, *Lectures on holographic methods for condensed matter physics*, [arXiv:0903.3246v3 [hep-th]].

[6] J. Tarrio, S. Vandoren, *Black holes and black branes in Lifshitz spacetimes*, JHEP **1109** (2011) 017 [arXiv:1105.6335 [hep-th]].

[7] M. Taylor, *Non-relativistic holography*, [arXiv:0812.0530v1 [hep-th]].

[8] U. Gursoy, E. Plauschinn, H. Stoof, S. Vandoren, *Holography and APRES sumrules*, JHEP **1205** (2012) 018 [arXiv:1112.5074 [hep-th]].

[9] U. Gursoy, V. Jacobs, E. Plauschinn, H. Stoof and S. Vandoren, *Lifshitz holography for undoped Weyl semimetals*, [arXiv:1209.2593 [hep-th]].

[10] A. Zyuzin, A. Burkov, *Topological response in Weyl semimetals and the chiral anomaly*, [arXiv:1206.1868v1 [cond-mat.mes-hall]].

[11] M. Peskin, D. Schroeder, *An Introduction to Quantum Field Theory*, ISBN 978-0-201-50397-5.

[12] Z. Wang, X-L Qi, S-C Zhang, *Equivalent topological invariants of topological insulators*, [arXiv:0910.5954v2 [cond-mat.str-el]].

[13] R. Shindou, L. Balents, *Artificial Electric Field in Fermi Liquids*, Physical Review Letters 97, 216601 (2006) [arXiv:0603089v2 [cond-mat.str-el]].

[14] D. Xiao, M-C Chang, Q. Niu, *Berry phase effects on electronic properties*, Reviews of modern physics, Volume 82, July-September 2010.

[15] N. Nagaosa, J. Sinova, S. Onoda, A. MacDonald, N. Ong, *Anomalous Hall Effect*, [arXiv:0904.4154v1 [cond-mat.mes.hall]].

[16] P. Goswami, S. Tewari, *Axion field theory and anomalous non-dissipative transport properties of (3+1)-dimensional Weyl semi-metals and Lorentz violating spinor electrodynamics*, [arXiv:1210.6352v1 [cond-mat.mes-hall]].

[17] S. Carroll, *Spacetime and Geometry*, ISBN 0-8053-8732-3.

[18] A Adams, A. Maloney, A. Sinha, S. Vazquez, *1/N Effects in Non-Relativistic Gauge-Gravity Duality* [arXiv:0812.0166 [hep-th]].

[19] B. de Wit, *Lecture notes Field Theory in Particle Physics*.

[20] T. Frankell *The Geometry of Physics: An Introduction*, ISBN 978-1107602601

[21] R. Contino, A. Pomarol, *Holography for Fermions*, [arXiv:0406257v2 [hep-th]].

[22] H. Stoof, K. Gubbels D. Dickerscheid, *Ultracold Quantum Fields*, ISBN 978-1-4020-8762-2

[23] H. Bruus, K. Flensberg, *Many-Body Quantum Theory in Condensed Matter Physics*, ISBN 0-19-856633-6.

[24] P. Allen, *Electron Transport* in *Conceptual Foundations of Material Properties:A standard model for calculation of ground- and excited-state properties* M. L. Cohen and S. G. Louie, editors ISBN 0444509763

[25] J. Duistermaat, J. Kolk, *Multidimensional Real Analysis II: Integration*, ISBN 0-521-82925-9.

Appendix A

Solving Integrals

A.0.3 First step analysis

It turns out to be important, before considering (5.47), to first have a look at the integration order when we would integrate over the first term of (5.47), after removing some constants,

$$\int d^3\mathbf{k}\left[\frac{1}{2}\frac{(k_3-\Delta k_3)}{(k_1^2+k_2^2+(k_3-\Delta k_3))^{3/2}}\right]=\int dk_3dk_2dk_1\left[\frac{1}{2}\frac{(k_3-\Delta k_3)}{(k_1^2+k_2^2+(k_3-\Delta k_3))^{3/2}}\right]=(*). \tag{A.1}$$

Take a look at where the divergence is in Figure A.1. Now the integral dk_1 of the integrand is well-

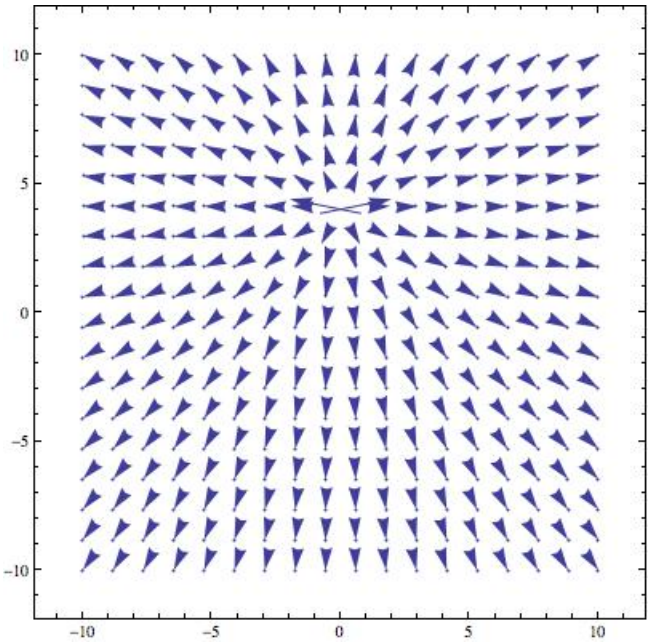

Figure A.1: The Berry curvature of (A.1) is plotted. Due to cylindrical symmetry we can consider the following intersection without any generality. The horizontal axes denote k_1 and the vertical axes k_3. The value for Δk_3 is 5.

defined, because $k_2 = 0$ and $k_3 = \Delta k_3$, the only configuration that k_1 could hit a pole, the integrand

vanishes. Thus

$$\begin{aligned}(*) &= \int dk_3 dk_2 \left[\frac{1}{2} \frac{k_1(k_3 - \Delta k_3)}{(k_2^2 + (k_3 - \Delta k_3)^2)\sqrt{k_1^2 + k_2^2 + (k_3 - \Delta k_3)^2}} \Bigg|_{k_1=-\infty}^{k_1=\infty} \right] \\ &= \int dk_3 dk_2 \left[\frac{k_3 - \Delta k_3}{k_2^2 + (k_3 - \Delta k_3)^2} \right] \\ &= (**)\end{aligned} \tag{A.2}$$

Now the integral over k_2 is well-defined, since for $k_3 = \Delta k_3$ the integrand vanishes,

$$\begin{aligned}(**) &= \int dk_3 \arctan\left(\frac{k_2}{k_3 - \Delta k_3} \right) \Bigg|_{k2=-\infty}^{k2=\infty} \\ &= \pi \int_{-\infty}^{\infty} dk_3 \frac{k_3 - \Delta k_3}{|k_3 - \Delta k_3|} \\ &= \pi \int_{-\infty}^{\infty} dk_3 \text{sign}(k_3 - \Delta k_3),\end{aligned} \tag{A.3}$$

and this last integral diverges. Without any loss of generality the order of dk_1 and dk_2 could have been swapped. But if if we start with integrating over k_3, the situation is different. This turns out to be essential for calculating (5.47).

Investigating the integration over the divergence in the case of starting with an integration over k_3, requires taking $k_1 = k_2 = 0$. This would yield an integrand,

$$\sim \frac{(k_3 - \Delta k_3)}{(k_3 - \Delta k_3)^{3/2}} = \frac{1}{(k_3 - \Delta k_3)^{1/2}}, \tag{A.4}$$

which is not integrable over k_3. Essentially the same thing would happen when first calculating the integral over dk_1 or dk_2 and then dk_3. Investigating the pole in this case requires $k_2 = 0$ or $k_1 = 0$, respectively,

$$\begin{aligned}\int dk_2 \left[\frac{1}{2} \frac{(k_3 - \Delta k_3)}{(k_1^2 + k_2^2 + (k_3 - \Delta k_3))^{3/2}} \right] \Bigg|_{dk_1=0} &= \int dk_1 \left[\frac{1}{2} \frac{(k_3 - \Delta k_3)}{(k_1^2 + k_2^2 + (k_3 - \Delta k_3))^{3/2}} \right] \Bigg|_{dk_2=0} \\ &\sim \frac{k_3 - \Delta k_3}{(k_3 - \Delta k_3)^2} \\ &= \frac{1}{(k_3 - \Delta k_3)},\end{aligned} \tag{A.5}$$

which again is not integrable over k_3.[1] Nothing strange happens here. Whatever way the integral is integrated it is divergent. In the next subsection we argue how we can handle (5.47).

A.0.4 Solution

What we learned from the last integral is that when solving (5.47) we may not split the integral blindly, because this action requires all integrals to be finite. Moreover, for $\Delta k_3 \neq 0$, the integral is

[1] It looks like this integral can be done using contour integration. This is not possible since for this integrand any closing contour has problems converging at ∞.

not absolutely integrable. This means that

$$\int \frac{d^3\mathbf{k}}{(2\pi)^3}\text{abs}\left[\frac{1}{2}\frac{(k_3-\Delta k_3)}{(k_1^2+k_2^2+(k_3-\Delta k_3))^{3/2}}-\frac{1}{2}\frac{(k_3+\Delta k_3)}{(k_1^2+k_2^2+(k_3+\Delta k_3))^{3/2}}\right]=\infty. \tag{A.6}$$

Although we do not present a mathematical proof, intuitively it is clear that when taking the absolute value of an integrand which is the sum of two integrands that diverge separately at different points, there is nothing canceling the positive valued divergences, since all contributions of the integrand are positive. Hence the integral of the absolute value of the integrand diverges. Note that this does not necessarily mean that the regular integral, without taking the absolute value of the integrant, diverges

A result of not being absolutely integrable is that we lose the property of freely interchanging integrals. This property is normally guaranteed by Fubini's theorem [25], which is a direct consequence of being absolutely integrable.

However, we know that this integral has to converge from the calculation involving the action formalism on page 49. As a consequence of having no Fubini's theorem to depend on, the Cartesian volume measure $d^3\mathbf{k}$ cannot blindly be identified with any combination of iterated integrals, because some orders of integration do not yield a converging value. We conclude that $d^3\mathbf{k} := dk_3dk_1dk_2 = dk_3dk_2dk_1$, simply because we show that any other combination of measures renders the integral non-convergent.

We start from the integration order $dk_3dk_2dk_1$. The following formula may be used,

$$\int dx\int dy(f(x,y)+g(x,y))=\int dx\left(\int dyf(x,y)+\int dyg(x,y)\right), \tag{A.7}$$

as long as the inner integrals are convergent. This is also why we are allowed to shift away Δk_2 and δk_1. Using (A.7) and the primitives calculated in (A.1), (A.2) and (A.3) on page 62,

$$\begin{aligned}
\sigma^{12} =& -\frac{e^2}{\hbar}\int\frac{d^3\mathbf{k}}{(2\pi)^3}\left[\frac{1}{2}\frac{(k_3-\Delta k_3)}{(k_1^2+k_2^2+(k_3-\Delta k_3)^2)^{3/2}}-\frac{1}{2}\frac{(k_3+\Delta k_3)}{(k_1^2+k_2^2+(k_3+\Delta k_3)^2)^{3/2}}\right]\\
=& -\frac{e^2}{\hbar}\int\frac{dk_3dk_2dk_1}{(2\pi)^3}\left[\frac{1}{2}\frac{(k_3-\Delta k_3)}{(k_1^2+k_2^2+(k_3-\Delta k_3)^2)^{3/2}}-\frac{1}{2}\frac{(k_3+\Delta k_3)}{(k_1^2+k_2^2+(k_3+\Delta k_3)^2)^{3/2}}\right]\\
=& -\frac{e^2}{\hbar}\int\frac{dk_3dk_2}{(2\pi)^3}\left[\frac{k_3-\Delta k_3}{k_2^2+(k_3-\Delta k_3)^2}-\frac{k_3+\Delta k_3}{k_2^2+(k_3+\Delta k_3)^2}\right]\\
=& -\frac{e^2}{\hbar}\pi\int_{-\infty}^{\infty}\frac{dk_3}{(2\pi)^3}[\text{sign}(k_3-\Delta k_3)-\text{sign}(k_3+\Delta k_3)]\\
=& -\frac{e^2}{\hbar}\pi\int_{-\Delta k_3}^{\Delta k_3}\frac{dk_3}{(2\pi)^3}[-2]\\
=& -\frac{e^2}{\hbar}(-\frac{4\pi}{(2\pi)^3}\Delta k_3)=\frac{e^2}{\hbar}\frac{\Delta k_3}{2\pi^2},
\end{aligned} \tag{A.8}$$

where in the line with the sign functions the finiteness might be more insightful from Figure A.2. When generalizing the answer for arbitrary σ^{ij}, as was discussed above equation (5.47), we obtain (5.51), as desired. Performing the integral starting from $dk_3dk_1dk_2$ yields the same approach and answer, because of the symmetry between k_1 and k_2.

Now we start from the integration over k_3. Investigation of the poles requires $k_1 = k_2 = 0$. In

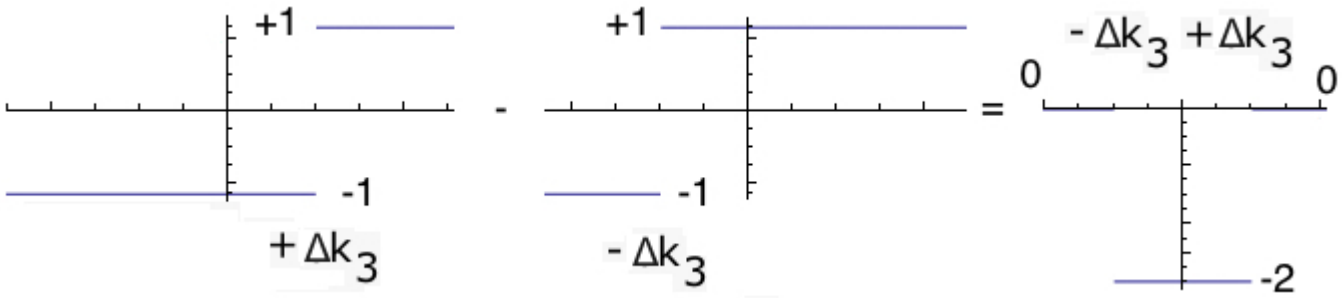

Figure A.2: These graphs show that the difference of sign functions gives us the desired factor of $4\Delta k_3$.

contrast to the monopole in (A.1), we now have two poles. The integrand looks like,

$$\begin{aligned}
&\sim \left[\frac{(k_3-\Delta k_3)}{(k_1^2+k_2^2+(k_3-\Delta k_3)^2)^{3/2}} - \frac{(k_3+\Delta k_3)}{(k_1^2+k_2^2+(k_3+\Delta k_3)^2)^{3/2}}\right]\Bigg|_{k_1=k_2=0} \\
&= \left[\frac{(k_3-\Delta k_3)}{((k_3-\Delta k_3)^2)^{3/2}} - \frac{(k_3+\Delta k_3)}{((k_3+\Delta k_3)^2)^{3/2}}\right] \\
&= \left[\frac{1}{(k_3-\Delta k_3)^2} - \frac{1}{(k_3+\Delta k_3)^2}\right].
\end{aligned} \tag{A.9}$$

It is clear that the integrand diverges for k_3 near $\pm\Delta k_3$. The last remaining case, is the one where we first integrate over k_1 and then k_3. The divergence is investigated by letting $k_2 = 0$. The case of first integrating k_2 is understood due to symmetry. Hence

$$\begin{aligned}
&\sim \int dk_1 \left[\frac{(k_3-\Delta k_3)}{(k_1^2+k_2^2+(k_3-\Delta k_3)^2)^{3/2}} - \frac{(k_3+\Delta k_3)}{(k_1^2+k_2^2+(k_3+\Delta k_3)^2)^{3/2}}\right]\Bigg|_{k_2=0} \\
&= \left[\frac{k_3-\Delta k_3}{(k_3-\Delta k_3)^2} - \frac{k_3+\Delta k_3}{(k_3+\Delta k_3)^2}\right] \\
&= \left[\frac{1}{(k_3-\Delta k_3)} - \frac{1}{(k_3+\Delta k_3)}\right],
\end{aligned} \tag{A.10}$$

which is divergent at $k_3 = \pm\Delta k_3$.

A.0.5 Change of variables

Along with changing the order of integration, we also have to be careful when changing variables. We want to use other coordinates because in the next section, when including the self-energy, it turns out that calculations using cylindrical coordinates are much easier. Hence it is shown why cylindrical coordinates may be used. En passant it is shown why spherical coordinates are not an allowed choice.

Transforming to cylindrical coordinates implies

$$\begin{aligned}
k_1 &\to r\cos(\phi), \\
k_2 &\to r\sin(\phi), \\
k_3 &\to h.
\end{aligned} \tag{A.11}$$

For the measures

$$\int_{-\infty}^{\infty} dk_3 \int_{-\infty}^{\infty} dk_2 \int_{-\infty}^{\infty} dk_1 \to \int_{-\infty}^{\infty} h \int_0^{2\pi} d\phi \int_0^{\infty} dr[r], \tag{A.12}$$

where $[r]$ denotes the Jacobian. Notice that the order of k_1 and k_2 with respect to k_3 does not change, also in new coordinates. This new choice of coordinates only "mixes" the k_1 and k_2, which commute anyway. We can now conclude that this is an allowed choice of coordinates, as long as we perform the integral over h as the last one. The integral is independent of ϕ, as we see,

$$\begin{aligned}
\sigma^{12} =& -\frac{e^2}{\hbar}\frac{1}{(2\pi)^3}\int_{-\infty}^{\infty}dh\int_0^{2\pi}d\phi\int_0^{\infty}dr[r]\left[\frac{1}{2}\frac{h-\Delta k_3}{(r^2+(h-\Delta k_3)^2)^{3/2}}-\frac{1}{2}\frac{h+\Delta k_3}{(r^2+(h+\Delta k_3)^2)^{3/2}}\right]\\
=& -\frac{e^2}{\hbar}\frac{1}{(2\pi)^3}\int_{-\infty}^{\infty}dh[2\pi]\int_0^{\infty}dr[r]\left[\frac{1}{2}\frac{h-\Delta k_3}{(r^2+(h-\Delta k_3)^2)^{3/2}}-\frac{1}{2}\frac{h+\Delta k_3}{(r^2+(h+\Delta k_3)^2)^{3/2}}\right]\\
=& -\frac{e^2}{\hbar}\frac{1}{2}\frac{1}{(2\pi)^2}\int_{-\infty}^{\infty}dh\left[\frac{h-\Delta k_3}{|h-\Delta k_3|}-\frac{h+\Delta k_3}{|h+\Delta k_3|}\right]\\
=& -\frac{e^2}{\hbar}\frac{1}{2}\frac{1}{(2\pi)^2}\int_{-\infty}^{\infty}dh[\mathrm{sign}(h-\Delta k_3)-\mathrm{sign}(h+\Delta k_3)]\\
=& -\frac{e^2}{\hbar}\frac{1}{2}\frac{1}{(2\pi)^2}\int_{-\Delta k_3}^{\Delta k_3}dh[-2]\\
=&\frac{e^2}{\hbar}\frac{1}{2\pi^2}\Delta k_3.
\end{aligned}\tag{A.13}$$

Hence we find the same result as before,

$$\sigma^{ij}=\frac{e^2}{\hbar}\epsilon^{ij\ell}\frac{1}{2\pi^2}\Delta\mathbf{k}_\ell.\tag{A.14}$$

Now we choose to go to spherical coordinates instead,

$$\begin{aligned}
k_1 &\to r\cos(\phi)\sin(\theta),\\
k_2 &\to r\sin(\phi)\sin(\theta),\\
k_3 &\to r\cos(\theta).
\end{aligned}\tag{A.15}$$

For the measures

$$\int_{-\infty}^{\infty}dk_3\int_{-\infty}^{\infty}dk_2\int_{-\infty}^{\infty}dk_1\to\int_0^{\infty}dr\int_0^{2\pi}d\phi\int_0^{\pi}d\theta[r^2\sin(\theta)].\tag{A.16}$$

We lose any clue of ordering, i.e. we mixed all measures, including k_3. It is clear that the integral over r has to be performed last to yield a converging answer. Because the integrand is independent of ϕ, $d\theta$ and $d\phi$ may switch order.

$$\begin{aligned}
\sigma^{12} =& -\frac{e^2}{\hbar}\frac{1}{(2\pi)^3}\int_0^{\infty}dr\int_0^{2\pi}d\phi\int_0^{\pi}d\theta[r^2\sin(\theta)]\left[\frac{1}{2}\frac{r\cos(\theta)-\Delta k_3}{(r^2+\Delta k_3^2-2r\Delta k_3\cos(\theta))^{3/2}}-(\Delta k_3\to-\Delta k_3)\right]\\
=& -\frac{e^2}{\hbar}\frac{1}{2}\frac{1}{(2\pi)^2}\int_0^{\infty}dr\left[\frac{r^2}{\Delta k_3^2}\left(\frac{r-\Delta k_3}{|r-\Delta k_3|}-\frac{r+\Delta k_3}{|r+\Delta k_3|}\right)-(\Delta k_3\to-\Delta k_3)\right]\\
=& -\frac{e^2}{\hbar}\frac{1}{2}\frac{1}{(2\pi)^2}\int_0^{\infty}dr\frac{r^2}{\Delta k_3^2}2\left(\frac{r-\Delta k_3}{|r-\Delta k_3|}-\frac{r+\Delta k_3}{|r+\Delta k_3|}\right)\\
=& -\frac{e^2}{\hbar}\frac{1}{(2\pi)^2}\int_0^{\infty}dr\frac{r^2}{\Delta k_3^2}(-2\theta(\Delta k_3-r))\\
=&\frac{e^2}{\hbar}\frac{1}{2\pi^2}\frac{1}{3}\Delta k_3.
\end{aligned}\tag{A.17}$$

Hence,

$$\sigma^{ij} = \frac{e^2}{\hbar}\epsilon^{ij\ell}\frac{1}{2\pi^2}\frac{1}{3}\Delta\mathbf{k}_\ell. \tag{A.18}$$

The above integral does not provide the right answer, as was expected. This occurs because when we would trace back the measures, some integration over "k_3" already has happened when integrating over θ and ϕ, which is not in the right order. Moreover, in the second and third line of (A.17) we see that if we would discard one of the monopoles, the total integral would still yield a finite value. This is not in accordance with the fact that we found that it diverges in (A.4) and (A.5). The integral of (A.17) does exist when taking into account the special ordering of measures, but it is the solution to an integral inequivalent to (5.47).

Acknowledgements, Dankwoord,

I enjoyed writing this thesis. I really start to like and appreciate the fields of physics it touches upon. For me this thesis is even more than the work produced and the knowledge gained. It was also a tour into the scientific world, which I enjoyed. During the summer of 2012 I participated in the String theory workshop in Amsterdam. Here I attended lectures of people like Sean Hartnoll and Herman Verlinde. I attended the Lorenz professor Lectures of Subir Sachdev in Leiden and also a talk by Juan Maldacena as Colloquiem Ehrenfesti. During these, and many other, events I was inspired by science and moreover, I met interesting people. Finally I also got a close look in the ITF in Utrecht and participated in the social and scientific dynamics. I can really say that I got attracted to science by the whole process.

Henk, ik wil je bedanken voor je vertrouwen in mij. Ik vind het heel fijn dat je vanaf het eerste moment benadrukte dat je een thesis, of wat dan ook, niet *onder* iemand schrijft maar *met* iemand. Ik voelde me gesterkt in het feit dat je zoveel geduld toont en je gezonde koppigheid heeft me heel vaak geprikkeld om toch iets dieper na te denken. Ik heb oprechte bewondering in je inzicht en kennis van natuurkunde en streef er zelf naar dit ook ooit te mogen vergaren in deze mate. Heel erg cool vond ik het hoe je mij door het maken van mijn presentatie heen loodste. Ik ga je opmerkingen over wiskundigen en snaartheoreten misschien nog wel het meest missen. Bedankt!

Vivian, ik vond de sessies waar we samen problemen analyseerde op een bord of bij de koffieautomaat erg leuk en leerzaam. Ik zal het waarschijnlijk nooit realiseren hoe luxe ik het had dat je altijd tijd maakte om mij te helpen als ik vast zat qua natuurkunde of moraal. Bedankt!

Verder mag ik niet vergeten Stefan Vandoren te bedanken voor zijn interesse in mijn scriptie en een luisterend oor voor vragen met bijbehorend advies. I also like to thank Yuri Kuznetsov for his help with complex and less complex integrals. Erik Plauschinn, thank you for explaining me the Palatini formalism so patiently. To Alessandro Sfondrini, thanks for being a victim of listening to the first version of my talk and providing me with useful tips and discussions. Bedankt en Thanks!

Graag wil ik ook Bram, Peter, Jeffrey, Joost, Laurent, Laura, Joey en Mathijs bedanken voor het proeflezen van mijn epistel en/of discussies over natuurkunde. Mathijs wil ik in het bijzonder bedanken voor het bijstaan in de eerste uren van mijn scriptie, als natuurkundige en als vriend. Emmeke, ondanks het feit dat jij niet helemaal in dit rijtje nerds thuishoort bewonder ik je geduld met mij als ik weer eens niets anders kon doen dan aan integralen denken. Jongens, Bedankt!

Tot slot wil ik mijn familie, hoe complex deze ook is, bedanken voor het feit dat jullie mijn studie altijd boven alles hebben gesteld. Hoewel ik jullie hiervoor nooit genoeg zal kunnen bedanken: Bedankt, Bedankt, Bedankt!